UNIVERSIDADE D
COIMBRA

Eduarda Leite Gomes

IMPACT OF GLYCANS IN THE DEVELOPMENT OF INFLAMMATORY BOWEL DISEASE-ASSOCIATED COLORECTAL CANCER

Dissertação no âmbito do Mestrado em Investigação Biomédica, ramo de Oncobiologia, orientada pela Professora Doutora Salomé Soares Pinho e apresentada à Faculdade de Medicina da Universidade de Coimbra

Julho de 2019

Impact of Glycans in the Development of Inflammatory Bowel Disease-Associated Colorectal Cancer

Eduarda Leite Gomes

Dissertation for the attribution of the master's degree in Biomedical Research – Oncobiology field, submitted to the Faculty of Medicine of the University of Coimbra, Portugal. The research work presented in this dissertation was performed at the Instituto de Investigação e Inovação em Saúde (i3S) / Instituto de Patologia e Imunologia Molecular da Universidade do Porto (IPATIMUP).

Dissertação apresentada à Faculdade de Medicina da Universidade de Coimbra para cumprimento dos requisitos necessários à obtenção do grau de Mestre em Investigação Biomédica – ramo de Oncobiologia. Este trabalho foi realizado Instituto de Investigação e Inovação em Saúde (i3S) / Instituto de Patologia e Imunologia Molecular da Universidade do Porto (IPATIMUP).

Supervisor: Salomé Pinho, phD, DVM

Internal Supervisor: Manuel Santos Rosa, phD

Co-supervisor: Ana Dias, phD

University of Coimbra

We thank the funding from the GEDII (Grupo de Estudo da Doença Inflamatória Intestinal) (reference DII4), through the project “Glycans in colitis-associated colorectal cancer”

"Nothing in life is to be feared,
it is only to be understood.
Now is the time to understand more,
so that we may fear less"

Marie Curie

AGRADECIMENTOS

À Professora Doutora Salomé Pinho, obrigada por me ter aceite no seu grupo e pela confiança que demonstrou ao longo de todo o meu percurso. Um sincero obrigada por me ter colocado o desafio deste projeto, que tanto amei, e por todo o crescimento pessoal e científico que me proporcionou. Obrigada pelo apoio, por toda a disponibilidade e acima de tudo pelo grande exemplo de paixão pela ciência.

Ao Professor Doutor Manuel Santos Rosa, meu orientador da Universidade de Coimbra, obrigada pela sua acessibilidade.

À Ana Dias, obrigada pela ajuda ao longo deste ano. Agradeço a confiança que me foi depositada e que me permitiu desenvolver autonomia e independência em todos os desafios.

À Mariana Silva, o meu maior obrigado. Obrigada por todo o conhecimento crítico e científico que me transmitiste. Obrigada por todos os momentos partilhados. Sem dúvida que tudo se torna melhor em boa companhia. Obrigada pela amizade, pela paciência e pelo apoio ao longo de todo o ano. Cresci muito contigo e sem ti nada seria possível.

Ao Professor Doutor Henrique Girão, coordenador do Mestrado em Investigação Biomédica, o meu sincero obrigada pelo programa que nos proporciona, sem dúvida que mudou a minha forma de ver o mundo da ciência. Obrigada por todo o apoio ao longo do percurso.

À Doutora Patologista Joana Alves, do Hospital de Santo António, agradeço todo a disponibilidade e todos os ensinamentos em termos histológicos.

A todos os membros do grupo Immunology, Cancer and Glycomedicine obrigada por me terem integrado tão bem e me terem feito sentir em casa. É sem dúvida um orgulho pertencer a este grupo, que em tão pouco tempo se tornou numa família durante todo o ano. À Márcia, obrigada pela pessoa incrível que és e pela grande amizade que criamos. À Inês, obrigada pela amizade, pelo otimismo e pela boa energia que transmites todos os dias. Ao Manel, obrigada pelas boas conversas e por todas as discussões científicas. À Vanda, obrigada pela disponibilidade. À Ângela, obrigada pelas palavras de apoio nos momentos certos. À Maria, obrigada pela tranquilidade que transmites. Obrigada por tudo a todos vocês, porque sem vocês este ano não teria sido a mesma coisa. Sem dúvida que deixaram uma grande marca na minha vida.

Aos membros da equipa Glycobiology in Cancer obrigada pela partilha de laboratório ao longo de quase toda a minha tese. Obrigada pela forma como me receberam, pelo convívio, pela amizade, pela boa disposição e pelo bom ambiente de laboratório.

Às minhas amigas de mestrado, à Nascimento, à Pelicano e à Dani, obrigada por terem sido um dos grandes pilares da minha tese. Obrigada pela amizade e pelo apoio que foram mesmo com toda a distância.

Aos amigos de Bioquímica, obrigada por terem tornado os anos da universidade os melhores anos da minha vida. A UMinho será sempre parte de mim! Obrigada em especial à Bruna, à Marta, ao Pinho, ao Gonçalo, à Marlene, ao Macedo, ao Tiago, ao Tony, ao Mário, à Carlota e à Inês. Ao Bruno, ao Vítor, à Madalena e à Joana, agradeço o papel que tiveram durante todo o percurso.

Aos meus amigos de infância, obrigada por estarem sempre presentes ao longo de todo o meu crescimento, quer a nível pessoal quer a nível profissional. Obrigada à Márcia e à Jéssica por estarem sempre presentes.

Por último e mais importante, àqueles que sempre contribuíram indiretamente para o meu sucesso, a minha família. Obrigada por todo o apoio incondicional. Obrigada avó por olhares sempre por mim. Um obrigada especial à minha Mãe por ser o maior pilar da minha vida e ao meu irmão por toda a cumplicidade e por ser o meu maior exemplo de vida.

0 mais sincero obrigada a todos!

ABSTRACT

Inflammatory Bowel Disease (IBD)-associated Colorectal Cancer is a major concern in the clinical management of patients with chronic IBD. The risk for Colitis-associated Colorectal Cancer (CAC) in Ulcerative Colitis (UC) and Crohn's disease (CD) patients is of 18% and 8%, respectively. Several evidences show that chronic inflammation of the colon is associated with cancer progression, however, the underlying molecular basis of inflammation-associated cancer progression remains poorly understood. Glycosylation is one of the most abundant protein posttranslational modification. It consists in the addition of carbohydrate structures to proteins and lipids by specific enzymes, the glycosyltransferases and glycosidases. Changes in glycosylation patterns play a fundamental role in each pathological step of cancer development and progression, such as cancer cell signaling, tumor cell-cell adhesion, cell-matrix interactions, cancer metabolism, angiogenesis, metastasis and tumor immune surveillance. In fact, it has been demonstrated that the immune system is tightly controlled by glycosylation. The *N*-acetylglucosaminyltransferase V (GnT-V) encoded by the *MGAT5* gene, catalyzes the synthesis of β1,6 GlcNAc branched *N*-glycans structures. Evidences showed that in IBD, *MGAT5* gene is downregulated on intestinal T cells, and the deficiency on branched glycans on intestinal T cells was associated with an hyperimmune response and increased disease severity. On the other hand, aberrant expression of complex branched *N*-glycans is associated with tumor progression and invasiveness. However, whether this differential expression of glycans in colitis and cancer contexts are relevant in tumor-immune cell interactions in CAC remains completely unknown.

The main aim of this thesis was to characterize the glyco-profile during CAC carcinogenesis, further assessing the impact of β1,6 GlcNAc branched *N*-glycan structures in the modulation of immune response along inflammation-associated cancer. Using a well-characterized cohort of CAC patients, our cross-sectional study revealed a distinct glycoprofile in stroma and epithelial cells, characterized by an increased and gradual expression of branched *N*-glycans along CAC carcinogenic cascade. Additionally, we observed that this altered glycosignature also impact immune response early in dysplastic conditions, suggesting the role of glycans in immunomodulation along CAC. Interestingly, our *in vivo* data on AOM/DSS-induced CAC mice model, showed that *Mgat5*$^{-/-}$ mice exhibit a decrease in the number of tumor lesions comparing with WT mice, concomitantly with an increased pro-inflammatory response predominantly governed by innate immune cells. This preliminary data supports the contribution of complex branched glycans in the creation of an immunosuppressive environment associated with CAC carcinogenesis.

Taken together, our findings support that the aberrant expression of branched *N*-glycans is implicated in the early stages of CAC development, through the modulation of the surrounding immune response. This new evidence generated in this master thesis needs to be further clarified and validated.

Key words: Cancer, Inflammatory Bowel Disease, Colitis-Associated Cancer, *N*-glycosylation, β1,6 GlcNAc branched *N*-glycans, *MGAT5,* immunosurveillance, AOM/DSS model.

RESUMO

O desenvolvimento de Cancro Colorretal associado à Doença Inflamatória Intestinal (DII) é a maior preocupação na estratificação de doentes com DII. O risco para o desenvolvimento de cancro em doentes de Colite Ulcerosa e de Doença de Crohn é de 18% e 8%, respetivamente. Diversas evidencias demonstram que a inflamação crónica do colon está associada com a progressão tumoral. No entanto, o mecanismo molecular por trás da inflamação associada à progressão para cancro ainda é pouco compreendido. A glicosilação é uma das modificações pós-tradução mais abundantes em proteínas. Este processo consiste na adição de carboidratos a proteínas e lípidos através de enzimas específicas, designadas glicosiltransferases e glicosidases. Alterações nos padrões de glicosilação desempenham um papel fundamental em cada etapa patológica do desenvolvimento e progressão do cancro, tal como na sinalização, na adesão célula-célula, na interação célula-matriz, no metabolismo, na angiogénese, na metastização e vigilância imunológica do tumor. De facto, foi demonstrado que o sistema imunitário é extremamente controlado pela glicosilação. A enzima *N*-acetilglucosaminiltransferase V, codificado pelo gene *MGAT5,* catalisa a síntese de estruturas de *N*-glicanos ramificadas. Evidências demonstraram que na DII, o gene *MGAT5* está negativamente regulado nas células T do intestino, e esta deficiência nos glicanos ramificados foi associada a uma resposta hiperimune e a um aumento da severidade da doença. Por outro lado, a expressão aberrante de *N*-glicanos ramificados está associada a progressão e invasão tumoral. No entanto, permanece por esclarecer se esta expressão diferencial de glicanos em contexto de colite e cancro é relevante na interação entre as células tumorais e as células imunes, durante o desenvolvimento de cancro colorretal associado à DII.

O objetivo desta tese foi caracterizar o perfil de glicanos durante o processo de carcinogénese, avaliando o impacto dos *N*-glicanos ramificados na modulação da resposta imune ao longo do cancro associado a inflamação. Usando uma coorte bem caracterizada de pacientes, o nosso estudo revelou um perfil de glicanos distinto no estroma e nas células epiteliais, caracterizado por um aumento gradual da expressão de *N*-glicanos ramificados ao longo da cascata de carcinogénese. Além disso, observamos que esse perfil alterado de glicanos também tem impacto na resposta imune em condições antecedentes ao desenvolvimento tumoral, evidenciando o papel dos glicanos na imunomodulação. Curiosamente, os nossos resultados, usando um modelo *in vivo* induzido por AOM/DSS, demonstraram que ratinhos *MGAT5*$^{-/-}$ apresentam uma diminuição do número de lesões tumorais comparativamente com ratinhos *WT,* com uma resposta pró-inflamatória predominantemente produzida por células imunes inatas. Estes resultados preliminares suportam a contribuição dos *N*-glicanos

ramificados na criação de um ambiente imunossupressor associado com o processo de carcinogénese.

Em conjunto, os nossos resultados sustentam a hipótese que a expressão anormal de *N*-glicanos ramificados está implicada nas fases iniciais do desenvolvimento de Cancro Colorretal associado à DII, através da modulação da resposta imune. Esta nova evidência descrita nesta tese precisa de ser melhor clarificada e consequentemente validada em estudos futuros.

Palavras-chave: Cancro, Doença Inflamatória Intestinal, Cancro associado a Colite, *N*-glicosilação, glicanos ramificanos, *MGAT5,* immunovigilancia, modelo AOM/DSS.

INDEX

FIGURE INDEX

TABLE INDEX

ABBREVIATIONS LIST

5-ASA	5-Aminosalicylic Acid
ABC	Avidin-Biotin-Peroxidase Complex
ALG	Asparagine-Linked *N*-Glycosylation
AOM	Azoxymethane
APCs	Antigen-Presenting Cells
ASGPR	Asialoglycoprotein Receptor
Asn	Asparagine
AUC	Area Under the Curve
BSA	Bovine Serum Albumin
CAC	Colitis-Associated Colorectal Cancer
CD	Crohn's Disease
cDNA	Complementary DNA
DESC	Dysplasia and early stage cancer
CHP	Centro Hospitalar Do Porto
CLR	C-Type Lectin Receptors
CRC	Colorectal Cancer
CRD	Carbohydrate-Recognition Domain
CTLA-4	Cytotoxic T Lymphocyte Antigen 4
DAB	3,3 Diaminobenzidine Tetrahydrochloride
DAI	Disease Activity Index
DC-SIGN	DC-Specific Intercellular Adhesion Molecule-3-Grabbing Non-Integrin
DCs	Dendritic Cells
DII	Doença Inflamatória Intestinal
dNTPs	Deoxynucleotides
Dol-P	Dolichol Phosphate
DSS	Dextran Sulfate Sodium
DTT	Dithiothreitol
ECCO	European Crohn's And Colitis Organization
ECM	Extracellular Matrix
EDTA	Ethylenediaminetetraacetic Acid Disodium Salt Dehydrate

ELISA	Enzyme-Linked Immunosorbent Assay
ER	Endoplasmic Reticulum
ERAD	ER-Associated Degradation
FACS	Fluorescent-Activated Cell Sorting
FAP	Familial Adenomatous Polyposis
FBS	Fetal Bovine Serum
FFPE	Formalin-Fixed Paraffin-Embedded
Foxp3	Forkhead Box P3
Fuc	Fucose
Fuc-VIII	Fucosyltransferase VIII
FVD	Fixable Viability Dye
Gal	Galactose
GalNAc	*N*-Acetylgalactosamine
gDNA	Genomic DNA
Glc	Glucose
GlcNAc	N-Acetylglucosamine
GNA	*Galanthus Nivalis*
GnT	N-Acetylglucosaminyltransferase
GPI	Glycosylphosphatidylinositol
HBSS	*Hank's Balanced Salt Solution*
HEPES	Hydroxyethyl Piperazineethanesulfonic Acid
HGD	High-Grade Dysplasia
HRP	Horseradish Peroxidase
HSA	Hospital De Santo António
IBD	Inflammatory Bowel Disease
IDT	Integrated Dna Technologies
IECs	Intestinal Epithelial Cells
IFN-γ	Interferon Gamma
IL	Interleukin
ITIMs	Tyrosine-Based Inhibitory Motifs
KO	Knockout

L-PHA	*Phaseolus Vulgaris Leucoagglutinin*
LacNAc	*N*-Acetyllactosamine
LGD	Low-Grade Dysplasia
LLO	Lipid-Linked Oligosaccharide
LSC	Late stage cancer
Man	Mannose
MGAT	Mannosidase Acetylglucosaminyltransferase
MHC	Major Histocompatibility Complex
Mincle	Macrophage-Inducible C-Type Lectin
MR	Mannose Receptor
MUC	Mucin
NaCl	Sodium Chloride
Neu5AC	*N*-Acetylneuraminic Acid
NK	Natural Killer
OST	Oligosaccharyltransferase
P/S	Penicillin Streptomycin
PBMCs	Peripheral Blood Mononuclear Cells
PBS	Phosphate-Buffered Saline
PBST	Pbs Tween
PD-1	Programed Cell Death Protein 1
PD-L1	Programmed Death-Ligand 1
PFA	Paraformaldehyde
RORγ	RAR-Related Orphan Receptor Gamma
ROS	Reactive Oxygen Species
RPMI	*Roswell Park Memorial Institute*
RT	Room Temperature
RT-qPCR	Quantitative Real-Time Polymerase Chain Reaction
Ser	Serine
Siglecs	Sialic Acid-Binding Immunoglobulin-Like Lectins
SLe	Sialyl Lewis
TAAs	Tumor-Associated Antigens

TAMs	Tumor-Associated Macrophages
Tbet	T-Box Transcription Factor TBX21
TCR	T Cell Receptor
TGF-β	Transforming Growth Factor B
Th	T Helper Cell
Thr	Threonine
TIL	Tumor-Infiltrate Lymphocytes
TMB	Tetramethylbenzidine
TNF-α	Tumor Necrosis Factor Alpha
Treg	Regulatory T Cells
UC	Ulcerative Colitis
WHO	World Health Organization
WT	Wildtype

INTRODUCTION

1. Cancer

Cancer is the second leading cause of death worldwide, with 17 million new cancer cases and 9.6 million deaths in 2018 [1, 2]. The World Health Organization (WHO) foresees 27.5 million new cancer cases each year worldwide by 2040, which consists in an increase of 61.7% of cancer incidence compared to 2018 [2].

Hanahan and Weinberg have been proposing a series of hallmarks of cancer, consisting on common characteristics of all types of cancer that confer malignant properties to tumor cells [3]. Normal cells evolve progressively to a neoplastic state, acquiring a series of cancer features, required to enable them to become tumorigenic and ultimately metastatic. The main hallmarks of cancer cells comprise: sustaining proliferative signaling, evading growth suppressors, resistance to cell death, enabled replicative immortality, angiogenesis, activating invasion and metastasis, dysregulation of cellular metabolism and avoiding immune destruction **(Figure 1)** [3, 4].

Over the past decades, several evidences have been showing that the tumor-associated inflammatory response contributes to tumorigenesis, facilitating neoplastic tissue to acquire malignant properties [4]. In fact, research community has extended this concept, revealing that the molecular and cellular basis of tumors can no longer be understood by enumerating the traits of cancer cells, but instead must encompass the contributions of the tumor microenvironment to tumorigenesis [4].

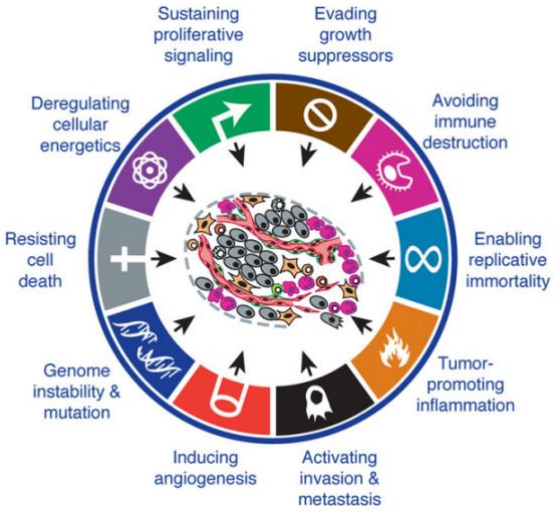

Figure 1 | Hallmarks of cancer. Hanahan and Weinberg in 2000 suggest that most cancers acquire the same set of functional capabilities during their evolution, through different mechanistic strategies. In 2011, the same authors proposed the additional of two new enabling characteristics: genome instability and mutation, as well as tumor-promoting inflammation. Adapted from [4].

1.1. Colorectal Cancer

Colorectal Cancer (CRC) was classified as the 3rd most common cancer in 2018 [2] and the 4th leading cause of cancer-related deaths in the world [5]. Even though approximately 30% of all CRC are associated with hereditary factors (including Familial Adenomatous Polyposis (FAP) and Lynch Syndrom) [6], the majority of CRC cases has been linked to somatic mutations and environmental factors, including sporadic CRC and Inflammatory Bowel Disease (IBD)-associated CRC. In fact, the extensive and chronic inflammation that characterizes IBD is associated with an increase risk for CRC development, in a process termed colitis-associated colorectal cancer (CAC) [7, 8].

1.1.1. Inflammatory Bowel Disease

IBD is a chronic and inflammatory idiopathic disorder of the gastrointestinal tract that includes Ulcerative Colitis (UC) and Crohn's disease (CD). In UC the inflammation is restricted to the colonic mucosa in a continuous pattern, while in CD the inflammation has multi-focus points and can be transmural, affecting any part of the gastrointestinal tract [9, 10]. The prevalence of IBD is increasing worldwide, being more prevalent in the industrialized countries, particularly in USA and north Europe (**Figure 2**). However, the incidence stabilized at the turn of 21st century in the developed countries, while it continues to rise in the newly industrialized countries [11].

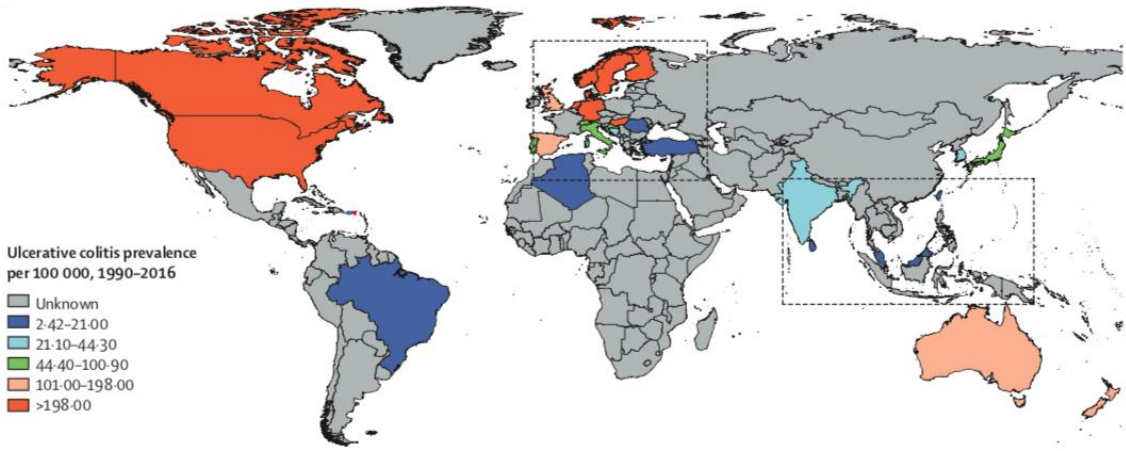

Figure 2 | Global prevalence of UC reported in 2018. Developed countries show higher disease prevalence, such as, USA and north Europe. Adapted from [11].

The precise etiology of IBD remains unclear. However, several factors are known to be key drivers of the disease pathogenesis, and thereby IBD is considered a multifactorial disease. Genetic predisposition, environmental factors and lifestyle (such as diet and stress) play

important roles in triggering the dysregulation of immune response, together with the development of dysbiotic conditions that contribute to the loss of gut homeostasis [9, 12]. Inflammatory processes can lead to tissue damage, which may interfere with the microbiome composition, triggering an uncontrolled activation of innate and adaptive immune system. These processes eventually culminate in physical symptoms, including increased frequency of bowel movements, mucus discharge, blood in the stool, severe diarrhea, abdominal pain and weight loss [10, 13].

UC is classified according to the extension of the disease (**Figure 3**), which leads to different symptoms. Proctitis is confined to the rectum and usually, UC begins with ulcerative proctitis. Left-sided colitis causes continuous inflammation throughout the left side of the colon. Ultimately, pancolitis is when the disease and inflammation occur throughout the entire colon [13].

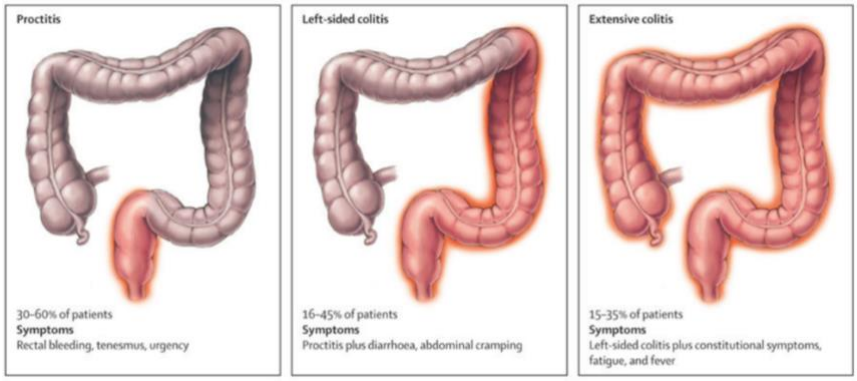

Figure 3| UC classification. UC is classified into different categories depending on the extension of the disease: Proctitis, Left-sided colitis and extensive colitis [13].

1.1.2. Inflammatory Bowel Disease-associated Colorectal Cancer

The risk of CRC development is the major concern in the clinical management of patients with chronic and severe inflammation in IBD. The risk for CAC development in UC and CD patients is of 18% and 8% after 30 years of disease onset, respectively [14, 15]. Although, CAC accounts in a small percentage of all CRC, it is responsible for 10-15% of annual deaths of IBD patients. Therefore, IBD patients (especially UC patients) undergo under a regular surveillance colonoscopy with biopsies to detect dysplasia and early cancer development, and very often undergo prophylactic colectomy [13, 16]. The European Crohn's and Colitis Organization (ECCO) created a guideline to stratify the risk of CAC development in IBD patients according to the extension and severity of the disease. Patients with extensive colitis and more than 8 years of

disease activity carry the highest risk of CAC, whereas left-sided colitis patients present an intermediate risk [17].

In CAC carcinogenesis the cancer stage arises from an inflammatory non-dysplastic mucosa that progresses to dysplasia and ultimately to invasive adenocarcinoma. Contrarily to sporadic CRC which develop from a polyp with an aberrant crypt, IBD dysplastic lesions are normally multiple and flat. The morphological criteria for dysplasia are based on a combination of cytological and architectural alterations of the crypt epithelium. Inflamed mucosa evolves into low-grade dysplasia (LGD), characterized by the nuclear hyperchromaticity, enlargement, and elongation, and then, progresses into high-grade dysplasia (HGD), characterized by an architectural aberration of the crypts, culminating in the development of carcinoma (**Figure 4)** [18, 19]. All of these histopathological changes are followed with molecular and cellular alterations, comprising genetic and epigenetic alterations, which are distinct from the sporadic form of CRC.

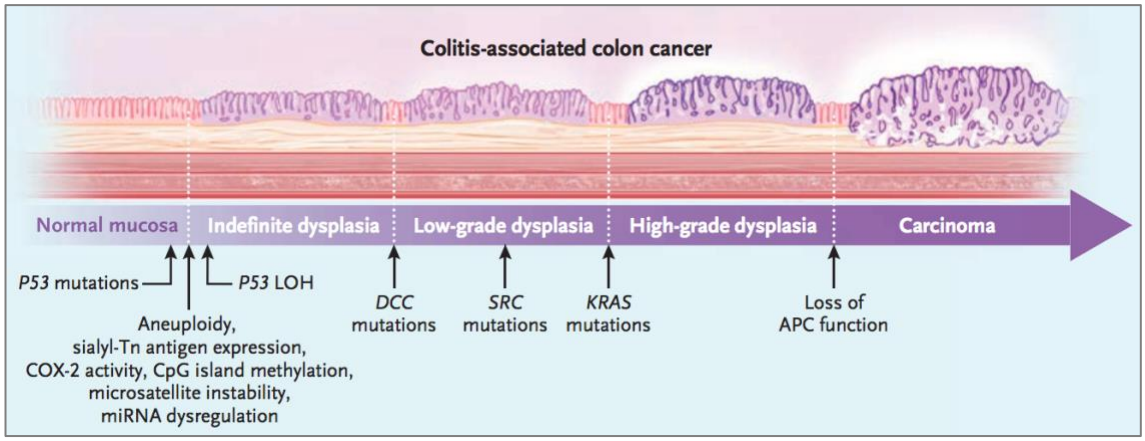

Figure 4| Histological and molecular steps of CAC development. Dysplastic lesions arise in the inflamed colonic mucosa and progresses through several grades of dysplasia, culminating in the development of carcinoma. Adapted from [19].

The underlying mechanisms that govern the transition from inflammation to cancer are still poorly understood. The development of CAC relies on the combination of genetic and epigenetic factors, as well as microbial and host influences mediated by IBD-associated inflammation [20]. The chronic inflammation can lead to tissue injury, resulting in excessive tissue regeneration and thereby, promoting the progression to carcinogenesis [21]. Immune cells present in the tumor microenvironment create an inflammatory environment, especially by the release of reactive oxygen species (ROS), which have the ability to cause genetic and epigenetic changes, as well as to sustain proliferation which ultimately induces the malignant process [7, 21, 22]. Another important factor in the development of CAC is the intestinal microbiota. Emerging evidence in this field suggest a crucial role of the gut microbiome on malignant transformation, either as a

direct trigger or as a consequence of the disease, contributing to the crosstalk between tumor and immune system [23, 24]. Abnormal communication between the altered gut microbiota (dysbiosis) and the immune system has been implicated in the etiopathogenesis of CAC [25, 26].

2. Immune system

2.1. Innate and adaptive immune cells

The immune system is a complex system of different cell types and soluble compounds conventionally known to protect us against pathogens and foreign substances, while simultaneously maintain tolerance towards self-antigens [27]. Based on antigen specificity and the timing of activation, immune cells are comprised in two distinct sections – innate and adaptive response. Innate immune cells are the first line of defense against microbes or injured cell products, including phagocytic cells (such as macrophages), natural killer (NK) cells and dendritic cells (DCs). In turn, adaptive response consists in later mechanisms and develops specific responses to infections by the expression of antigen-specific receptors, including T and B lymphocytes as major players [28, 29].

Macrophages are highly specialized phagocytes that can be either classified into M1 or M2 type, according to the produced cytokines. M1 macrophages, activated by microbial products and interferon gamma (IFN-γ), express high levels of pro-inflammatory cytokines (tumor necrosis factor alpha (TNF-α), interleukin (IL)-1, IL-6, IL-12 and IL-23) and are capable of ROS production. Paradoxically, M2 macrophages, activated by IL-4, IL-10 and IL-13, increase the expression of anti-inflammatory cytokines IL-10 and transforming growth factor β (TGF-β), and downregulate the expression of IL-12 and major histocompatibility complex (MHC) class II, crucial for the induction of immune responses [7, 30].

NK cells recognize potential target cells without the need for immunization or pre-activation compared with T lymphocytes, which first require instruction by antigen-presenting cells (APCs). The activation of NK cells depends upon the presence of cytokines such as IL-15, IL-12, and IL-18, promoting the release of the IFN-γ. They are rich in perforin and granzyme-containing granules, which are responsible for NK cell-mediated killing [31-33].

DCs, known as APCs, are crucial regulators of the inflammatory response by bridging innate and adaptive immunity. DCs are specialized in antigen recognition and uptake. Briefly, after the antigen uptake, DCs become activated and travel to the lymph nodes, where occurs antigen presentation to naïve T lymphocytes, via MHC, providing the required stimuli for T cell

activation. Likewise, DCs secrete different cytokines that incite T cell polarization into different effector T cells [34-36].

Lymphocytes have an important role in adaptive immunity and can be either B or T lymphocytes. B cells, bone marrow-derived lymphocytes, are responsible for the production of antibodies. T cells, thymus-derived lymphocytes, modulate cellular immunity regarding to their phenotype and function. T cells can be divided in different classes: T cell receptor (TCR)$\alpha\beta^+$ MHC class II-restricted $CD4^+$ T cells, subdivided in regulatory T cells (Treg cells), which suppress immune responses, and $CD4^+$ T helper cells (Th cells), which can range between Th1, Th2, Th9 and Th17; TCR$\alpha\beta^+$ MHC class I-restricted CD8$\alpha\beta^+$ lymphocytes, characterized by the cytotoxic granules; and a smaller subsets of T lymphocytes, the TCR $\gamma\delta^+$ T cells (γδ T cells). The phenotypes of different subsets of effector $CD4^+$ cells, Th1, Th2, Th9 and Th17, depend on the expression of specific transcription factors, such as T-box 21 (*TBX21*, known as Tbet), Gata-3, PU.1 or RAR-related orphan receptor gamma (Rorγ), respectively. Treg cells also depend on the expression of a specific transcription factor, the forkhead box P3 (Foxp3) [29, 37].

2.2. Chronic inflammation and tumorigenesis

In the gastrointestinal tract, intestinal epithelial cells (IECs) act as a physical barrier crucial for intestinal homeostasis, and play a major role in the regulation of the inflammatory response of the intestine, further orchestrating the network of interactions between the microbiota and the surrounding stromal and immune cells present in the sub-mucosa [24, 35]. Barrier dysfunction results in pathological interactions between the epithelium, microbiome and the immune system, leading to disruption of homeostasis, and consequently to pathological inflammation and, eventually, to tumorigenesis [9, 24].

The first evidence associating inflammation to cancer development was made by Rudolf Virchow in the 19th century [38]. However, this field has only emerged during the last decades, where the role of inflammation in tumorigenesis became more accepted. Several types of inflammation, such as autoimmunity and chronic inflammation, can preceded tumor development and can contribute to the oncogenic cascade, such as hepatitis and hepatocellular carcinoma or colitis and CRC [7]. Several studies from CAC patients and murine models of CAC showed that activated neutrophils, fibroblasts, DCs, macrophages and T cells contribute to tumor growth through the production of cytokines (**Figure 5**) [39].

Intestinal macrophages are key players in tissue development, regeneration and homeostasis, due to its plasticity and ability to change phenotype and function. In chronic inflammation, M1 macrophages are important players contributing to tumor initiation and

progression. In fact, ROS production can activate the NF-κB pathway, which in turns lead to secretion of TNF-α and other pro-inflammatory cytokines, promoting tumor proliferation and development, a pathway also well-established in CAC [40, 41].

In the gastrointestinal mucosa, T cells also play a central role in maintaining barrier function and controlling the delicate balance between immune activation and immune tolerance [37]. Over the past years, the role of T cells in inflammation has been of paramount importance to understand their influence in chronic inflammatory diseases and consequently, in the development of inflammation-associated cancers. However, whereas some pro-inflammatory cells can elicit tumor progression, others can suppress the carcinogenic process as part of the host antitumor immune response. Therefore, there is a dual role of T cells during inflammation-associated tumor development [42]. The central role of $CD4^+$ T cells in chronic inflammation, such as IBD, highlighted them as possible promotors of tumor development. Th2 cells are critical regulators of intestinal homeostasis, however, when dysregulated and hyperactivated may lead to serious consequences. In fact, UC is a modified Th2 disease, supported by the predominant expression of IL-13, IL-5, IL-6 and IL-4, suggesting that this subtype of Th cells play a role in tumor-promoting effect [42, 43]. Concerning Th1 immune cells, they are responsible for the secretion of cytokines, such as IFN-γ, TNF-α and IL-6. Similarly, Th1 response seems to promote tumor development at the transition point from IBD to CRC, by the release of TNF-α and IL-6, which culminates in the activation of NF-κB and STAT3 pathways, respectively [42]. Other inflammatory factors implicated in the pathogenesis of CAC are Th17 cells-released cytokines. Th17 cells release IL-17, IL-21 and IL-22, providing a pro-inflammatory environment and thus, contributing to the pathogenesis of immune-inflammatory diseases and tumor progress [44].

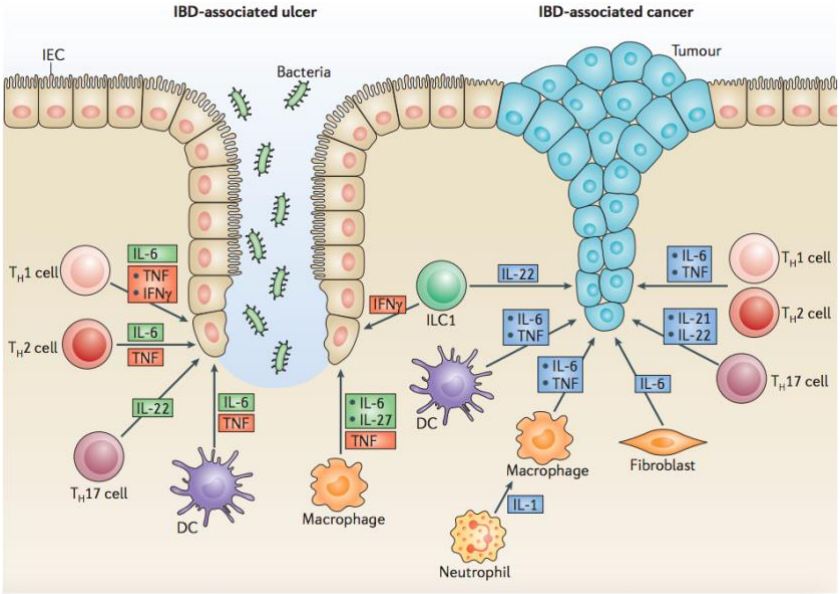

Figure 5| The crucial role of immune system and inflammatory cytokines on the battlefield: mucosal healing and CAC development [39].

2.3. Tumor microenvironment and cancer immunoediting

The tumor microenvironment is composed by different types of immune cells that include innate immune cells, such as macrophages, polymorphonuclear leukocytes, natural killer (NK) cells and dendritic cells (DCs), as well as adaptive immune cells, comprising T and B lymphocytes. These immune cells intercommunicate with each other and with the tumor cells by direct contact and by cytokines and chemokines production [28, 45].

Tumor-associated macrophages (TAMs) are important immune cells present in tumors. The role of macrophages in tumorigenesis has been controversial engaging in a dual relationship with cancer. However, most TAMs are considered to have properties of polarized M2 cells, promoting tumor growth by the secretion of cytokines, growth factors, inflammatory substrates and proteolytic enzymes that participate in critical carcinogenic processes, such as angiogenesis, invasion and metastasis. TAMs can also suppress T lymphocyte activation and proliferation [46-49].

Concerning NK cells, they are important in the recruitment of other immune cells, such as DCs, and thus, are key players in cancer immunosurveillance and antitumor immunity [50]. Although NK cells have been documented to infiltrate primary tumors and mediate a potent antitumor cytotoxicity, they typically comprise only a minor population, suggesting a mechanism of evading anti-tumor immunity by neoplastic cells [31].

DCs are also found throughout the tumor mass. Although the role of DCs in tumor microenvironment is still poorly recognized, the cross-presentation is well stablished to be necessary for inducing a cytotoxic $CD8^+$ T cell response [51].

Tumor-infiltrating lymphocytes (TILs) are a major component of the tumor microenvironment, where T cells are specific for tumor-associated antigens (TAAs). Cytotoxic $CD8^+$ T and $CD4^+$ Th1 cells are the principal weapons of immunity against cancer. The “helper” function of $CD4^+$ T cells improves the efficacy of cytotoxic $CD8^+$ T cells. $CD8^+$ T cells are proficient exterminators of malignant cells, through the release of cytokines, such as IFN-γ and TNF-α, the production of cytotoxic granules, containing perforin and granzymes, and by inducing tumor cell apoptosis [52]. Although accumulations of these effector T cells in the tumor might be considered as evidence of immune surveillance by the host, they can be ineffective in arresting tumor growth. In fact, Treg cells may contribute to the inhibition of the anti-tumor T cell responses. These cells accumulate in the tumor microenvironment and may impair the activation, survival and expansion of anti-tumor T cells through the production of TGF-β, IL-10 and the immune-inhibitory receptor cytotoxic T lymphocyte antigen 4 (CTLA-4) [53].

Overall, the tumor microenvironment is constantly an evolving entity that has a diverse cellular composition, with various pro-inflammatory and anti-inflammatory mediators that in combination determine how tumors will develop and respond to therapy.

The knowledge that immune cells in tumor microenvironment play a dual role in cancer progression, gave rise to the concept of cancer immunoediting (**Figure 6**). Cancer immunoediting is a dynamic process composed by three sequential phases: elimination, equilibrium, and escape. In the elimination phase, immune cells work together to detect and destroy cancer cells. However, if anti-tumor immunity is unable to completely eliminate the transformed cells, cancer cells undergo a clonal selection and may enter into the equilibrium phase. In this phase cancer cells edit its reporter of TAAs and re-shape tumor microenvironment to become immunosuppressive, then, entering in the escape phase, in which immune system are no longer able to recognize TAAs. Cancer cells can use different immune escape strategies such as the downregulation of MHC class I molecules to evade detection by cytotoxic $CD8^+$ T cells and/or an increased expression of ligands for the inhibitory receptors, such as the programmed death-ligand 1 (PD-L1) [54, 55].

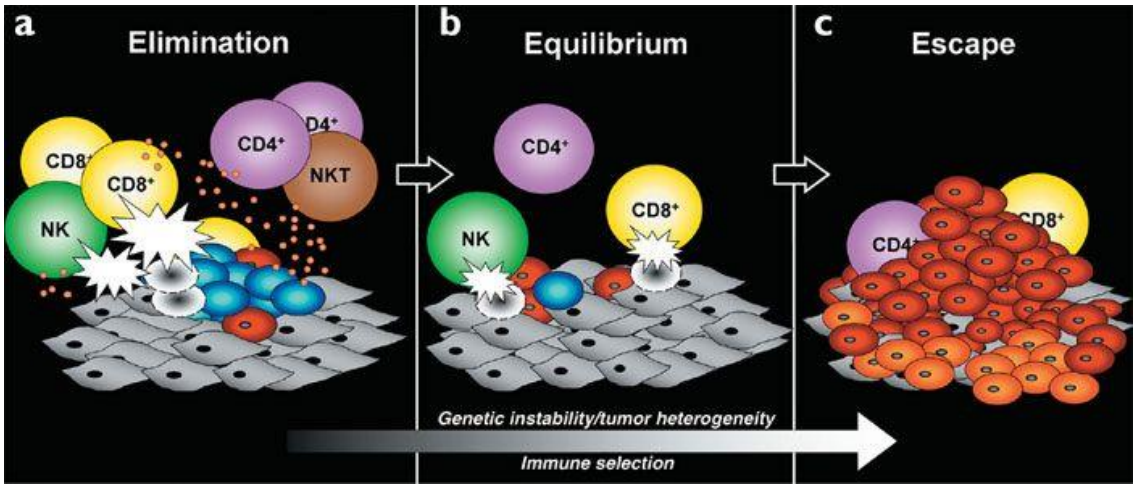

Figure 6| Cancer immunoediting. The three phases of cancer immunoediting hypothesis: elimination, equilibrium and finally the escape of cancer cells to the immune response [55].

3. Protein Glycosylation

The field of glycobiology had its first steps during the first half of the 20th century when it was elucidated the biochemistry and structure of simple and complex glycans. However, this area has only recently emerged as a crucial field of molecular and cellular biology, physiology and biomedicine [56, 57], highlighting its impact on both homeostatic and pathological conditions such as autoimmune diseases and cancer [58, 59]. Glycans play important roles in several biological processes, including cell-cell and cell-extracellular matrix (ECM) adhesion, receptor activation, molecular trafficking and clearance, endocytosis and signal transduction [60]. Glycans are ubiquitously expressed in essentially all cells in nature, being crucial to all living forms [56]. For instance, in mammalians, the glycome (biological repertoire of all glycan structures of an organism) appears to be higher than the proteome. All of these glycans contain a huge amount of important biological information that regulate fundamental cellular and molecular mechanisms in health and disease [60].

Glycosylation is one of the most abundant posttranslational modifications of proteins and lipids in a higher abundance than phosphorylation modifications. This process consists in the glycosidic linkage of carbohydrate structures to other saccharides, proteins or lipids through a complex enzymatic process producing different families of glycoconjugates (**Figure 7**) [58]. The glycosylation process is prominent in the lumen of the endoplasmic reticulum (ER) and in the Golgi apparatus [61]. The biosynthesis of these structures is determined by multiple factors, including the abundance and trafficking of glycoprotein substrates, as well as the levels of expression/activity of glycosyltransferase and glycosidase enzymes, crucial in this biological process [62].

It is estimated that 50% of all mammalian proteins are modified by glycans through the covalent attachment of sugar molecules, revealing the importance of this protein alteration [63]. Protein glycosylation encompasses two main types of glycans: *N*-glycans and *O*-glycans. *N*-glycosylation occurs through amide linkage to asparagine (Asn) residues in a consensus sequence Asn-X-Ser/Thr, where X represents any amino acid excluding proline. On the other hand, *O*-glycosylation occurs through the attachment of sugar residues to side chains of serine (Ser) or threonine (Thr) [64].

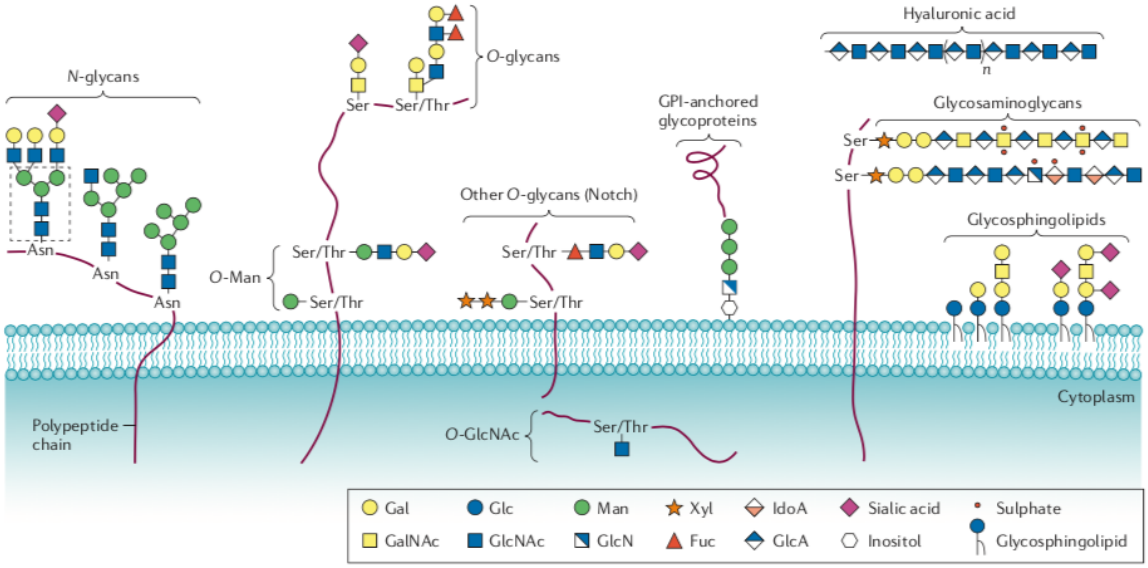

Figure 7| Common classes of glycoconjugates in mammalian cells. Glycans can be found in various macromolecules forming different families, such as the *N*-glycans, *O*-glycans, glycosaminoglycans, glycolipids (glycosphingolipids) and glycosylphosphatidylinositol (GPI)-linked proteins [58].

3.1. N-Glycosylation

In eukaryotic organisms, more than half of all proteins are glycoproteins and about 90% of them are expected to carry *N*-linked glycans, with an average of 1 to 9 *N*-linked glycans per polypeptide chain [65], reiterating the importance of *N*-glycosylation in eukaryotic biology.

N-glycans in eukaryotic cells share a common core structure: Mannose(Man)α1-3(Manα1-6)Manβ1-4N-Acetylglucosamine(GlcNAc)β1–4GlcNAcβ1–Asn-X-Ser/Thr being further modified in three major types: high-mannose, in which only Man residues lengthen the core; complex *N*-glycans, in which GlcNAc extend the core; and hybrid *N*-glycans, in which Man extends the Manα1-6 arm and one or two GlcNAcs extend the Manα1-3 arm (**Figure 8**) [66].

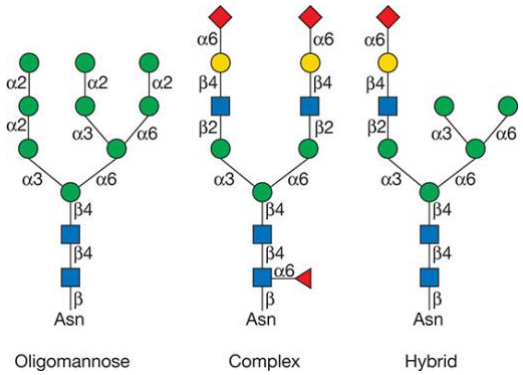

Figure 8| Types of N-glycans. *N*-Glycans at Asn-X-Ser/Thr sequons in eukaryote glycoproteins are of three general types: high-mannose or oligomannose, complex, and hybrid [66].

These structures are initially synthesized as a lipid-linked oligosaccharide (LLO) precursor in the ER membrane, resulting from the attachment of GlcNAc residue to the lipid

carrier dolichol phosphate (Dol-P). The glycan is built upon this residue followed by the addition of one GlcNAc and five Man residues. Then, the glycan is translocated to ER luminal membrane site, where is decorated with more four Man and three Glucose (Glc) residues. These initial steps are carried out by multiple asparagine-linked *N*-glycosylation (ALG) processing enzymes. Subsequently, the oligosaccharide assembled on Dol-P is transferred *en bloc* to the side-chain Asn residue of the glycoprotein by oligosaccharyltransferase (OST). Before leaving the ER, the glycoprotein suffers a trimming of two Glc residues which results in the formation of a $GlcMan_9GlcNAc_2$ structure (**Figure 9**) that acts as a ligand for the membrane-bound or soluble lectin chaperones, calnexin and calreticulin. These carbohydrate-binding proteins (known as lectins) bind to glycans and control protein folding, determining whether the newly made membrane and secreted proteins continue to the Golgi apparatus or targeted for ER-associated degradation (ERAD) pathway [62, 67-69].

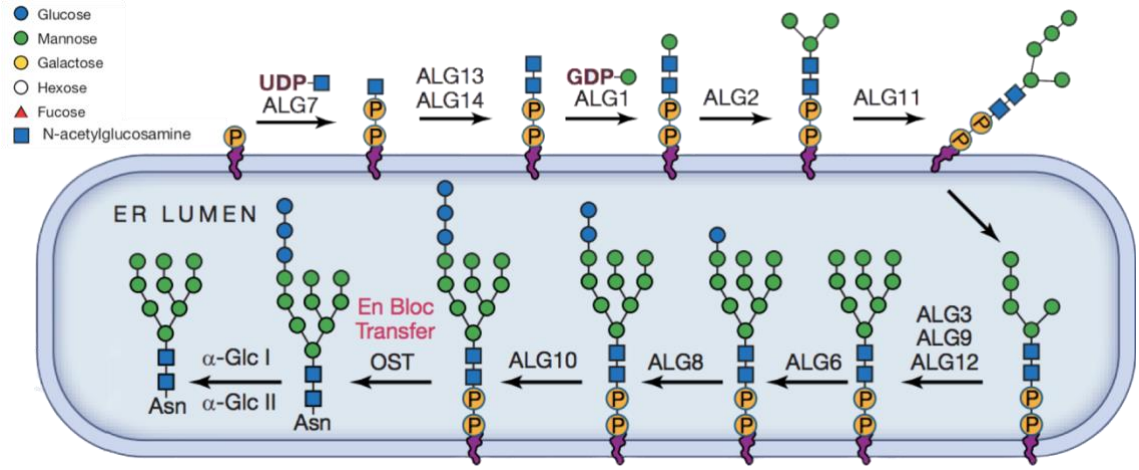

Figure 9| General process of *N*-linked glycan construction in the ER. Adapted from [70].

In the *cis*-Golgi, the glycosidases α1-2 mannosidase IA and IB (MAN1A1, MAN1B1) remove the Man residues from the glycoprotein giving rise to $Man_5GlcNAc_2$, a key intermediate in the pathway to hybrid and complex N-glycans. Biosynthesis of hybrid and complex *N*-glycans starts in the *medial*-Golgi by the action of *N*-acetylglucosaminyltransferase I (GnT-I, encoded by Mannosidase Acetylglucosaminyltransferase (*MGAT*)*1*), which adds a GlcNAc residue to the glycan structure [66]. Afterwards, *N*-glycans are trimmed by α-mannosidase II enzymes (MAN2A1, MAN2B1), which remove the terminal α1-3Man and α1-6Man residues, and a second GlcNAc residue is added by the action of *N*-acetylglucosaminyltransferase II (GnT-II, encoded by *MGAT2*). Additional branches can be initiated by the addition of β1-4GlcNAc branch to the Manα1-3 core by *N*-acetylglucosaminyltransferase IV (GnT-IV, encoded by *MGAT4*) and/or the addition of β1,6GlcNAc arm to the Manα1-6 by *N*-acetylglucosaminyltransferase V (GnT-V protein, encoded by *MGAT5*). Complex and hybrid structures may also carry a bisecting GlcNAc

residue that is added to the β-Man of the core by *N*-acetylglucosaminyltransferase III (*MGAT3* gene, GnT-III protein) (**Figure 10**) [66].

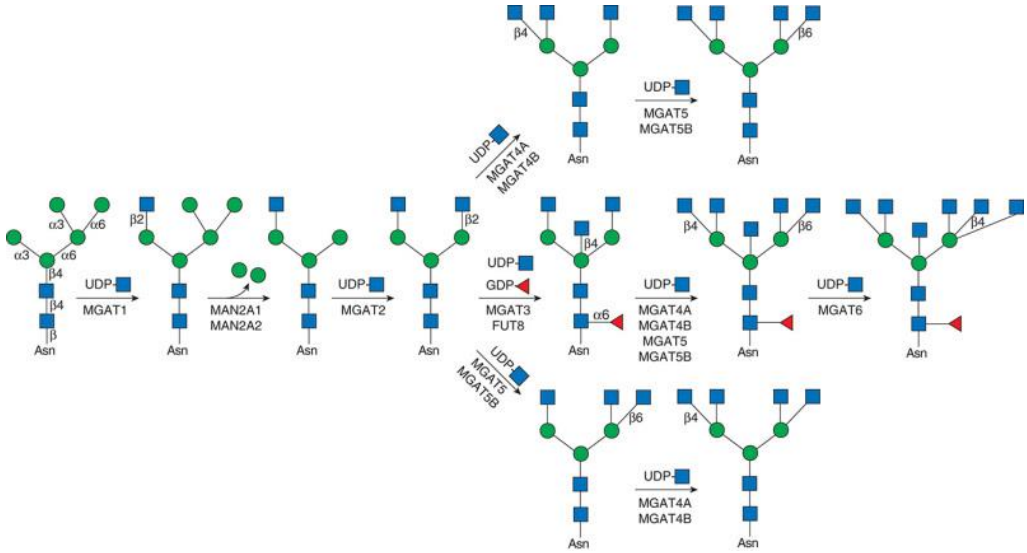

Figure 10| *N*-glycosylation pathway occurring in Golgi apparatus, which determines the branching and core modification of complex *N*-glycans [66].

The final step of glycosylation is the maturation, which occurs at the *trans*-Golgi. In this stage, hybrid and branched *N*-glycans can be extended with different carbohydrate structures, giving rise to higher glycan diversity. For instance, addition of α1-6 fucose (Fuc) to the Asn-linked GlcNAc is the major core modification in vertebrate *N*-glycans. Furthermore, the majority of glycans can be extended at GlcNAc branch with, for instance, poly-*N*-acetyllactosamine (poly-LacNac) and/or capped with Fuc, galactose (Gal), *N*-acetylgalactosamine (GalNAc), *N*-acetylneuraminic acid (Neu5Ac) and sialic acid in the elongated branches, which are important for lectins and antibodies binding [66].

4. Glycosylation patterns in pathological conditions

4.1. Role of glycans in cancer

Tumor cells display a wide range of alterations that result in an aberrant glycosylation profile. These aberrant glycosylation patterns play fundamental roles in all pathological steps of cancer development, such as cancer signaling, tumor cell-cell adhesion and cell-matrix interactions, cancer metabolism, angiogenesis, metastasis and tumor immune surveillance [58, 71]. Altered expression of glycans can be attributed to an altered conformation of the peptide backbone, a dysregulation of the glycosyltransferase's transcription levels or their mislocalization, dysregulation of the chaperon genes and/or altered abundance of the sugar nucleotide donor and cofactors [58].

Changes in glycosylation is a hallmark of cancer being often observed in cancer cells. The most widely-occurred glycosylation alterations include incomplete glycosylation synthesis leading to the expression of truncated *O*-glycan structures (such as Tn or Sialyl Tn), aberrant overexpression of complex branched *N*-glycans, abnormal core fucosylation and increased terminal extension of the sialylated glycans, such as sialyl Lewis X (SLe^x) and A (SLe^a) (**Figure 11**). Additionally, changes in the expression of carbohydrate receptors (such as the glycan binding proteins: galectins, C-type lectin receptors (CLRs) and sialic acid-binding immunoglobulin-like lectins (siglecs)) has also been observed in cancer [58].

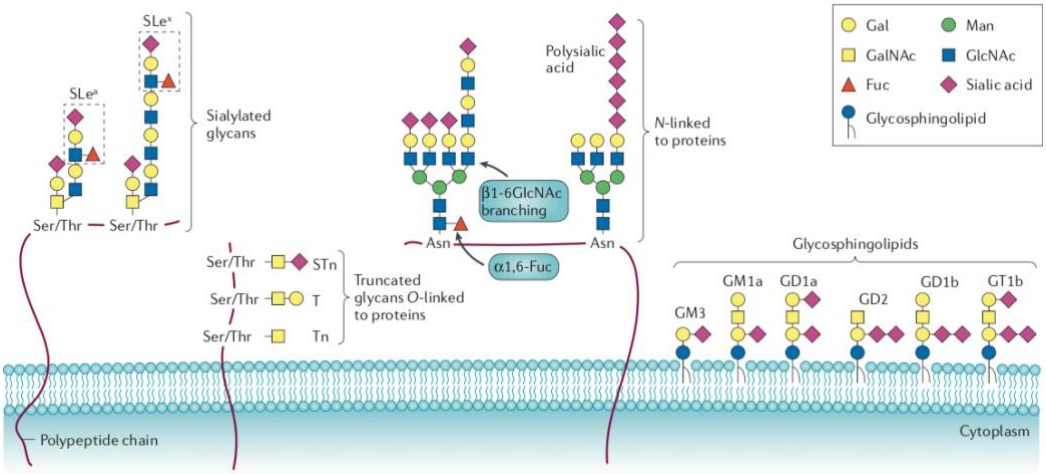

Figure 11| Altered tumor-associated glycans. The most widely-occurred glycosylation alterations include increased terminal extension of sialylated glycans, truncated *O*-glycans and aberrant complex *N*-glycans [58].

Concerning *N*-glycosylation, the overexpression of complex β1-6-GlcNAc *N*-linked glycans are one of the most well-characterized cancer-associated glycosignatures, being correlated with cancer malignancy and poor prognosis [72]. The increased expression of these structures is due to upregulation of the GnT-V enzyme, encoded by the *MGAT5* gene. *MGAT5* expression is regulated by the RAS-RAF-MAPK signaling pathway that is frequently up-regulated in cancer. Indeed, *MGAT5*-deficient mice showed significant decreased tumor growth and metastasis [73, 74].

In fact, branched *N*-glycans have been implicated in the modulation of cell-cell adhesion in cancer, affecting an important adhesion molecule, namely E-cadherin. The overexpression of GnT-V in this membrane glycoprotein leads to its mislocalization into the cytoplasm, resulting in a downregulation of adherent-junctions, which in turns contribute to an increase in tumor motility and invasiveness [75]. In contrast, the GnT-III, an enzyme encoded by the *MGAT3* gene, which catalyzes the addition of bisecting GlcNAc *N*-glycans, counteracts GnT-V activity, having a significant role in suppression of cancer metastasis. Accordingly, the presence of this enzyme stabilizes E-cadherin at the cell membrane contributing to its proper adhesive functions and consequently to the suppression of tumor progression and metastasis [76, 77]. In fact, many studies suggest that there is an enzymatic competition in cancer between GnT-III and GnT-V that dictates the course of tumor progression [78, 79].

Other *N*-glycan signature associated with cancer is the core fucosylation, which consists in the addition of α1,6-fucose to the core structure through the action of fucosyltransferase VIII (Fuc-VIII, encoded by *FUT8* gene). In fact, overexpression Fuc-VIII has been associated with tumor cell growth and malignancy in several cancer such as lung cancer and breast cancer [58, 80].

The overall increased sialylation is also an important cancer-associated alteration. Particularly, an increase in α2,6-linked sialylation was pinpointed as a predictive marker of poor prognosis in colon cancer [81]. In *N*-glycans, expression of polysialic acid is also often present in high-grade tumors [58].

4.2. Role of glycans in immune responses

Glycoimmunology is a promising area in health and life sciences. Alterations in protein glycosylation both at the cell surface and on secreted glycoproteins can positively and negatively regulate the immune responses interfering in the modulation of tumor microenvironment and immunogenicity [82]. Such regulation results from the complex interplay between glycoproteins and glycan-binding proteins – such as galectins, CLRs and siglecs [83]. All these lectins contain

one or more carbohydrate-recognition domain (CRD), responsible for the interaction with specific glycan structures or sugar residues [84].

Galectins are a family of animal lectins, highly conserved, with affinity for *N*-acetyllactosamine (Galβ1-3GlcNAc or Galβ1-4GlcNAc) of *O*- and *N*-linked glycoproteins. These carbohydrate-binding proteins can modulate processes that include mitosis, apoptosis, cell-cycle progression, as well as mediate cell–cell and cell–extracellular matrix adhesion. In immune system, galectins are highly expressed in activated T and B lymphocytes, Treg cells, macrophages and DCs [85]. Interestingly, the expression of galectins in tumor cells is altered compared with their normal counterparts, and these altered expression correlates with the aggressiveness of the tumor cells. In fact, galectin-1 and galectin-3 have been associated with the initiation of the transformed phenotype of tumors [84, 85]. Galectin-1 functions as an immunosuppressant by selectively modulate T cell and DCs responses, by skewing the balance between anti- and pro-inflammatory environment, through the promotion of apoptosis of Th1 and Th17 cells, induction of IL-10-producing Treg cells and activation of IL-27-producing DCs [86, 87]. Galectin-3 is also involved in tumor growth, metastasis and immune suppression. This lectin produced by tumor cells bind to TCR-complex *N*-glycans and reduce $CD4^+$ T cell activation [88]. Additionally, galectin 3 can also interact with complex branched glycans present on CTLA-4, a checkpoint inhibitor, preventing its endocytosis [89].

CLRs are calcium-dependent carbohydrate binding proteins and include a large family of receptors that are divided into 17 subgroups. These molecules were originally named for their ability to bind carbohydrates in a Ca^{2+}-dependent manner through conserved amino acid residues. C-type lectins containing EPN (Glu–Pro–Asn) amino acid motif have specificity for mannose-type carbohydrates, such as DC-specific intercellular adhesion molecule-3-grabbing non-integrin (DC-SIGN) and mannose receptor (MR). On the other hand, lectins that contain QPD (Gln–Pro–Asp) motifs recognize specifically galactose-type or GalNAc-type carbohydrates, such as macrophage galactose lectin (MGL) and DC-asialoglycoprotein receptor (DC-ASGPR) [84, 90, 91]. C-type lectins can be found as transmembrane proteins or as secreted molecules, and have been implicated in tumor invasion, metastasis and immune suppression. For instance, in cytotoxic NK cells these lectins facilitate the recognition of the cancer cells via MHC class I, which trigger inhibitory signaling pathways [90]. However, recognition of tumor-associated glycans, by C-type lectins including macrophage-inducible C-type lectin (mincle), MGL and DC-SIGN can suppress antitumor immune responses. In fact, truncated *O*-glycans (such Tn structures) in mucin (MUC)-1 interacts with MGL and instructs DCs to suppress the protective antitumor responses [92].

Siglecs are well known glycan-binding proteins for their specificity for sialic acid-containing glycans, either in *O*- or *N*-glycans. Siglecs can affect regulatory mechanisms that control immune responses. Classically, siglecs negatively regulate cell signaling through the presence of immune receptor tyrosine-based inhibitory motifs (ITIMs). Siglec-1 is preferentially expressed on macrophages; siglec-2 is mainly expressed on B cells; siglec-8 on eosinophils and siglec-9 are expressed on myeloid-derived DCs, while siglec-5 on plasmocytic DCs [84]. Over the years, several evidences showed that siglecs are implicated in immune evasion and cancer progression [93]. In fact, siglec-9 can bind to MUC-1 promoting the release of factors associated with tumor progression [94].

The effects of the overexpression of complex branched *N*-glycans by the tumor cells on the modulation of the immune response in the tumor microenvironment is a relatively unexplored field. Nonetheless, it was showed that decreased *MGAT5* gene was associated with activate $CD4^+$ T cells and suppression of breast cancer progression [95]. Concerning the impact of glycans in the immunosuppressive phenotype found in tumors, a recent study showed that IL-10 upregulates *MGAT5* expression on $CD8^+$ T cells, and this was associated with an increase of antigen threshold required for T cell activation [96].

In the context of IBD, several reports have been demonstrating the importance of these branched carbohydrate structures on the regulation of the immune system. Demetriou et al., showed that a deficiency in GnT-V enzyme decreases the threshold for T cell activation by directly enhancing TCR clustering and consequently hyperactivating T cell immune response [97]. Accordingly, in IBD, our group, has shown that active UC patients exhibit a decrease of these structures on $CD4^+$ colonic T cells associated with an hyperimmune response [98]. Furthermore, the lack of complex branched *N*-glycans was recovered with the metabolic supplementation of GlcNAc and associated with a controlled T cell mediated immune response [99]. Importantly from the clinical point of view, the levels of expression of branched N-glycans were considered a potential clinical biomarker able to predict therapy response in UC patients [100]. In IBD context, macrophages also seem to play a role in UC pathogenesis. Contrarily to T cell-mediated immune response, it has been reported that upregulation of *MGAT5* gene exhibited higher susceptibility to experimental colitis and consequently aggravates CAC development, which was abolished in conditions of macrophage depletion, suggesting that complex branched *N*-glycans may have different roles in different immune cells [101].

Overall, this compelling body of evidences demonstrate the crucial role of the complex branched *N*-glycans as key orchestrators of the immune response as well as essential regulators of the process of cancer development and progression. In fact, evidences from our group showed that in inflammatory conditions, such as IBD, complex glycans are downregulated in T

cells leading to an hyperimmune response and high disease severity. On the other hand, complex branched *N*-glycans are overexpressed in cancer epithelial cells, which is associated with tumor progression. However, what remain unknown is the impact of these branched glycan structures along the course of CAC carcinogenesis.

AIM

The main goal of this thesis project is to explore whether a differential expression of glycans in colitis and cancer mediated by *MGAT5* glycogene constitutes a new mechanism that tips the balance between intestinal inflammation and cancer development. In order to clarify how glycans modulate inflammation-promoting cancer and tumor progression we aimed to:

1. Characterize the glycosignature of both epithelial and immune compartment *in situ* during CAC carcinogenesis, using a subset of human clinical samples;

2. Assess the impact of changes in glycosylation of T cells during CAC progression, using human fresh colonic biopsies from patients that have evolved in the carcinogenesis cascade;

3. Explore the mechanistic impact of complex branched *N*-glycans in colitis-associated colorectal cancer development, using a CAC mouse model in two different glycoengineered animals (WT and *MGAT5*$^{-/-}$ mice).

MATERIALS AND METHODS

Patients' Cohort and colonic biopsies collection

The study includes 7 patients from the Gastroenterology Department of Centro Hospitalar do Porto-Hospital de Santo António (CHP/HSA), Porto, Portugal, that were diagnosed with IBD and prograde in the carcinogenic cascade. Four of these patients only prograde until LGD, two prograde to HGD, and one develop CRC. All the 7 patients were studied by analyzing the formalin-fixed paraffin-embedded (FFPE) samples at different stages of disease course (evaluated in the department of pathology in the CHP/HSA). From these 7 patients we have analyzed 41 FFPE biopsies that were classified into colitis, LGD, HGD and CRC. For each patient we selected the FFPE from the dysplastic/neoplastic region (LGD or HGD) and from the adjacent and distant region of the lesion (adjacent colitis or distant colitis). Some FFPE that we had some douts in the classification were evaluated by the pathologist Dra. Joana Alves in the CHP/HSA. The age and gender were not exclusion factors in this cohort.

Moreover, 13 FFPE samples of colitis patients were selected and subdivided according to the risk of CAC development (based on the ECCO guideline [17]). **Colitis patients** are classified according to the endoscopic activity from Mayo 1 to 3. **Low risk** of CAC development includes patients with more than 8 years of diagnosis with low endoscopic activity (Mayo 1). **Intermediate risk** includes patients with more than 8 years of diagnosis of extensive colitis (Mayo 2 and 3). **High risk** patients include more than 8 years of diagnosis with pancolitis. Additionally, 5 FFPE samples of healthy controls were selected.

From these cohort we also collected fresh colonic biopsies (n=2 patients) to isolate the T lymphocytes to further analyze by flow cytometry or gene expression profile. The fresh biopsies were collected in the CHP/HSA from colonic lesion, adjacent mucosa and distant mucosa from the lesion (whenever possible). Fresh biopsies were also collected from healthy controls (n=2) and from UC patient (n=1). All the fresh biopsies were subjected to histological examination and classification by the department of pathology in the CHP/HSA, and all the patients signed informed consent about this research.

Isolation of $CD3^+$ T Cells from Fresh Human Colonic Biopsies and Blood: *Ex Vivo* Culture of T Cells

Fresh colonic biopsies and peripherial blood were collected from patients of our cohort, IBD patients and healthy individuals.

The fresh biopsies of our cohort were representative of different colonic regions: dysplastic lesion, adjacent mucosa and distant/normal mucosa to the dysplastic region. The tissue was immediately conserved on ice in *Hank's Balanced Salt Solution* (HBSS) (Sigma, MI,

USA) medium with 1% penicillin streptomycin (P/S) 10,000 µg/mL (Gibco, Paisley, UK) and 0,1% Gentamicin 50 mg/mL (Gibco, Paisley, UK). Biopsies were subjected to a mechanic digestion by gently tightened the tissue with tweezers in the HBSS medium. The medium with the released cells were filtered by a 70 µm Cell strainer (Corning, New York, USA) and centrifuged for 10 min at 300g, FACS buffer (phosphate-buffered saline (PBS, pH=7,4) containing fecal bovine serum (FBS) 2%) with 1 mM Ethylenediamine tetraacetic acid (EDTA) was added and the cells were centrifuged to proceed for the $CD3^+$ T cells isolation [99].

Isolation of peripheral blood mononuclear cells (PBMCs) was performed by a density-gradient centrifugation, which allows the sample separation according to their densities (**Figure 12)**. The blood was added carefully upon the LymphoPrep™ solution (Stemcell™ Technologies, Oslo, Norway), preventing them from mixing, with a ratio of 2:1, and then, the samples were centrifuged at 800g for 30 minutes at room temperature (RT) with no brake and no acceleration. PBMCs interface were collected, and the cells were washed several times with PBS and centrifuged at 300g for 10 min.

$CD3^+$ T cells were isolated from both biopsies and PBMCs using the EasySep™ Human T Cell Isolation Kit (Stemcell™ Technologies, Vancouver, Canada), that negatively selects the $CD3^+$ T cells. Isolation cocktail (50 µL/mL per sample) was added and incubated for 5 min at RT and then it was added the RapidSpheres™ (40 µL/mL per sample). Finally, the tube was placed into the magnet for 5 min and the isolated cells were collected. The T cells enrichment results from the use of several antibodies that recognize different molecules at the leukocyte cell surface in order to deplete them from the mononuclear cell population through the use of dextran-coated magnetic particles.

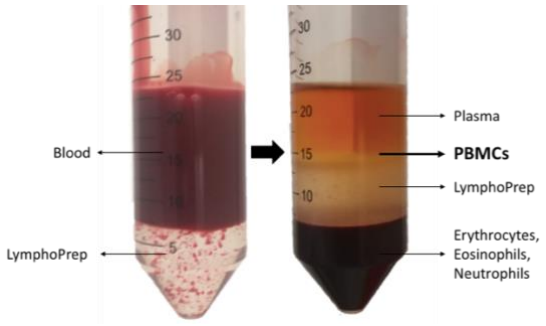

Figure 12| The separation of the different layers occurs after density gradient centrifugation, represented on the right, showing the mononuclear cell layer which was recovered by aspiration.

Animals and experimental procedure

CAC development was explored using a chemical induced mouse model. The model consists in the repeated dextran sulfate sodium (DSS) administration combined with the treatment with the genotoxic agent azoxymethane (AOM) [102]. This model was induced in both males and females C57BL/6 mice, in *Mgat5* wildtype (WT) (n=34) and knockout (KO) mice (*Mgat5*$^{-/-}$) (n=34) (mouse model established and provided by Prof. Michael Pierce, CCRC, Georgia University, Athens, USA). In AOM/DSS group, WT mice (n=18) and *Mgat5*$^{-/-}$ mice (n=17) were injected with 8 mg/kg AOM (Sigma, MI, USA) intraperitoneally. The other group (only with DSS) received an intraperitoneal injection with 0.9% sodium chloride (NaCl). One week later, all the groups received 2% DSS (MP Biomedicals) in their drinking water for 7 days, followed by 2 weeks of recovery. Mice received other 2 cycles of 1.5% DSS for 5 days intercalated with 2 weeks of recovery [103]. The clinical scores (stool consistency, rectal blood and body weight loss) were evaluated in the animals 3-5 times a week and the disease activity index (DAI) was calculated by the mean of the parameters abovementioned [104]. After each DSS cycle the mice were evaluated by colonoscopy (using the Mainz Coloview System with the assistance of Dra. Sofia Lamas, DVM) and the animals were sacrificed after each cycle to follow the disease progression. After the third cycle animals were monitored by colonoscopy in order to see the tumor development and were sacrificed at day 99. Schematic diagram for the model is represented in the **figure 13**.

All procedures involving animals were conducted in conformity with i3S guidelines in compliance with national and international laws and policies on the protection of animals used for scientific purposes (Directive 2010/63/EU, Guide for the Care and Use of Laboratory Animal. 8º edition, 2011).

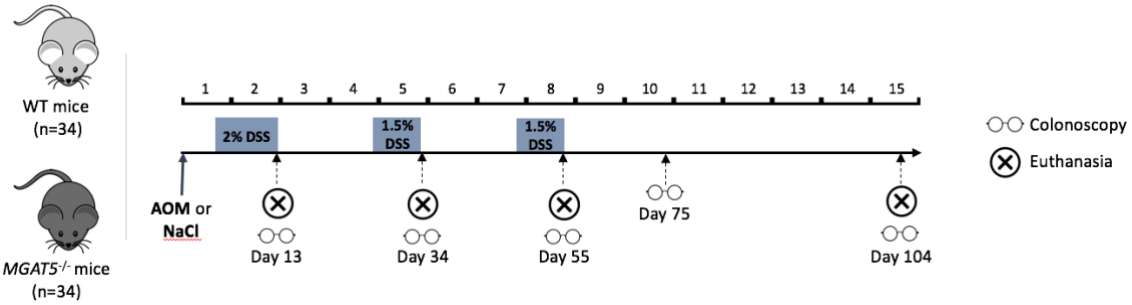

Figure 13 | Experimental procedure of the AOM/DSS group (injection with AOM chemical agent) and the DSS control group (injection with NaCl 0.9%) along the 15 weeks.

Sample Preparation

Mice were sacrificed by inhalation of terminal anesthesia doses of isoflurane and tissue were collected. Upon opening the colon, the entire luminal surface was observed, and the lesion size was measured in the last time point. A small portion of the distal and proximal colon was bisected to *ex vivo* culture the tissue to analyze the cytokine production. Distal colon from AOM/DSS group and DSS group was bisected longitudinally in three equal portions. One portion was stored in *RNAlater* stabilization solution (sigma, MI, USA) for further RNA analysis (not explored in this thesis) and other for flow cytometry analysis (collected for *Roswell Park Memorial Institute* (RPMI) medium (Gibco, Paisley, UK)). Spleen, cecum and the other portion of the colon were fixed in 4% formaldehyde (Enzymatic) for further paraffin embedding and processing by the histology service at i3S, Porto.

Tissue digestion and isolation of the mice mononuclear cells

In both *in vivo* groups (AOM/DSS and DSS groups), mouse mononuclear cells were collected from the mice colon samples to understand the immune and glyco-profile in the different groups and different genetic models.

An optimization procedure was needed during the time course of euthanasia. In the first time point, tissue was digested with 1 mM dithiothreitol (DTT) (Sigma, MI, USA) solution in HBSS medium (with 1% P/S and 0.1% Gentamicin) twice during 10 min in agitation to desaturate the proteins of the colon mucosa. Then, the tissue was washed with HBSS medium containing 0.5 mM EDTA and 25 mM hydroxyethyl piperazineethanesulfonic acid (HEPES) buffer, for 3 times during 20 min and mechanical digestion was performed using the gentleMACs dissociator machine (Miltenyi Biotec). Cells were centrifuged and filtered to follow for flow cytometry. In the initial time point, we verified that this procedure compromised the cell viability and a different protocol was stablished for the following time points. Tissue was digested using the gentleMACs dissociator with 0.9 mg/ml Collagenase IV (stock ≥ 125 U/mg) (Sigma, MI, USA) in RPMI medium with the enzyme cofactors (1 mM $CaCl_2$ and 1 mM $MgCl_2$), followed by incubation for 45 min at 37 ºC in agitation. Colon samples were mechanical digested again with the tissue dissociator and centrifuged for 10 min at 4 ºC 300g. The cells were washed with FACS buffer and filtered. After centrifugation, cells were added carefully upon the LymphoPrep™ solution with a ratio of 2:1, and then, the samples were centrifuged at 800g for 30 min at RT with no brake and no acceleration. Finally, the mononuclear cell layer was collected, and cells were centrifuged to follow for flow cytometry staining. On the last time point, epithelial cells, deposited on the bottom, were also collect and analyzed.

Histopathological analysis

FFPE samples from our cohort, as well as the mice colon samples, were sliced with 4 µm of thickness using a paraffin microtome (Microm HM335E) and adherent to silane coated microscope slides APTACA®.

Hematoxylin and eosin staining was performed to evaluate histologically the FFPE samples from human and mice. Hematoxylin stains nucleic acids in blue-purple, while the eosin stains in pink the non-specific proteins in the cytoplasm.

Sections were deparaphined in xylene (twice for 10 min), dehydrated with a decreasing concentration of ethanol (100%-70%, for 5 min each) and washed with water for 10 min. Samples were embedded 4-7 times in hematoxylin (Richard-Allan Scientific™ Modified Mayer's Hematoxylin, Thermo Scientific, DE, USA), washed with water for 5 min, and embedded in ammoniacal water 1% for 1 min to differentiate the nuclei. The slides were washed again for 5 min in water and 1 min in ethanol 95% and then embedded in eosin (Eosin-Y, Thermo Scientific, DE, USA) for 2 min. Finally, the samples were intensively washed with ethanol 95%, diaphanized with xylol and mounted with Entellan rapid mounting medium (Merk, Darmstadt, Germany).

Histological evaluation of the mice samples were performed by the pathologist Dra. Joana Alves in the CHP/HSA.

Lectin histochemistry and Immunohistochemistry

Histochemistry is a common microscopy-based technique that uses specific antibodies or ligants that labeled an antigen target in cells of a tissue section.

The staining of glycans was performed by the modified avidin-biotin-peroxidase complex (ABC) method [105]. Colon biopsies sections were deparaphined in xylene, dehydrated with a gradual decreasing concentration of ethanol (100%-70%) and washed with water. Sections were then treated with hydrogen peroxide 3% in methanol for 10 min to block the endogenous peroxidase activity. After washing the slides in PBS, sections were incubated with bovine serum albumin (BSA) 10% diluted in PBS in a humid chamber for 20 min at RT. Biotinylated lectins diluted in PBS were added to the slides at RT in a humid chamber: *Phaseolus vulgaris Leucoagglutinin* (L-PHA) lectin, that specifically recognizes the β1,6-GlcNAc branched *N*-glycan structures (1:150, 1h, ZA1219A, Vector Laboratories, Burlingame, USA) and *Galanthus nivalis* (GNA) lectin, that specifically recognizes terminal α1-3-linked mannose (1:150, 1h, ZD0417, Vector Laboratories, Burlingame, USA) (**Figure 14**). Sections were then washed with PBS and incubated with ABC solution (Vectastain® ABC Kit, Vector Laboratories, Burlingame, USA) for 30 min at RT, 1:100 in PBS. After washing with PBS, sections were stained for 5-8 min with

0.05% 3,3 diaminobenzidine tetrahydrochloride (DAB). Finally, sections were counterstained with hematoxylin, washed with water, dehydrated with a gradual increasing concentration of ethanol (70%-100%) and xylol, and mounted. Negative controls were performed using PBS instead of lection solution.

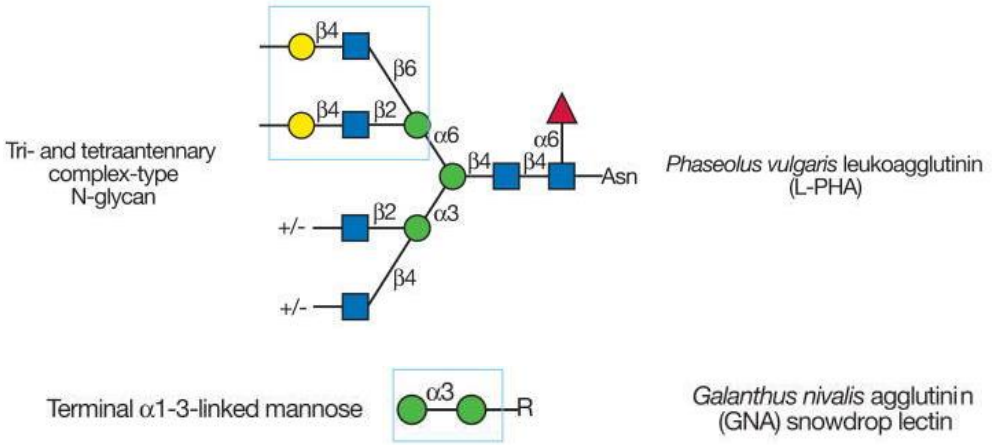

Figure 14| Complex structure β1,6-GlcNAc branched is recognized by L-PHA, and terminal α1-3 linked mannose is recognized by GNA.

Immunohistochemistry for $CD3^+$ T cells was performed by using the horseradish peroxidase (HRP) polymer detection kit (UltraVision™ Quanto Detection System HRP, Thermo Scientific, DE, USA) according to the manufacter's recommended protocol. Colon biopsies sections were deparaphined, dehydrated and washed. Heat-induced antigen retrieval was done with citrate buffer (10 mM citric acid, pH=6) for 45 minutes in a steam cooker (Ufesa), left to cool for 10 minutes at RT and washed with PBS. Incubation with the rabbit IgG anti-human CD3 monoclonal primary antibody (clone EP449E, Thermo Scientific, DE, USA) diluted at 1:300 in BSA 5% was performed overnight (O.N) at 4ºC. The recommended protocol was performed and slides were stained for 5-8 min with DAB. Finally, sections were washed, counterstained with hematoxylin, washed again, dehydrated and mounted. Positive controls were included, namely sections of IBD patients, which previously showed to display prominent expression of CD3.

RNA extraction

Three to five slices from FFPE biopsies samples of the patient cohort with 10 µm of thickness were cut using a paraffin microtome (Microm HM335E) and total RNA was extracted using the Recover All™ Total Nucleic Acid Isolation Kit (Invitrogen, CA, USA) according to the manufacture's recommended protocol. Samples were deparaphined with 100% xylene during 5 min at 50 ºC, centrifuge for 2 min at maximum velocity and washed twice with 100% ethanol. The pellet was then left to dry at RT for approximately 2 hours. Digestion buffer with protease

from the kit was added and incubated at 50 ºC for 15 min and posteriorly at 80 ºC for 15 min. The lysate was then transferred to a column with a filter cartridge (that retains the RNA) after the addition of an isolation additive solution with 100% ethanol for the nucleic acid isolation. The filter was extensively washed with Wash 1 and Wash 2/3 solutions from the kit, using centrifugations of 30 sec at 10 000 rpm. To remove genomic DNA (gDNA) DNase mix from the kit was added for 30 min at RT and washed again with Wash 1 and twice with Wash 2/3 solutions. To recover the RNA, elution solution was added to the filter.

For the fresh biopsies, RNA was extracted using the RNAqueous®-Micro Kit RNA Isolation (AM1931, Invitrogen, CA, USA), according to the manufacture's recommended protocol. T cells from the colon biopsies was stored in RNA later reagent to stabilize the cellular RNA during the period of storage. Cells were centrifuged and the pellet was resuspended in the lysis solution from the kit. After a period of vortex, 100% ethanol was added, and the mix was transferred to a micro filter cartridge. The samples were centrifuged, washed with Wash 1 solution and twice with Wash 2/3 solution. Finally, to recover the RNA elution buffer was added to the filter.

RNA concentration was measured using a Nanodrop 1000 UV-Vis Spectrophotometer system (Thermo Scientific, DE, USA) and stored at -80 ºC.

Real-time qPCR

Quantitative real-time polymerase chain reaction (RT-qPCR) is a commonly used assay to determine the expression profile of a specific gene of interest.

Total RNA from FFPE samples or T lymphocytes from colon biopsies samples was transcribed into complementary DNA (cDNA). RNA from FFPE samples and biopsies samples was transcribed to cDNA using the SuperScript™ IV Reverse Transcriptase (Invitrogen, CA, USA), using 300 ng and 100 ng of RNA, respectively. RNA was diluted in nuclease free H_2O, and random primers (0,1 µg/uL) and deoxynucleotides (dNTPs, 1 mM) were added. In the T100™ Thermo Cycler (Bio-Rad Laboratories, CA, USA), the samples were heated at 65 ºC for 5 min, followed by 1 min in 4 ºC. The reactional mix (with the buffer solution, RNase OUT enzyme (40 units/µL), DTT reagent and reverse transcriptase IV enzyme (150 units)) was added and the samples were subjected to PCR on the T100™ Thermo Cycler (23 ºC x 10 min, 52 ºC x 10 min, 80 ºC x 10 min, 4 ºC x ∞; Bio-Rad Laboratories, CA, USA).

To perform the RT-qPCR, cDNA is amplified using gene-specific probes combined with a fluorescent reporter molecule that enable the quantification of the PCR product in real time.

The RT-qPCR was performed in a MicroAmp™ Fast Optical 96-Well Reaction Plate and the cDNA was amplified using the probes represented in the **table 1** to quantify the *MGAT5*,

MAN2A1, *ST6Gal1, PDCD1, IFNγ, TBS21, Foxp3, RORC, CD3E* and *18S*. Quantification was acquired with 7500 Software v2.3 following the run method: holding stage: 50 ºC x 20 sec and 95 ºC x 10 min, cycling amplification: 95 ºC x 15 sec and 60 ºC x 1 min during 45 cycles. The mRNA expression of the genes of interest was normalized using the housekeeping gene *18S* or the *CD3E* mRNA levels (ΔCt). RQ values were calculated by the $2^{-\Delta CT}$ method.

Table 1 | Probes used in RT-qPCR for the amplification of genes of interest.

GENE	DESCRIPTION	PROBE	SUPPLIER
MGAT5	α-1,6-Mannosylglycoprotein 6-β *N*-Acetylglucosaminyltransferase	Hs00159136_m1	TaqMan™
MAN2A1	Mannosidase α class 2A member 1	Hs01123597_m1	TaqMan™
ST6Gal1	ST6β-galactoside α-2,6-sialyltransferase 1	Hs00949382_m1	TaqMan™
PDCD1	Programmed Cell Death 1	Hs01550088_m1	TaqMan™
IFNγ	Interferon gamma	Hs00989291_m1	TaqMan™
TBX21	T-box transcription factor	Hs00203436_m1	TaqMan™
Foxp3	Forkhead box P3	Hs01085834_m1	TaqMan™
RORC	RAR Related Orphan Receptor C	Hs00172858_m1	TaqMan™
CD3E	T-cell surface glycoprotein CD3 epsilon chain	Hs01062241_m1	TaqMan™
18S	18S ribosomal RNA	Custom_Human (custom by P.Oliveira)	Integrated DNA Technologies (IDT)

Flow Cytometry: human T cells and mice mononuclear and epithelial cells

Fluorescent-activated cell sorting (FACS) is a fluorescent-based method that allows the quantification of lived cells according to the different chemical and physical properties. This technique enables the use of different fluorochrome-conjugated antibodies against several molecules, which allows the simultaneous analysis of different families of cells in a sample.

Antibodies, lectins and the correspondent fluorochromes for human and mice samples are described in **table 2**.

To evaluate the glycoprofile in the *ex vivo* culture of human T cells, isolated T cells from the colon biopsies and peripherial blood samples were washed with PBS and centrifuged at 300g for 5 min at 4 ºC, followed by the staining of dead cells with Fixable viability dye (FVD) (1:2000) for 30 min on ice and dark. Cells were washed and biopsies were stained at the surface with lectins. Biopsies and blood were stained for L-PHA and SNA (that specifically recognizes the alpha 2,6-linked sialic acid) (1:1000) for 15 min. Cells were washed with FACS buffer (PBS with 1% FBS) and stained at the surface with antibodies. Biopsies and blood were stained for CD45 (1:300),

CD8 (1:300), CD4 (Pacific blue – 1:100 or PercP-Cy5.5 - 1:200) and Programed Cell Death Protein 1 (PD-1) (1:100) on ice and dark for 30 min. Cells were washed and stained with streptavidin (1:200) for 30 min. Finally, the cells were fixed with 2% paraformaldehyde (PFA) during 30 min, centrifuged and resuspended in FACS buffer for analysis by flow cytometry.

To evaluate the glyco and immune (innate and adaptive) profile of the cells from mice's colon, flow cytometry was performed in the different time points of disease course. Cells were washed and stained with FVD (1:2000) for 30 min on ice and dark. Further, cells were stained with lectins: L-PHA, GNA, SNA (1:1000) for 15 min, followed by the staining of CD45 (1:400), CD3 (1:100), CD4 (1:300), CD8 (1:500), PD-1 (1:400), CD24 (1:800), MHCII (1:800), CD64 (1:200), CD11c (1:100), CD11b (1:400) and CD206/MMR (1:200), on ice and dark for 30 min. On the last time point, epithelial cells were also stained for the lectin L-PHA (1:1000), CD45 (1:400), MHC-I (1:200) and PD-L1 (1:1000). Cells were washed and stained with streptavidin (1:200) for 30 min. Finally, the cells were fixed with 2% PFA for 30 min, centrifuged and resuspended in FACS buffer. For the last two time points, cells were also stained for the transcription factors, Foxp3 (1:200) and Tbet (1:200) in order to understand the immune profile of $CD4^+$ T cells, using the Foxp3/Transcription Factor Staining Buffer Set (eBioscience). In this protocol, after the extracellular staining cells were fixed for 30 min on ice with the fixation buffer from the kit and permeabilized for 10 min at RT with the permeabilization buffer. Then, cells were blocked with 2% rat serum for 10 min, followed by staining with the intracellular antibodies Foxp3 and Tbet.

Data acquisition was performed in the FACS Canto v.2 flow cytometer (BDBioscience), using the FACSDiva software (BDBioscience). The files were then analyzed with FlowJo software version vX.10.0.

Enzyme-Linked Immunosorbent Assay (ELISA)

The cytokines released from mice explants (supernatants collected) were analyzed by ELISA assay following the manufacturer's instructions. The cytokines analyzed were IFN-γ, TNF-α, IL-1β, IL-17A (Invitrogen, CA, USA) and IL-10 (R&D Systems, Minnesota, EUA). This procedure starts with plate coating with the specific cytokine capture antibody O.N at 4 ºC (for IFN-γ, TNF-α, IL-1β, IL-17A) or at RT (IL-10). Then, plate was washed several times, reagent diluent from each specific kit was added for 1 hour at RT and the specific standards for each cytokine and mice samples were added for 2 hours at RT. Detection antibody was added to all wells for 1 hour (for IFN-γ, TNF-α, IL-1β, IL-17A) or 2 hours (for IL-10) at RT, and the streptavidin or avidin conjugated with HRP was added for 30 min at RT. Finally, tetramethylbenzidine (TMB) substrate solution 1x was added for 15 min, sulfuric acid (2N H_2SO_4) was added to stop the reaction and

the plate was measured at 450 nm and 570 nm using the Biotek MQX200 uQuant Microplate Reader.

Table 2 | Lectins and monoclonal anti-human and anti-mouse antibodies used in flow cytometry analysis, the respective clones and conjugation fluorescence molecules, as well as their supplier.

REACTIVITY	mAB	CLONE	CONJUGATION	SUPPLIER
Human	**FVD**	-	APC-eFluor 780	eBioscience
Human	**CD45**	HI30	Brilliant Violet 510	Biolegend
Human	**CD4**	RPA-T4	eFluor 450	eBioscience
Human	**CD4**	RPA-T4	PerCP-Cy5.5	Biolegend
Human	**CD8**	RPA-T8	PE-Cy7	BD Pharmingen
Human	**CD279 (PD-1)**	J43	PerCP-eFluor 710	eBioscience
Human/mouse	**SNA**	-	Cy5	Vector laboratories
Human/mouse	**L-PHA**	-	Fluorescein	Vector laboratories
Human/mouse	**GNA**	-	Fluorescein	Vector laboratories
Mouse	**CD45**	30-F11	FITC	eBioscience
Mouse	**CD45**	30-F11	PE-Cy7	eBioscience
Mouse	**CD3**	17A2	eFluor 506	eBioscience
Mouse	**CD4**	RM4-5	eFluor 450	eBioscience
Mouse	**CD8a**	53-6.7	PE-Cy7	eBioscience
Mouse	**CD279/PD-1**	J43	PE	eBioscience
Mouse	**Foxp3**	FJK-16S	APC	eBioscience
Mouse	**Tbet**	eBio4B10	PerCP-Cy5.5	eBioscience
Mouse	**CD24**	M1/69	PE	eBioscience
Mouse	**MHCII**	M5/114.15.2	PE-Cy5	eBioscience
Mouse	**CD64**	X54-5/7.1	APC	eBioscience
Mouse	**CD11c**	N418	eFluor 450	eBioscience
Mouse	**CD11b**	M1/70	eFlour 506	eBioscience
Mouse	**CD206/MMR**	15-2	PE-Cy7	eBioscience
Mouse	**MHCI**	AF6-88.5.5.3	FITC	eBioscience
Mouse	**PD-L1**	MIH5	PerCP-eFluor 710	eBioscience
Mouse	**Streptavidin**	-	PE	eBioscience

FITC: fluorescein isothiocyanate; **PE**: phycoerythrin; **APC**: allophycocyanin; **PerCP**:peridinin chlorophyll protein; **Cy5** or **7**: Cyanine 5 or cyanine 7

Statistical analysis

RQ values were used to compare transcription rates and the statistical significance of results was determined by non-parametric kruskal-wallis test or parametric Student t-test. DAI values were used to calculate the Area Under the Curve (AUC) and statistical significance was assessed by multiple t-test. For the analysis of the spleen and colon size 2way ANOVA and for

comparison of the lesions size unpaired Student t-test was done. For the MFI and percentage from mice FACS analysis and ELISAS 2way ANOVA and 1way ANOVA tests were performed. All the data were analyzed using the GraphPad Prism 7 Software (GraphPad Software). Results were considered statistically significant with p values of less than 0.05.

RESULTS

1. Increased expression of complex branched *N*-linked glycans along CAC: a switching event in the CAC carcinogenesis?

1.1. Increased expression of complex branched *N*-linked glycans is associated with high risk colitis to cancer

To better study and understand the impact of complex branched *N*-glycans in the progression of colitis to CAC, we have analyzed a series of colitis with different cancer-associated risks (low, intermediate and high risk). We performed RT-PCR analysis of two important glycogenes: *MAN2A1* gene, which encodes for the enzyme responsible for the removal of the terminal α1-3Man and α1-6Man residues after the action of GnT-I, and *MGAT5* gene, which encodes for the GnT-V enzyme that catalyzes the addition of β1,6-GlcNAc branched glycans. The results showed a significantly higher *MAN2A1* mRNA expression levels in the colitis cases associated with high risk to evolve to CRC when compared to normal colonic samples (**Figure 15A**). Concerning *MGAT5* mRNA expression, the same profile was observed. High risk colitis presents a higher expression when compared to the other cases, with statistical significance when compared with the normal group (**Figure 15B**). These preliminary evidences suggest that overexpression of complex carbohydrate structures may be involved in the progression of colitis to cancer.

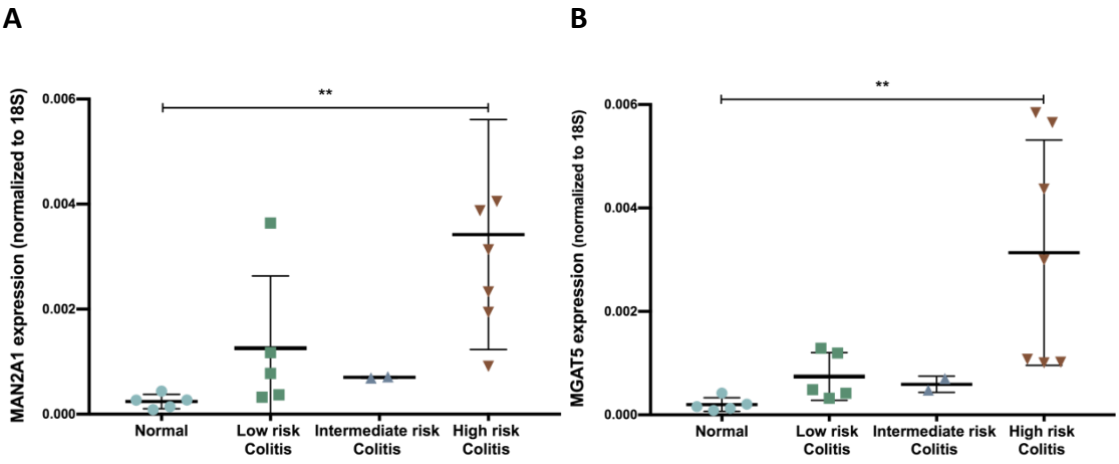

Figure 15| Increase *MAN2A1* and *MGAT5* mRNA expression in colitis with high risk to evolve to CAC. (A) Relative *MAN2A1* mRNA expression is increased from normal (n=5) to high risk colitis (n=7). **(B)** Relative *MGAT5* mRNA expression is increased from normal to high risk colitis. No statistical differences were observed in the other groups. The two graphs suggest that colitis with higher risk to prograde to cancer show increased expression of genes related with the expression of complex branched N-glycans. *MAN2A1* and *MGAT5* mRNA expression was normalized for the house keeping gene *18S* in all cases. Statistical significance was assessed by Kruskal-Wallis test, with Dunn's test for multiple comparisons: **p ≤ 0.01.

1.2. Increased expression of β1,6-GlcNAc branched *N*-linked glycans along CAC carcinogenesis

The expression of β1,6-GlcNAc branched and high-mannose *N*-glycans structures were evaluated along CAC using lectin histochemistry. FFPE biopsies were divided into different groups – inflammed mucosa distant from the dysplastic region; colitis adjacent or in the site of dysplasia; LGD and HGD. The results of histochemistry in the different samples were evaluated by three independent observers that analyzed the expression of β1,6-GlcNAc branched and high-mannose *N*-glycans in two tissue components: in lamina propria infiltrate (stroma) and in epithelial cells. The results showed a increased expression of L-PHA along CAC in which distant colitis display the lower levels of expression of branched glycans in the intestinal inflammatory infiltrate (20% L-PHA non and 40% L-PHA weak) and HGD (100% L-PHA weak), which gradually increase in LGD (21,4% L-PHA medium and 7,1% L-PHA strong) and in "colitis-associated dysplasia" (25% L-PHA medium and 16,7% L-PHA strong). Interestingly, in epithelial cells, L-PHA expression showed a constant increase along the CAC carcinogenesis, showing a higher expression in LGD (42,9% L-PHA medium and 14,3% L-PHA strong) and HGD (100% L-PHA medium). On the contrary, we observed a decrease in the high-mannose *N*-glycans along disease progression in lamina propria infiltrates, and no expression of GNA was observed in epithelial cells (**Figure 16A and 16B**). The staining with CD3 was used to identify the intestinal inflammatory infiltrate at the level of lamina propria (**Figure 16A).**

To validate these results, we have performed RT-PCR for *MAN2A1* and *MGAT5* gene in order to evaluate the expression of the correspondent glycogenes at the transcriptional level. The results showed an increase in the expression of *MAN2A1* gene in the colitis adjacent to dysplasia, suggesting that these alterations appear to occur prior to the progression to dysplasia acting as a potential trigger of cancer development (**Figure 16C**). When considering *MGAT5* mRNA expression we have observed a gradual increase along CAC carcinogenesis, and interestingly, this upregulation start to occur in the colitis adjacent to the dysplastic region (**Figure 16D**).

These data show an altered glycosignature in both lamina propria and and epithelial cells along CAC development. In general, these results suggest that branched *N*-glycans appear to be more expressed in epithelial cells along CAC carcinogenesis, which is in accordance with the pro-malignant effect of the branched glycans. On the other hand, in lamina propria, branched *N*-glycans appear to be more expressed in the first stages of carcinogenesis, while high-mannose *N*-glycans appear to decrease in the immune infiltrate along the cascade, suggesting that this increase in complexed structures may be a switching event for CAC progression.

A

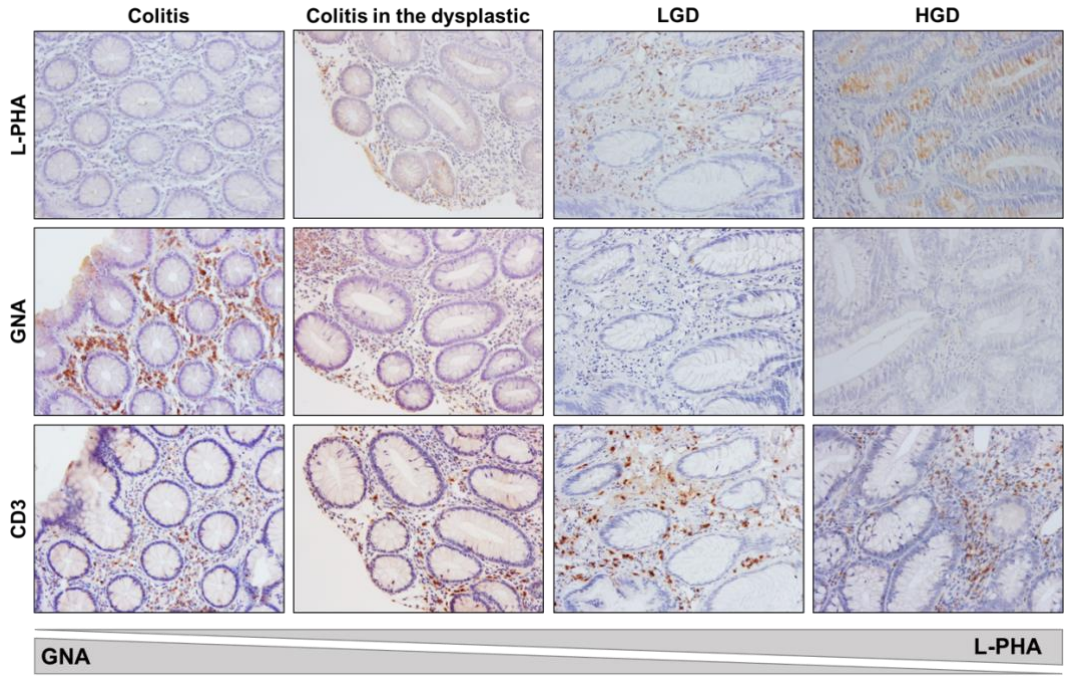

B

		L-PHA								GNA				
		Stroma				Epithelial				Stroma				
	n	L-PHA non	L-PHA weak	L-PHA medium	L-PHA strong	L-PHA non	L-PHA weak	L-PHA medium	L-PHA strong	n	GNA non	GNA weak	GNA medium	GNA strong
Distant Colitis	10	2 (20%)	4 (40%)	4 (40%)	0	6 (60%)	4 (40%)	0	0	9	3 (33,3%)	2 (22,2%)	1 (11,1%)	3 (33,3%)
Colitis adjacent to dysplastic region	12	3 (25%)	4 (33,3%)	3 (25%)	2 (16,7%)	4 (33,3%)	6 (50%)	2 (16,7%)	0	11	3 (27,3%)	4 (36,4%)	4 (36,4%)	0
LGD	14	3 (21,4%)	7 (50%)	3 (21,4%)	1 (7,1%)	3 (21,4%)	3 (21,4%)	6 (42,9%)	2 (14,3%)	14	8 (57,1%)	6 (42,9%)	0	0
HGD	1	0	1 (100%)	0	0	0	0	1 (100%)	0	1	1 (100%)	0	0	0

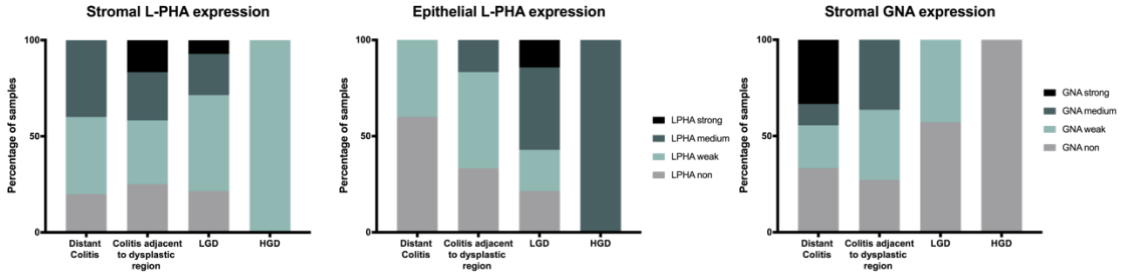

C

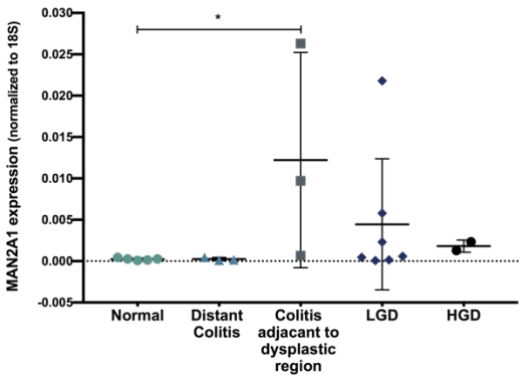

D

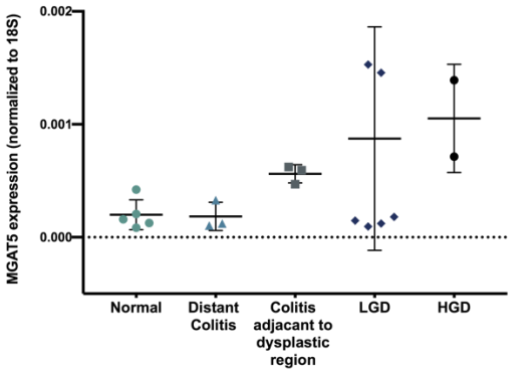

Figure 16| Alteration in branched and high-mannose *N*-glycans profile in immune and epithelial cells along CAC carcinogenesis. (A) Immunohistochemistry for L-PHA (recognizes the β1,6GlcNAc-branched *N*-glycans), GNA (recognizes high-mannose N-glycans) and CD3 (stains for T lymphocytes). L-PHA display increased expression in colon stroma of the low-grade dysplasia (LGD) and colitis adjacent to the dysplasia samples with a decreased in the high-grade dysplasia (HGD). In epithelial cells, L-PHA showed an increase along the carcinogenic cascade. A high staining for GNA was observed in the colitis distant from the dysplastic region, observing a decrease along the cascade. For CD3 it was observed that the carcinogenic cascade is accompanied with T lymphocytes infiltrate. **(B)** Table and schematic representation of the qualitative evaluation of the L-PHA (n=37 samples) and GNA (n=35 samples) staining in the stromal and epithelial compartment of the different groups. The percentage of L-PHA staining increase in the epithelial cells along CAC carcinogenesis, with an increase in the stroma of LGD and adjacent colitis samples. GNA did not show expression in epithelial cells and decreased along the cascade in the stroma. No statistical significance was observed. **(C)** Relative *MAN2A1* mRNA expression is increased from normal (n=5) to colitis adjacent to dysplastic region (n=3). No statistical differences were observed in the distant colitis (n=3), LGD (n=7) and HGD (n=2). **(D)** Relative *MGAT5* mRNA expression showed a gradual increase along CAC carcinogenesis. *MAN2A1* and *MGAT5* mRNA expression was normalized for the house keeping gene *18S* in all cases. Statistical significance was assessed by Kruskal-Wallis test, with Dunn's test for multiple comparisons: *$p \leq 0.05$.

1.3. Longitudinal study: glycans' profile along carcinogenesis in a set of patients with CAC

In order to describe the impact of glycans during the progression of colitis to dysplasia we have been performing a longitudinal analysis per patient. As example, a case study will be presented – CAC1 patient. CAC1 is a 69-year-old man that was diagnosed with UC in 1985. In 2009, a LGD lesion in the transverse colon was detected, and the patient started the clinical and endoscopic surveillance. In 2012, the patient was submitted to surgery to perform an ileum-ceco-colectomy. However, 3 years later the patient developed LGD in the rectum and was submitted to total colectomy. Along the years, the patient only used the standard therapy, 5-aminosalicylic acid (5-ASA), to control the colitis activity.

The lectin histochemistry was performed in the biopsies collected from 2010/2011. The results showed an increased expression of complex branched *N*-glycans (L-PHA staining) with a concomitant decrease in high-mannose structures (GNA staining) in the dysplastic region (from the transverse colon). On the other hand, we observed a decrease in complex branched *N*-glycans and increase in high-mannose *N*-glycans in the distant colitis (from the descendent colon). Interestingly, an increase in L-PHA staining in the colitis prior to dysplasia (in the rectum) was observed. In the same case, in 2010/2011 we also observed higher expression of GNA in the lamina propria immune infiltrate, and this expression was lost during the progression to LGD (in the rectum) in 2014/2015. Once again, concomitantly with the development of LGD (in 2015), we have observed an increased expression of L-PHA with the simultaneous decreased in GNA (**Figure 17**).

The longitudinal study of this case suggests, in a preliminary way, that CAC progression appear to be accompanied with an increase in β1,6-GlcNAc branched *N*-glycans in the lamina propria infiltrate together with a decrease in high-mannose *N*-glycans, and these alterations seem to precede the development of dysplasia.

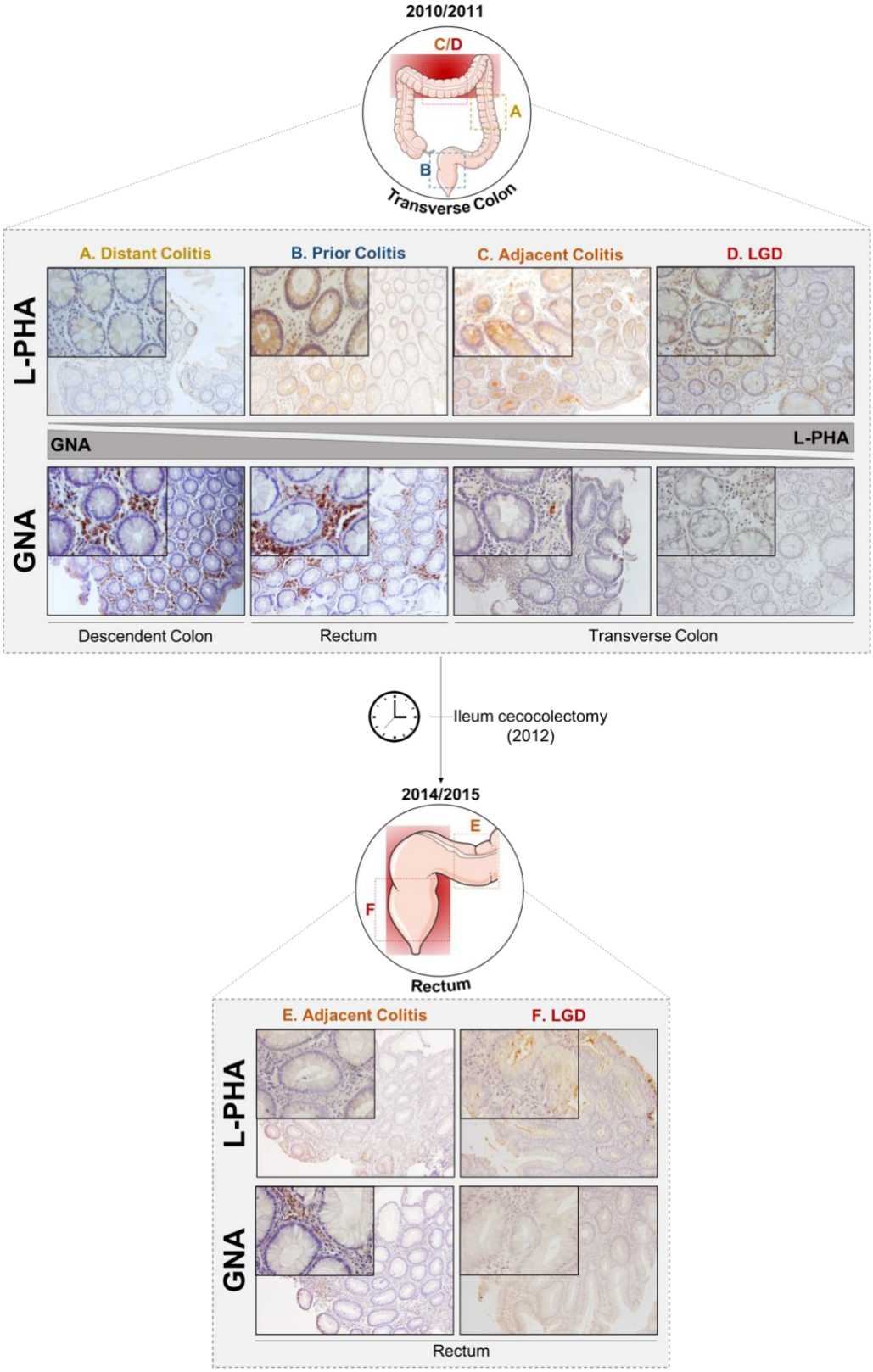

Figure 17| Longitudinal analysis of CAC1 patient showed an increase expression of complex branched *N*-glycans and decrease expression of high-mannose *N*-glycans in the evolution to low-grade dysplasia (LGD). Histochemistry for L-PHA (recognizes the β1,6 GlcNAc-branched N-glycans) and GNA (recognizes high-mannose glycans). Results showed an increase in the L-PHA expression in LGD, adjacent colitis and prior colitis, while GNA expression decrease. Interestingly, the high expression of GNA in prior colitis (2010/2011) was lost when patient prograde to LGD in the rectum (2014/2015).

2. Alterations in the glyco-phenotype of intestinal and blood T lymphocytes during colitis-dysplasia progression

In order to evaluate the glycans profile in *ex vivo* T lymphocytes from LGD patients we have performed an overall characterization of the blood and intestinal lamina propria lymphocytes using fresh colonic biopsies from healthy controls (n=2), colitis-mayo 3 patient (n=1) and LGD patient (n=1) by flow cytometry. We observed that the percentage of $CD4^+$ and $CD8^+$ T cells was altered between patients and healthy controls. As expected, colonic lamina propria $CD4^+$ T cells population was increased in colitis patient, while lamina propria $CD8^+$ T cells population was increased in LGD patient, suggesting an increase in cytotoxic lymphocytes in dysplasia (**Figure 18A**). Concerning the percentages in the blood, we also observed an increase in $CD4^+$ T cells in colitis patient, while $CD8^+$ T cells showed a decrease in both colitis and LGD patient (**Figure 18B**).

The $CD4^+$ T cells showed an interesting increase in β1,6 GlcNAc branched *N*-glycans structures (higher L-PHA) in intestinal lamina propria of LGD patient comparing with colitis and normal condition. Colitis patient showed a decrease in L-PHA and increase in α-2,6 sialic acid (higher SNA) comparing with normal condition (**Figure 19A**). In the blood, a similar L-PHA profile was observed, while SNA expression decreased in the LGD patient (**Figure 19B**). Results from PD-1 expression, a marker for T cell activation and a key immune checkpoint in cancer immunity, showed an increase in lamina propria $CD4^+$ T cells in colitis patient and a decrease in LGD patient, with no major differences in the blood (**Figure 19C**).

In the $CD8^+$T cells, we have observed a slight increase in β1,6 GlcNAc branched *N*-glycans structures in LGD patient comparing with colitis condition. Like in $CD4^+$ T cells, the $CD8^+$ T cells from colitis patient showed an increase in SNA (**Figure 20A**). In the blood, a similar L-PHA profile was observed, while SNA expression decreased in the LGD patient (**Figure 20B**). Results from PD-1 levels showed an increase in lamina propria $CD8^+$ T cells from colitis patient, and an increase in the blood from LGD patient (**Figure 20C**).

Overall, these results suggest that *ex vivo* T cells from CAC patients display alteration in the glycosylation profile in which an increase expression of β1,6 GlcNAc branched *N*-glycans appear to accompany malignant transformation as observed *in situ* in the stroma component.

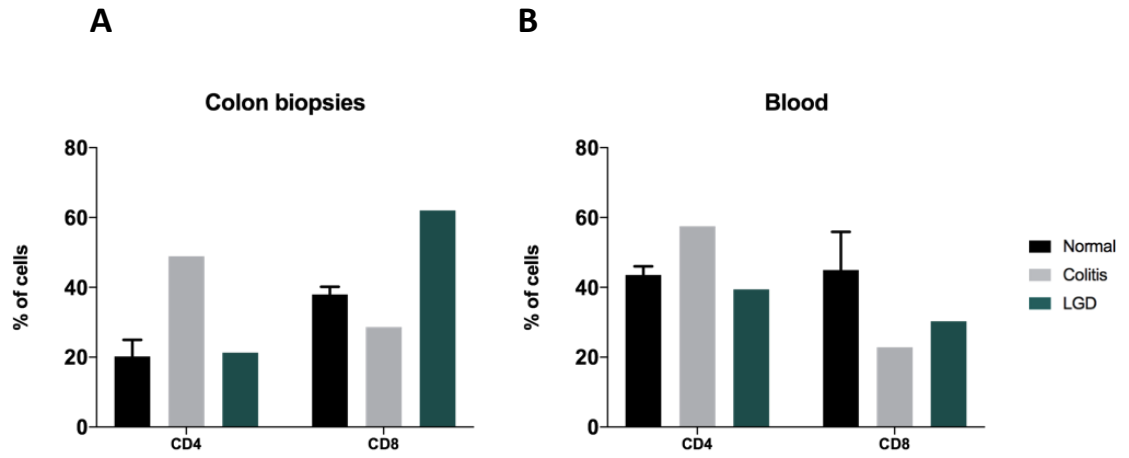

Figure 18| Percentage of CD4⁺ T cells and CD8⁺ T cells in fresh colonic biopsies and blood from normal, colitis and low-grade dysplasia (LGD) patients. (A) In colon biopsies, the percentage of CD4⁺ T cells is increased in colitis patient (n=1), while the percentage of CD8⁺ T cells is higher in LGD patient (n=1). **(B)** In blood samples, the percentage of CD4⁺ T cells is also higher in colitis patient, but the percentage of CD8⁺ T cells decrease in both colitis and LGD patient when compared with normal individuals (n=2). No statistical analysis was applied since the number of samples is very few.

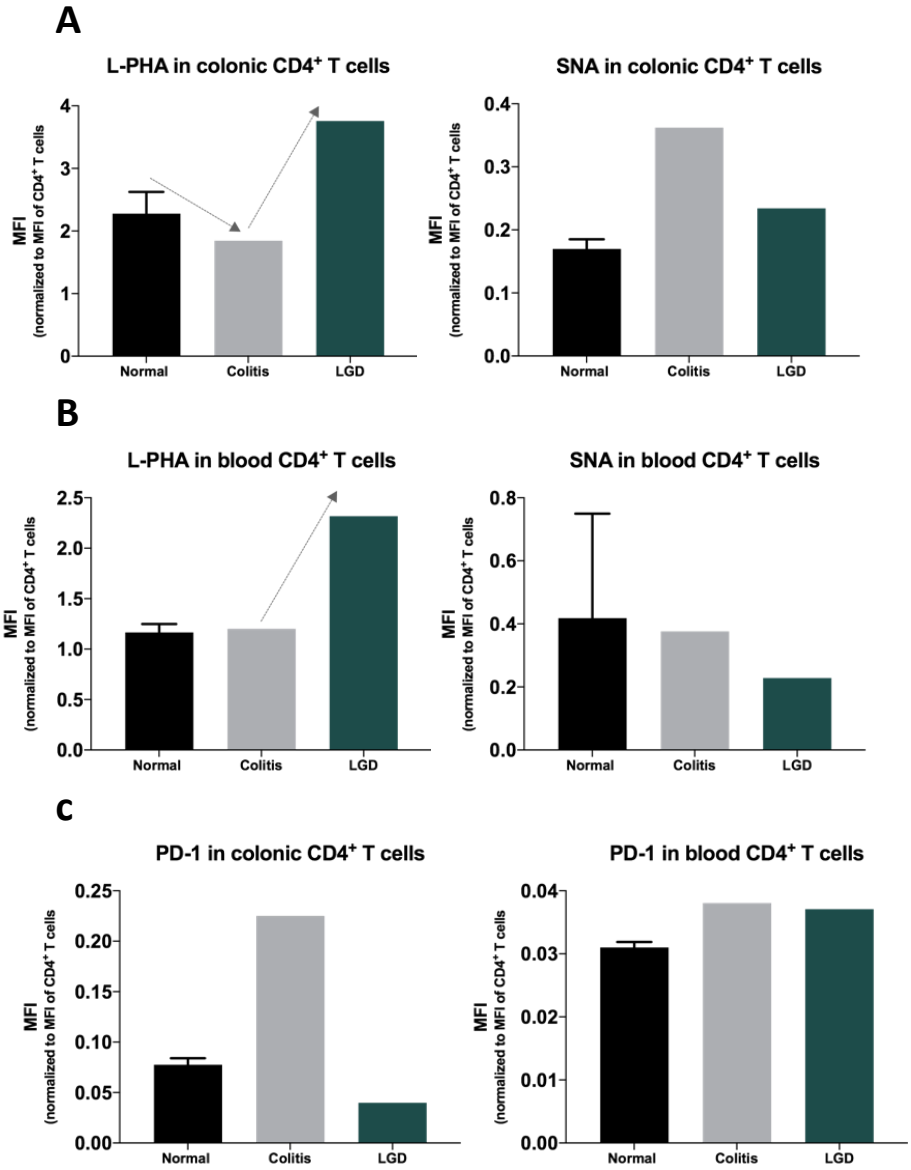

Figure 19| Glycosylation profile and PD-1 expression in colonic and blood CD4⁺ T cells. (A) L-PHA and SNA expression in colonic CD4⁺ T cells. Colitis showed a slightly decrease in L-PHA and an increase in SNA by flow cytometry. Low-grade dysplasia (LGD) showed a substantial increase in L-PHA. **(B)** L-PHA and SNA expression in blood CD4⁺ T cells. LGD showed a significant increase in L-PHA. **(C)** PD-1 expression in both colonic and blood CD4⁺ T cells. In colonic CD4⁺ T cells, PD-1 showed an increase in colitis patient with a decrease in LGD patient, while in blood, no major differences were observed. No statistical analysis was applied since the number of samples is very few.

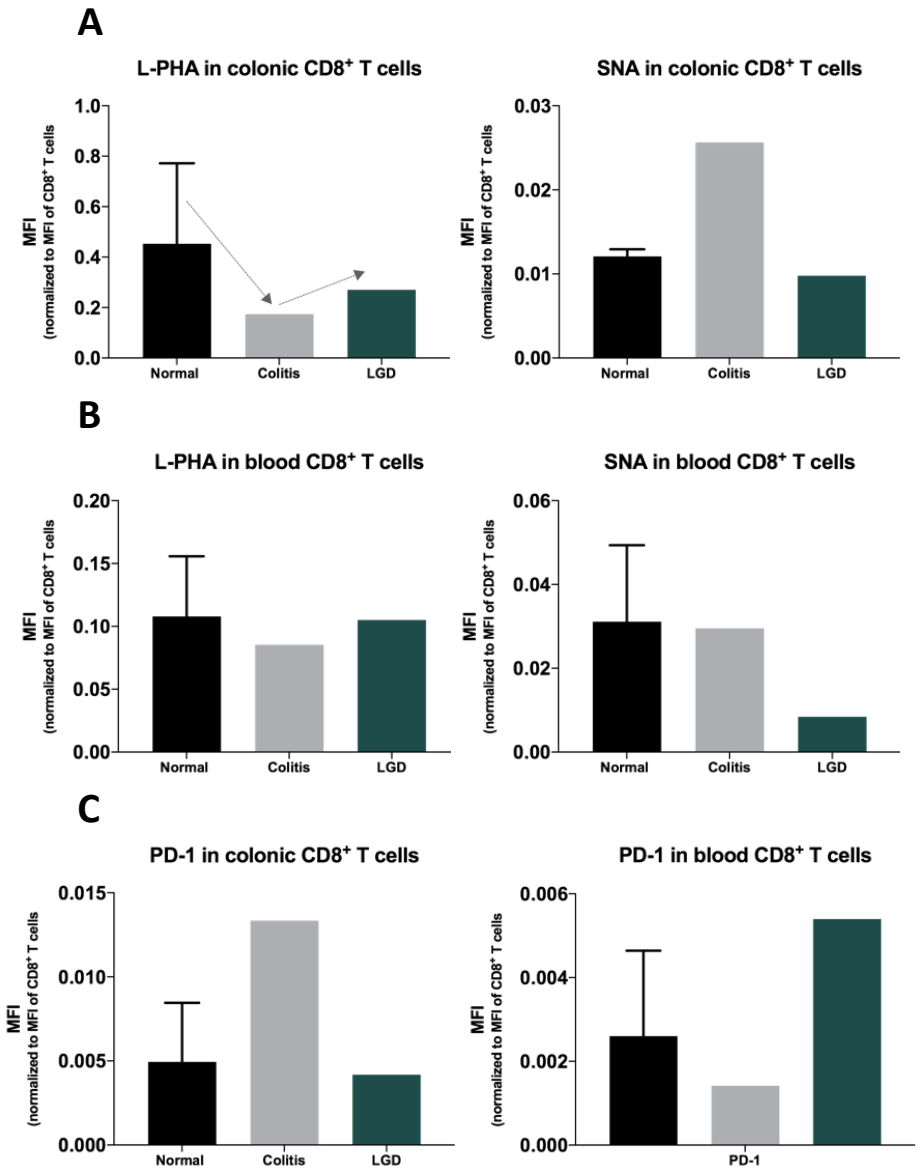

Figure 20| Glycosylation profile and PD-1 expression in colonic and blood CD8⁺ T cells. (A) L-PHA and SNA expression in colonic CD8⁺ T cells. Colitis showed a decrease in L-PHA and an increase in SNA by flow cytometry. Low-grade dysplasia (LGD) showed an increase in L-PHA compared to colitis **(B)** L-PHA and SNA expression in blood CD8⁺ T cells. LGD showed a slightly increase in L-PHA compared to colitis and a decrease in SNA compared to normal blood. **(C)** PD-1 expression in both colonic and blood CD8⁺ T cells. In colonic CD8⁺ T cells, PD-1 showed an increase in colitis patient, while in blood, PD-1 showed higher expression in LGD patient. No statistical analysis was applied since the number of samples is very few.

3. Intestinal lamina propria T lymphocytes display a different glycogene profile associated with a differential immune response.

RNA from $CD3^+$ intestinal lamina propria T lymphocytes was extracted from biopsies diagnosed with LGD (n=1), adjacent mucosa to dysplasia (n=1) and distant/normal mucosa (n=1) of the same patient. The results showed an increase in *MGAT5*, *MAN2A1* and *ST6Gal1* transcriptions, in both LGD and mucosa close to dysplasia, with a more evident increase in LGD sample when compared to normal mucosa, suggesting an increase in the complex glycan structures (**Figure 21A**).

The analysis of the immunogenes expression revealed an increased expression in *TBX21* gene expression (that encodes for the Tbet transcription factor typically expressed by Th1 cells) in the adjacent mucosa to dysplasia (**Figure 21B**). Additionally, expression of IFN-γ gene is increased in the adjacent mucosa to dysplasia when compared to normal mucosa, with a slightly decrease in the LGD when compared to adjacent mucosa (**Figure 21C**). Together, these two results suggest that lamina propria $CD4^+$ T cells in the LGD show a decrease in the pro-inflammatory profile concomitant with the increase in *MGAT5* gene when compared to adjacent mucosa. Results also showed an increased expression of *RORC* gene, expressed in Th17 cells, in the adjacent mucosa to dysplasia and LGD (**Figure 21D**), while the expression of the transcription factor *Foxp3*, expressed in Treg cells, decreased in these two biopsies (**Figure 21E**). Finally, expression of *PDCD1* gene, which encodes for PD-1, is increased in LGD T lymphocytes. (**Figure 21F**). Together, these altered gene expression profile suggest that immune system may be repressed in the dysplastic region allowing tumor progression.

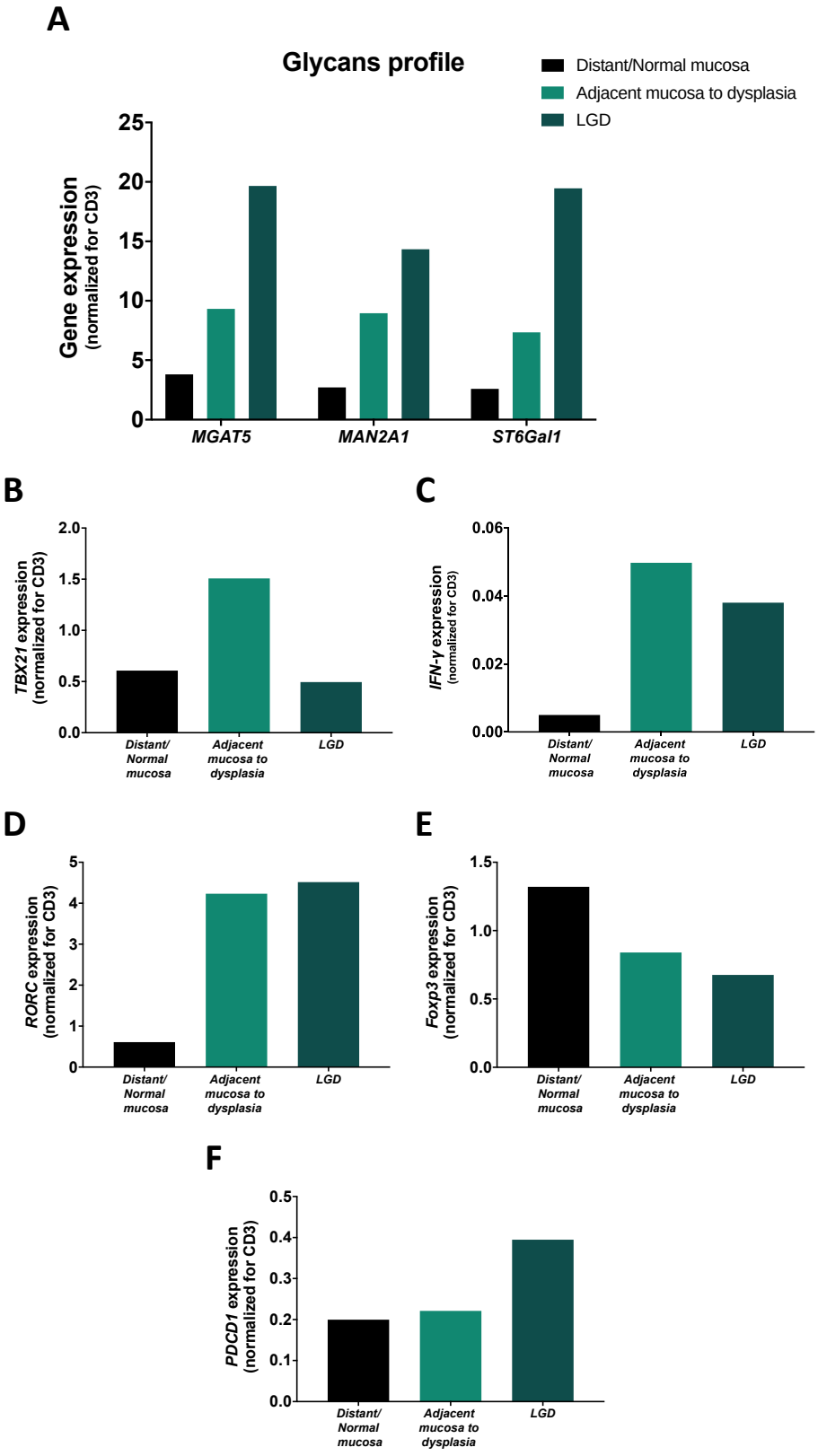

Figure 21| Alterations in the expression of complex glycans genes and immune genes in T lymphocytes from low-grade dysplasia (LGD) and adjacent mucosa to dysplasia. (A) Increased expression of *MGAT5*, *MAN2A1* and *ST6Gal1* mRNA levels in the adjacent mucosa to dysplasia and more evidently in LGD. **(B)** Expression of *TBX21* gene, which encodes the transcription factor Tbet (expressed in Th1 cells) is increased in adjacent mucosa to dysplasia. **(C)** Expression of *IFN-γ* gene is increased in adjacent mucosa to dysplasia, with a slightly decrease in LGD compared to adjacent mucosa. **(D)** Expression of *RORC* gene, expressed in

Th17 cells is increased in adjacent mucosa to dysplasia and LGD. **(E)** Expression of Foxp3 gene, expressed in Treg cells, is decreased in adjacent mucosa to dysplasia and LGD. **(F)** Expression of *PDCD1* gene, which encodes for PD-1 receptor, is increase in LGD T lymphocytes. All mRNA expression genes were normalized for the *CD3* gene. No statistical analysis was applied since the number of samples is very few (n=1).

4. Impact of β1,6-GlcNAc branched *N*-linked glycans along CAC carcinogenesis: an *in vivo* model

4.1. AOM/DSS mouse model of CAC

In order to better understand the impact of β1,6-GlcNAc branched *N*-linked glycans in the course of CAC development, we used an *in vivo* model that consists on repeated DSS cycles combined with the genotoxic agent AOM, which leads to colitis-dependent neoplasia. This model was performed in two different mouse groups with different genetic backgrounds – WT mice and KO mice for the gene *Mgat5* (*Mgat5*$^{-/-}$ mice), which encodes for the enzyme responsible for the production of β1,6-GlcNAc branched *N*-linked glycans. Over the course of disease induction, animals pass through a sequential pathological process, including inflammation–LGD–HGD–carcinoma [103]. Therefore, this model becomes ideal to dynamically dissect the impact of glycans, particularly complex branched glycans, in the carcinogenic cascade using different time points along the inflammation-cancer pathway.

For this purpose, we also used a control group that was submitted to three cycles of DSS, but instead of intraperitonially injection of AOM, we injected saline solution. However, the results from this group will not be the main focus of this thesis. All the animals were submitted to the following scheme with different time points of euthanasia (at the end of 1st, 2nd, 3rd DSS cycle and at day 104) (**Figure 22C**). Throughout disease induction, animals presented relatively high levels of DAI, particularly during DSS cycles. The first cycle corresponds to acute inflammation, while in the following cycles inflammation becomes chronic (**Figure 22A**). Even though DSS cycles were performed in all groups, we can observe, by results from AUC in the DSS group, that KO mice showed a higher AUC in the first and second cycle compared with WT mice, suggesting that *Mgat5*$^{-/-}$ mice have more susceptibility to inflammation during acute phase and during the transition for chronic inflammation. However, during the third cycle we observed a reversion, whereas WT mice showed higher AUC (**Figure 22B**). These results suggest that during the course of inflammation, KO mice acquire some resistance to DSS cycles.

During AOM/DSS mouse model, we monitored the animals by colonoscopy, observing mucosal alterations with visible inflammation and lesion development. Differences between WT and KO mice in the colonoscopies were not conclusive, but pictures from the open colon showed a macroscopic decrease in the extension of the lesions in the KO mice (**Figure 22D**).

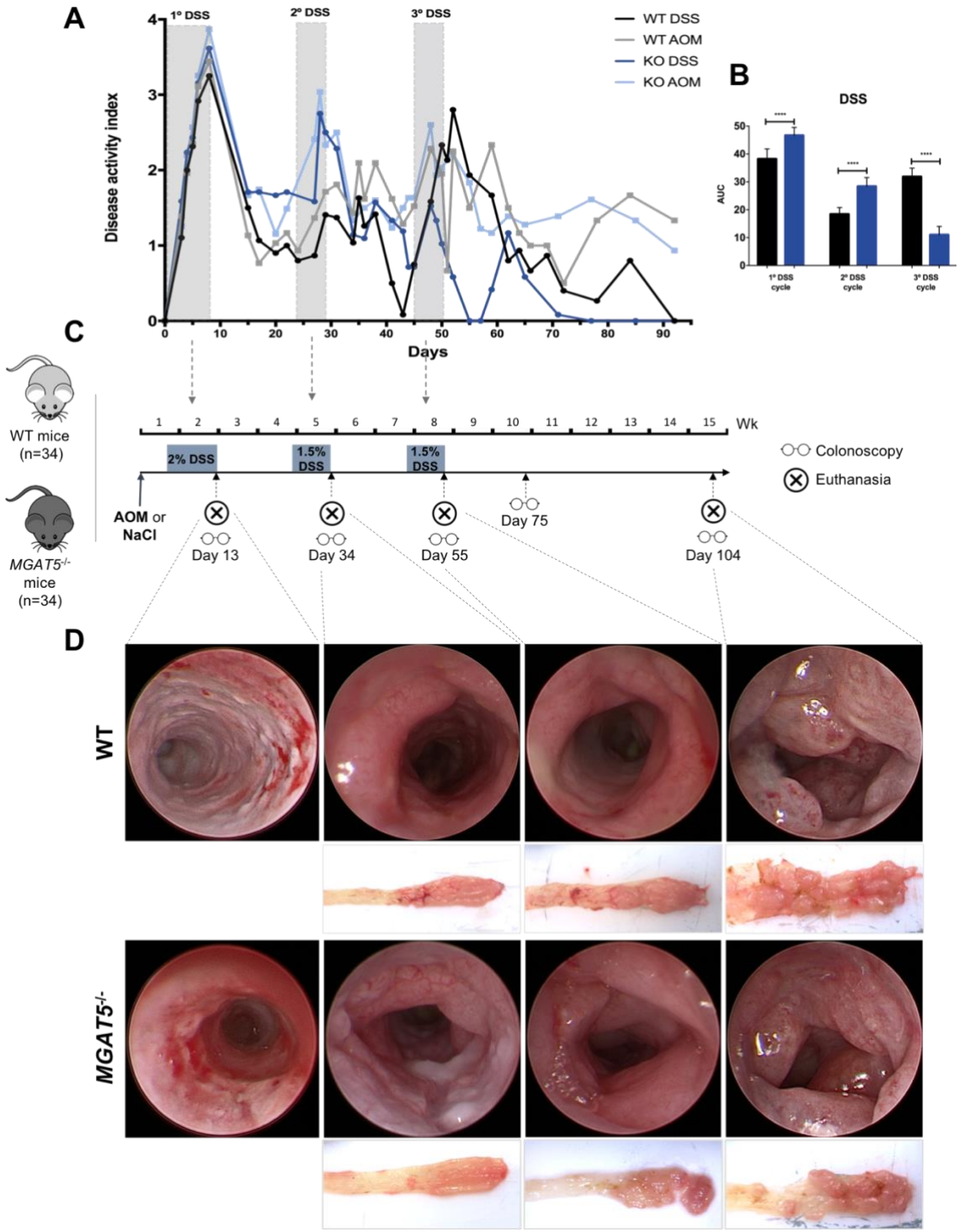

Figure 22| Disease activity index (DAI) curves, experimental procedure and macroscopic observation of the CAC mouse model in WT and *Mgat5*$^{-/-}$ mice. (A) DAI of the AOM/DSS groups (WT and KO) and DSS groups (WT and KO). DAI = (Body weight loss score + Stool consistency score + rectal blood score)/3. We observed a well-defined first peak in the first DSS cycle, corresponding to acute inflammation, and two other mitigated peaks of inflammation corresponding to chronic inflammation. **(B)** Area under the curve (AUC) of the two DSS groups, WT and KO, showed a higher disease activity in the KO mice during the first cycle and the reversal during the third cycle. Statistical significance was assessed by multiple t-test: ****p ≤ 0.0001. **(C)** Experimental procedure of the AOM/DSS group and DSS group. **(D)** Endoscopic images of colonic inflammation and neoplasia evolution and general observations of the colon in the AOM/DSS group (WT and KO) on different euthanasia time points (day 13, day 34, day 55 and day 104).

4.2. *Mgat5*$^{-/-}$ mice display a delay in CAC development

In this AOM/DSS model, after each euthanasia time point, colon and spleen length was measured. No differences were observed in the colon length (**Figure 23A**), whereas spleen length shows to be smaller in the KO mice, suggesting a higher immune infiltrate in the periphery such as in the colon (**Figure 23B**). Number and size of the lesions were also measured in the last time point of euthanasia, showing no differences between the two groups. However, results showed a remarkable decrease in the number of lesions (p=0,051) in *Mgat5* KO mice comparing with WT mice. *Mgat5* KO mice display a smaller number of larger lesions (more than 7 mm^2) (p=0,06), suggesting the impact of a deficiency in complex branched structures in suppression of tumor development and progression (**Figure 23C**).

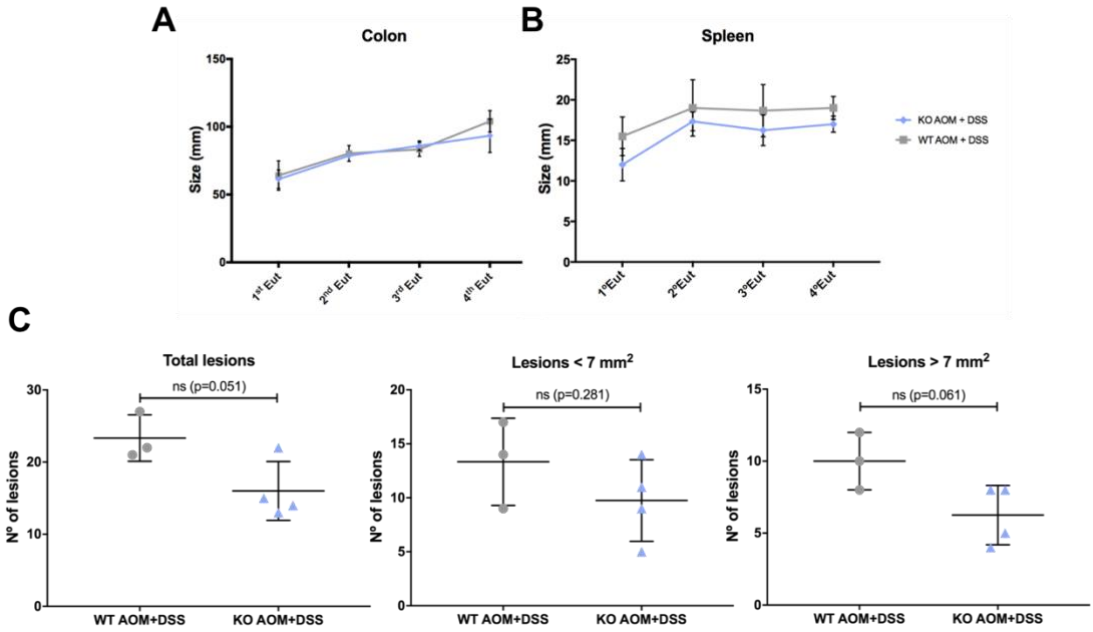

Figure 23| *Mgat5*$^{-/-}$ mice display a decrease in the number of lesions. (A) Colon length of the AOM/DSS group (WT and KO) along the CAC model of carcinogenesis. **(B)** Spleen length of the AOM/DSS group (WT and KO) along the CAC model of carcinogenesis. Results show a smaller size of the spleen in the *Mgat5*$^{-/-}$ mice, suggesting that immune cells may be infiltrating the peripheral organs. Statistical significance of the colon and spleen was assessed by two-way ANOVA, with Turkey's multiple comparisons test, with no significance **(C)** Number of total, smaller (<7 mm^2) and larger (>7 mm^2) lesions. KO mice showed less number of total lesions with a smaller number of larger lesions compared with the WT mice. Statistical significance was assessed by Student t-test: ns, not significant.

Histopathological analysis was carefully performed by a Pathologist confirming that colon samples collect at the end of the first DSS cycle (1st euthanasia) were inflamed mucosa; in the end of the second (2nd euthanasia) and third (3rd euthanasia) DSS cycle it was observed dysplasia and early stage cancer (DESC) in both genotypes, and in the last time point (4th euthanasia) all samples were considered adenocarcinomas. The histopathological analysis in the last time point of euthanasia, late stage cancer (LSC), WT mice presented more advanced lesions with a more invasive and undifferentiated phenotype when compared to *Mgat5*$^{-/-}$ mice (**Figure 24**).

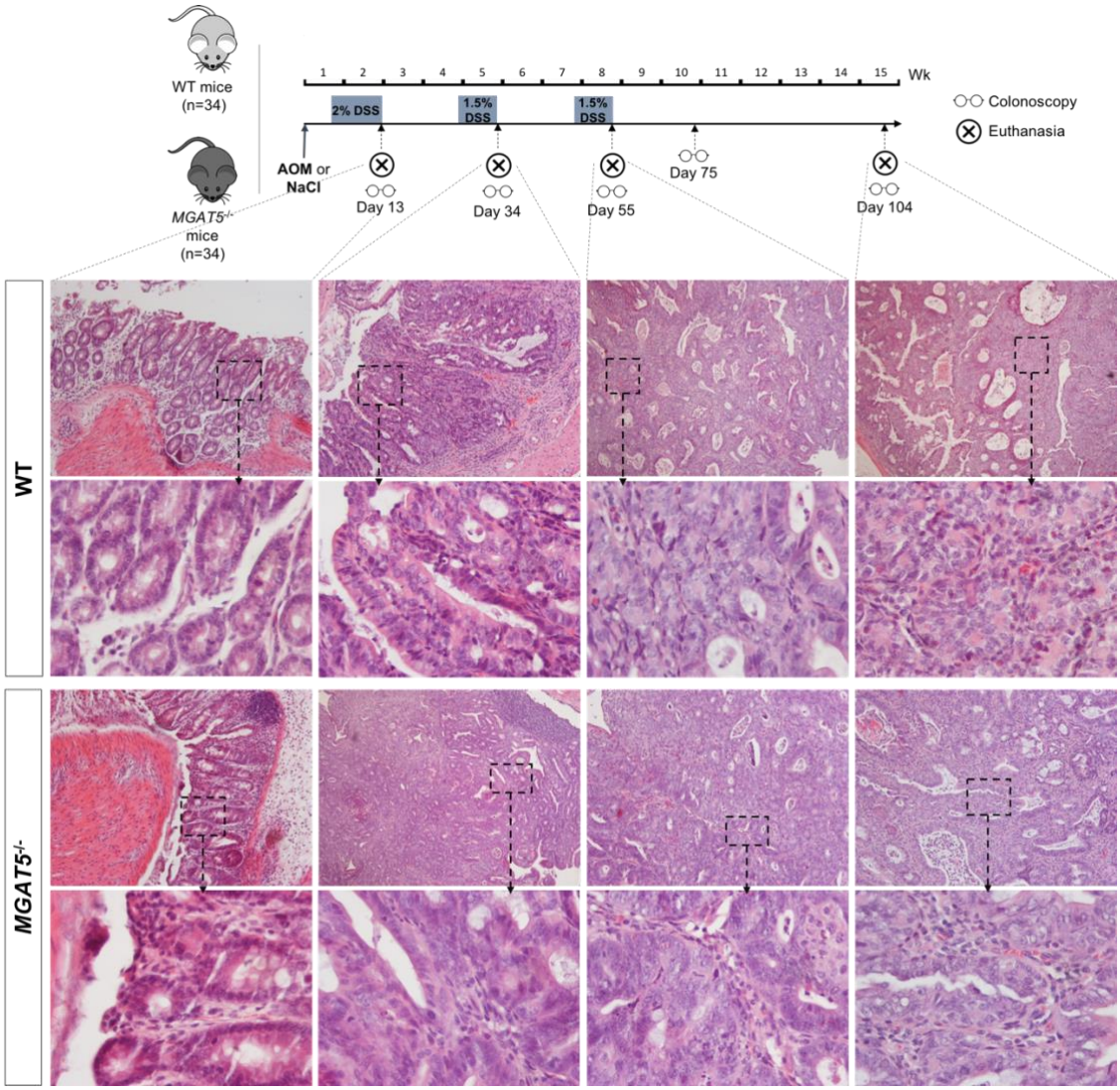

Figure 24| Histopathological examination of the AOM/DSS group (WT and *Mgat5*$^{-/-}$ mice) during CAC mouse model. Hematoxylin and eosin staining of the colon of AOM/DSS group (WT and KO) on different euthanasia time points (day 13, day 34, day 55 and day 104). Top panel: ×40 original magnification; bottom panel: ×200 original magnification.

4.3. CAC carcinogenesis is accompanied by alterations in T cells-glycans' profile

In order to evaluate the effects of *in vivo* glycosylation alterations in the regulation of adaptive immune cells along the carcinogenic cascade in WT and *Mgat5*$^{-/-}$ mice we have characterized the immune profile of those mice by flow cytometry. We found that the percentage of lymphocytes decreases along disease progression in both genotypes (**Figure 25A**). Results also showed a decrease in CD4^{+} T cells over time, but with a continuous increase in PD-1 expression, suggesting that even though CD4^{+} T cells are being less expressed in the tissue they are more activated. Interestingly, PD-1 expression is higher in the KO mice in the two last time points of euthanasia corresponding to later stages of adenocarcinoma (**Figure 25B**). In fact, in these malignant stages of the *Mgat5* KO mice, a slightly higher expression of *Foxp3* (**Figure 25C**) and *Tbet* (**Figure 25D**) transcription factors was observed, indicating the importance of Treg and Th1 in tumor immunosurveillance. Concerning CD8^{+} T cells no major differences were observed between the WT and KO mice (**Figure 25E**). It was interestingly to notice that PD-1 expression was not observed in the DSS group (supplementary data 1), suggesting that this alteration may be mediated by the carcinogenic process.

The glycans´ profile was also assessed in *ex vivo* T cells from both mice models with CAC. The results showed that intestinal T cells from WT mice showed an increased staining with L-PHA, reflecting the increased expression β1,6-GlcNAc branched *N*-linked glycans, that was gradually observed along the carcinogenic cascade, with the higher levels of branched glycans detected in the third time point (DESC). As expected, *Mgat5* KO mice did not show any expression of complex branched *N*-glycans (**Figure 26A**). Concerning high-mannose *N*-glycans structures in CD4^{+} T and CD8^{+} T cells, we found out that KO mice showed a higher expression of GNA in the second time point (DESC) (**Figure 26B**). Furthermore, we observed alterations in α-2,6 sialic acid structures, measured by SNA staining. CD4^{+} T cells from KO mice showed an increase in α-2,6 sialylation predominantly in the second time point (DESC). In CD8^{+} T cells a similar profile was observed but with no statistical significance (**Figure 26C**).

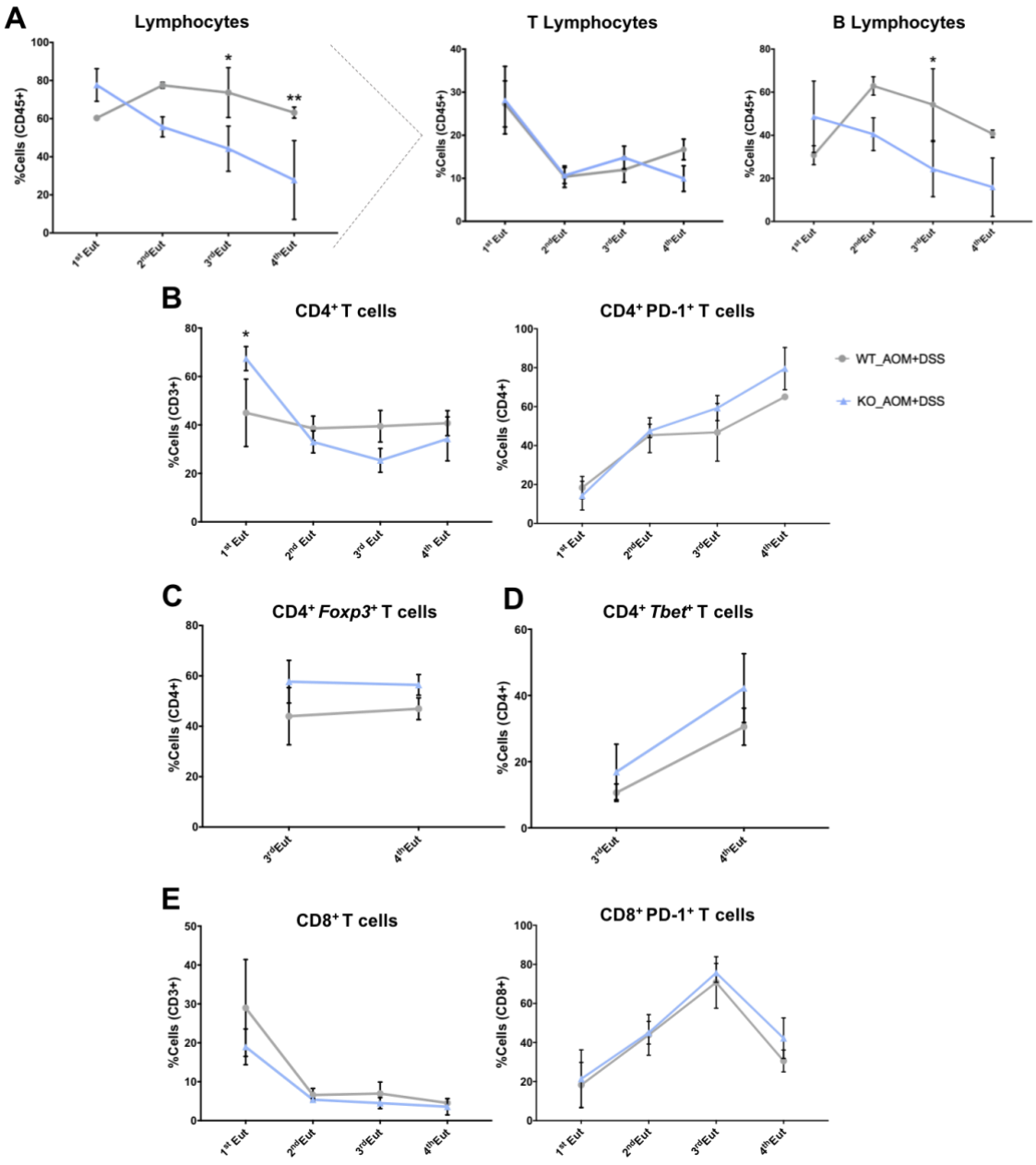

Figure 25| *Mgat5*$^{-/-}$ mice appear to show more PD-1 expression and more Treg and Th1 immune response. (A) Adaptive immunity decreases along CAC development, with a higher decrease in B lymphocytes in the KO mice. **(B)** CD4^{+}T cells shows higher expression of PD-1 in the *Mgat5* KO mice. **(C)** In the two last time points, *Mgat5* KO mice showed more CD4^{+}Foxp3^{+}T cells, which indicates a higher Treg expression. **(D)** In the two last time points, *Mgat5* KO showed more CD4^{+}Tbet^{+}T cells, which indicates a higher Th1 immune response. **(E)** CD8^{+}T cells shows a decrease in PD-1 expression in both groups in the last time point of euthanasia (late stage cancer (LSC)). Statistical significance was assessed by two-way ANOVA, with Turkey's multiple comparisons test: *p ≤ 0.05, **p ≤ 0.01.

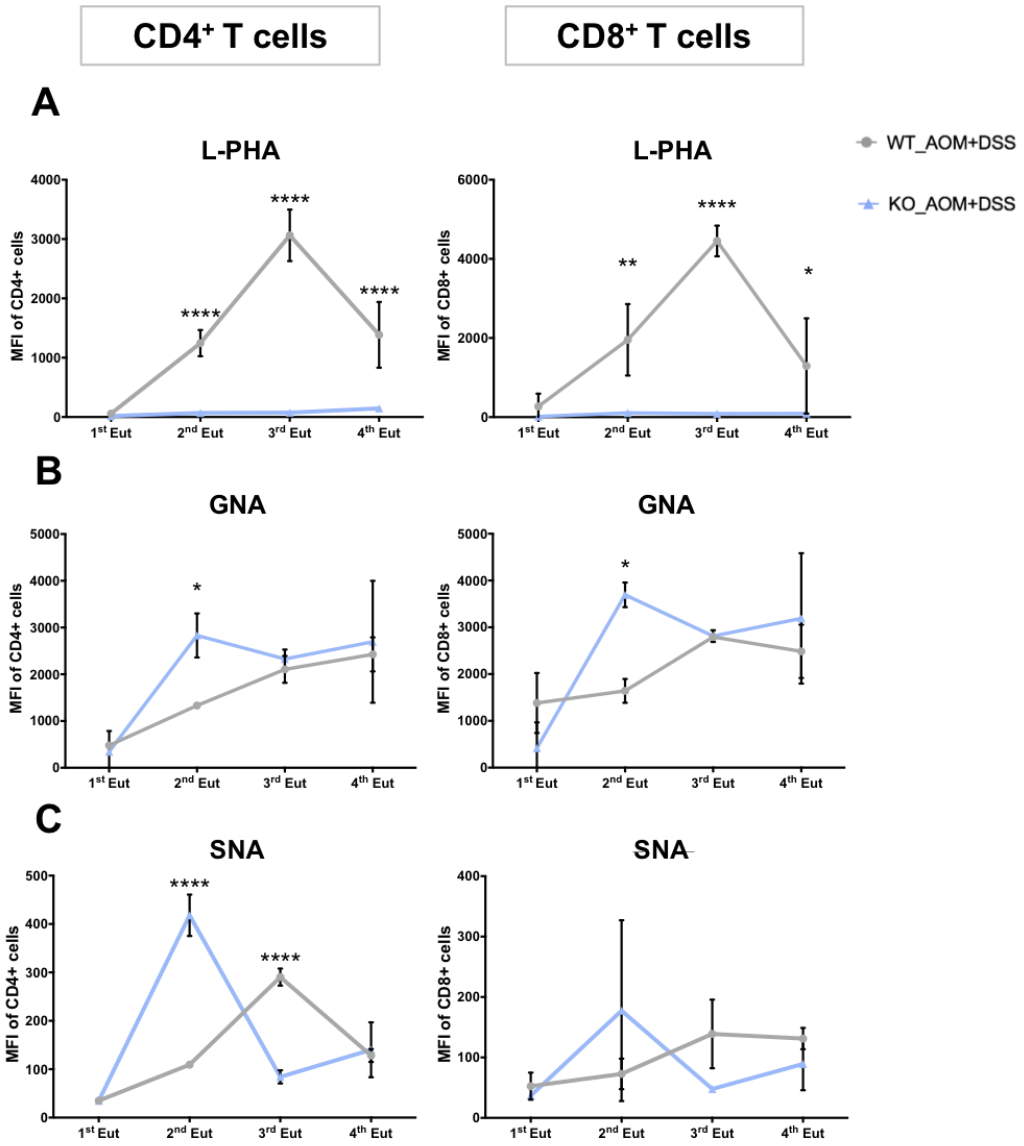

Figure 26| CAC development is accompanied with an increase in β1,6 GlcNAc branched *N*-glycans structures in both CD4⁺ and CD8⁺ T cells with a decrease in late stage cancer (LSC). (A) CD4⁺ T cells and CD8⁺ T cells showed an increase in L-PHA until the third euthanasia with a marked decrease in the last time point of euthanasia (LSC). KO mice did not show any expression of L-PHA, as expected. **(B)** GNA showed an increase in KO mice in the second time point (dysplasia and early stage cancer (DESC)). **(C)** SNA showed an increase in KO mice in the second time point and an increase in WT mice in the third time point. Statistical significance was assessed by two-way ANOVA, with Turkey's multiple comparisons test: *p ≤ 0.05, **p ≤ 0.01, ****p ≤ 0.0001.

4.4. *Mgat5*$^{-/-}$ mice have higher infiltration with myeloid cells and NK cells along disease progression.

Innate immune response was also analyzed in colonic inflammatory infiltrate during the carcinogenic cascade of AOM/DSS mouse model. By flow cytometry analysis we found out that the percentage of innate immune cells increases in the KO mice during disease progression, while in WT mice the percentage of innate cells remains constant in the different time points (**Figure 27A**). The percentage of monocytes and eosinophils were also higher in the *Mgat5* KO mice (**Figure 27B and 27C**). Interestingly, NK cells increased in the KO mice earlier in the carcinogenic cascade (DESC), while in WT mice NK cells only showed an increase in the last time point (LSC). This increased recruitment of NK cells in KO mice support the impact in the delay of tumor progression comparing with WT mice that showed more aggressive and advanced lesions (**Figure 27D**). Regarding DCs, no differences were observed until the third time point of euthanasia (DESC) between the two genotypes, however, an increased percentage of these cells in LSC time point was observed in the KO mice, highlighting the importance of these cells in tumor immunity (**Figure 27E**).

Taking into consideration the importance of C-type lectins in the modulation of immune response, we have also evaluated the expression of MR in DCs and macrophages in the last time point (LSC). Both WT and KO mice in AOM/DSS group showed a decrease in MR when compared with DSS group, suggesting that a deficiency in these receptors is required for tumor progression. However, no differences were observed between WT and KO mice in the AOM/DSS group (**Figure 27F**). Concerning macrophages, the results showed a higher percentage of these immune cells in the colon of *Mgat5* KO mice, at early stages (DESC). In LSC time point, WT mice displayed an increase percentage of macrophages equal to the percentage in KO mice (**Figure 27G**). In these immune cells, MR also presented a reduction in both WT and KO mice from AOM/DSS group, when compared with the DSS group. Moreover, KO mice from AOM/DSS group express slightly less MR when compared with WT mice from AOM/DSS group (**Figure 27F**). Altogether, these observations suggest the relevance of innate immune cells in the delay of tumor growth observed in KO mice, further indicating that the absence of complex *N*-glycan structures may lead to a more activated innate immune system.

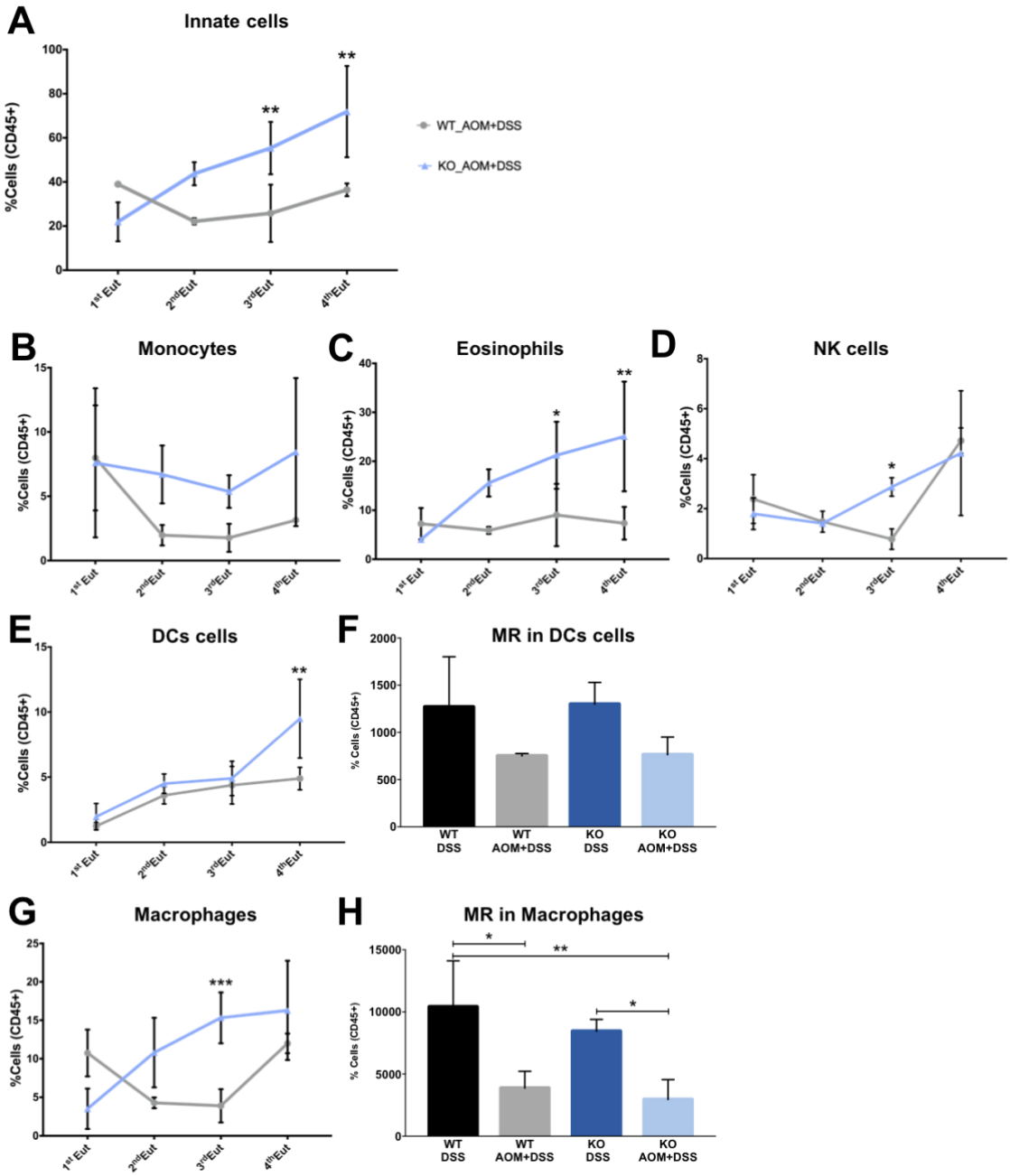

Figure 27| AOM/DSS *Mgat5*$^{-/-}$ mice showed higher innate immune infiltrate. (A) Innate immune cells increased in the *Mgat5* KO mice along CAC development. **(B)** *Mgat5* KO mice showed more monocytes. **(C)** *Mgat5* KO mice showed more eosinophils expression along CAC development. **(D)** *Mgat5* KO mice showed an early expression of natural killer (NK) cells. **(E)** *Mgat5* KO mice showed higher dendritic cells (DCs) in the last time point (late stage cancer (LSC)). **(F)** Mannose receptor (MR) expression was measured in the last time point (LSC), and AOM/DSS group showed a decrease in MR expression in DCs compared to DSS group, but no differences were observed between WT and KO mice. **(G)** *Mgat5* KO mice showed higher macrophages **(H)** MR expression from the last time point (LSC), showed a decrease in MR expression in macrophages from AOM/DSS group compared to DSS group. In the AOM/DSS group, KO mice showed a higher decrease. Statistical significance was assessed by two-way ANOVA, with Turkey's multiple comparisons test: *p ≤ 0.05, **p ≤ 0.01, ***p ≤ 0.001. For MR graphs, statistical significance was assessed by one-way ANOVA with Turkey's multiple comparisons test: *p ≤ 0.05, **p ≤ 0.01.

4.5. Colonic explants from *Mgat5*$^{-/-}$ mice-developing CAC exhibit higher levels of pro-inflammatory cytokines

We have evaluated the cytokine production of the supernatants from *ex vivo* cultures of the mice colonic explants. The results showed that IFN-γ, mainly produced by NK cells, Th1 and cytotoxic CD8^{+} T cells, is increased in the *Mgat5*$^{-/-}$ mice (**Figure 28A**). Likewise, TNF-α, a cytokine produced by M1 macrophages, NK cells, Th1 and cytotoxic CD8^{+} T cells, showed higher levels in the last time point of euthanasia (LSC) in the KO mice (**Figure 28B**). IL-17A, a cytokine released by Th17 cells, shows higher levels in the WT mice, however, with high standard deviation. Moreover, this cytokine shows an increase in the second, third and last time point of euthanasia in both groups, suggesting that may be important in CAC carcinogenesis (**Figure 28C**). Concerning IL-1β levels, mainly released by macrophages and dendritic cells, we found that in the first time point of euthanasia (time point of colitis) KO mice showed higher levels of this cytokine, with no differences in the followed time points (**Figure 28D**). Finally, IL-10, mainly released by M2 macrophages and Treg cells, showed higher expression in the first and last time point in both groups, with a slight increase in KO mice, however, with high standard deviation (**Figure 28E**).

Overall, *Mgat5*$^{-/-}$ mice shows high levels of pro-inflammatory cytokines, suggesting a more effective immune response against tumor progression.

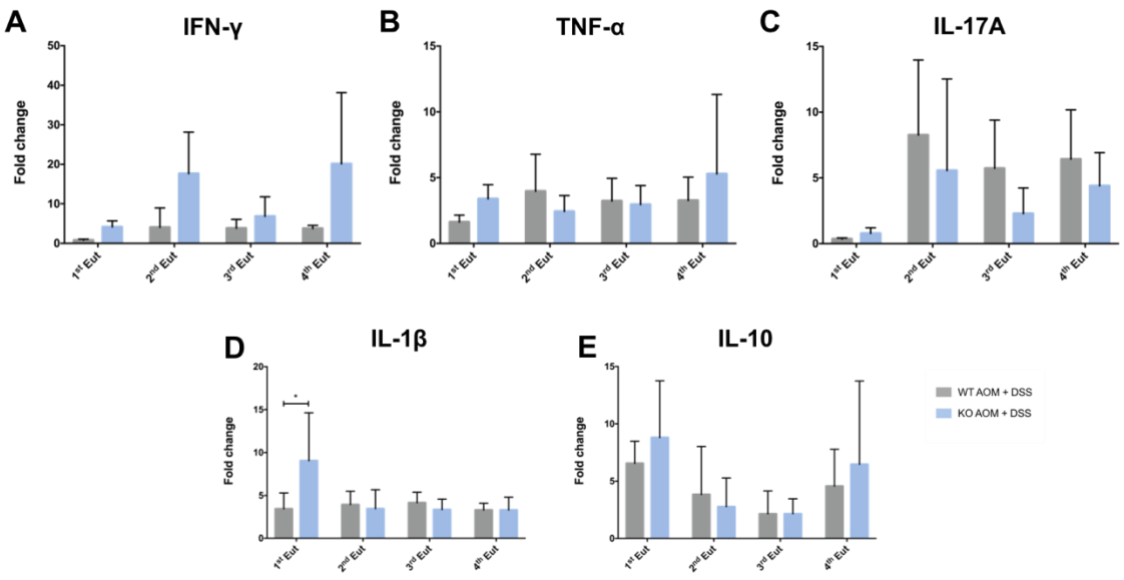

Figure 28| Cytokine profile in the supernatants from *ex vivo* cultures showed higher levels of IL-17A in WT mice, whereas IFN-γ and TNF-α showed higher levels in the last time point (late stage cancer (LSC)) in *Mgat5*$^{-/-}$ mice. (A) IFN-γ production showed higher levels in KO mice. **(B)** TNF-α showed higher levels in KO mice in the last time point of euthanasia (LSC). **(C)** IL-17A showed higher levels in the WT mice in the second, third and last time point of euthanasia (dysplasia and early stage cancer (DESC) and LSC), but with high standard deviation. **(D)** IL-1β expression showed higher levels in the KO mice in the first time point of euthanasia (colitis). **(E)** IL-10 expression was higher in the first and last euthanasia (colitis and LSC), but

with high standard deviation. Statistical significance was assessed by two-way ANOVA, with Sidak's multiple comparisons test: *p ≤ 0.05.

4.6. CAC development is accompanied by an increased expression of complex branched *N*-glycans in epithelial cells. Depletion of branched *N*-glycans results in a higher expression of MHC-I at epithelial cell surface.

Epithelial cells were isolated in the last time point of euthanasia (LSC). We found out that PD-L1 expression did not show significant differences between different groups, however KO mice appears to show higher expression of this receptor (**Figure 29A**). Interestingly, MHC class I shows higher expression in the KO mice from AOM/DSS group when compared with WT mice from AOM/DSS group, suggesting that epithelial/tumor cells from KO mice may be more easily recognized by the immune system (**Figure 29B**). Concerning the expression of β1,6-GlcNAc branched *N*-linked glycans, we found out that WT mice from AOM/DSS group showed higher expression of L-PHA compared to WT mice from DSS group, suggesting that these structures play a role in the carcinogenesis process. As expected, *Mgat5* KO mice did not show expression of L-PHA (**Figure 29C**). These results suggest that complex branched *N*-glycans also have impact on epithelial cells, modulating how the immune system can recognize the cancer cells.

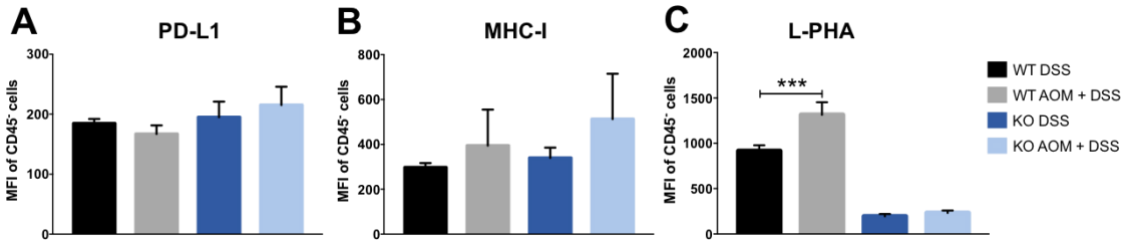

Figure 29| CAC development is accompanied with an increased in β1,6 GlcNAc branched *N*-glycans structures in epithelial cells and *Mgat5* KO mice showed higher MHC class I. (A) KO mice appear to show higher expression of PD-L1 in the last time point of euthanasia (late stage cancer (LSC)). **(B)** AOM/DSS KO mice showed higher MHC class I expression in the last time point of euthanasia (LSC). **(C)** AOM/DSS WT mice showed higher L-PHA expression in the last time point of euthanasia (LSC) comparing to DSS group, which is related with the expression of β1,6 GlcNAc branched *N*-glycans structures. Statistical significance was assessed by one-way ANOVA with Turkey's multiple comparisons test: ***p ≤ 0.001.

DISCUSSION

Cancer is a critical heath problem due to its high incidence, prevalence and poor survival. In fact, CAC is of major concern in the clinical management of patients with chronic IBD [7], however, the mechanisms underlying CAC development remain to be fully clarified. Our study aims at elucidating whether the changes in the glycosylation profile of the microenvironment influence cancer development and progression.

One of the most frequent posttranslational modifications in proteins is glycosylation that has been demonstrated to regulate their structures and functions. In fact, changes in glycosylation is a well-known feature associated with major diseases, such as cancer and inflammation [106]. Accumulating evidences have shown that in chronic inflammatory conditions, such as IBD, complex branched *N*-glycans, produced by GnT-V enzyme, are downregulated in T cells leading to a higher disease severity. On the other hand, aberrant glycosylation is a universal feature of cancer cells, and, in fact, overexpression of β1,6-GlcNAc branched *N*-linked glycans is associated with an increase of tumor development, progression and metastasis in several types of cancer. Taking into consideration these evidences, some questions have arisen regarding the progression from colitis to cancer. As in the other tumor types, in CAC are the glycans also altered? Which type of glycans are present? What is the impact of tumor glycosylation on the immune system? If the immune system is so activated in IBD, how does it allows tumor development? Will glycans have any impact on the modulation of the immune system that allows the progression from colitis to cancer?

In order to answer these questions, a well-organized strategy was defined, through the evaluation of human clinical samples and a CAC mouse model, using different methods and technologies. Taking into consideration the complexity of CAC, which remain poorly understood, our study will open doors to better understand the relevance of *N*-glycans in modulating immune responses and consequently, tumor onset.

Our results demonstrate that overexpression of glycogenes related with the synthesis of complex branched *N*-glycans is associated with high risk colitis to progress to CRC, suggesting that, alterations in the glyco-profile appear to occur prior to the progression to dysplasia. Furthermore, this increased expression of glycogenes and β1,6-GlcNAc branched *N*-linked glycans in epithelial cells was observed along CAC carcinogenesis. This is the first observation of glycosylation alterations along CAC development.

In colonic lamina propria, complex branched *N*-glycans also increased in colitis prior to dysplasia and in LGD whereas non-branched, high-mannose structures, decreased from colitis to dysplasia. In agreement, Demetriou and colleagues, demonstrated that mice deficient in

MGAT5 gene and lacking GnT-V enzyme (resulting in a reduction of complex branched *N*-glycans) display a significantly increase in TCR clustering, promoting a decrease in the threshold of T cell activation, which result in a hyperimmune response and increase susceptibility to immune-mediated diseases [97]. Moreover, in IBD, our group previously showed that intestinal T cells from UC patients display a deficiency in branched glycans associated with hyperactivation of T cell mediated immune response [98, 99]. Furthermore, the enhancement of branched *N*-glycans was associated with a controlled T cell-mediated immune response. Together, these evidences, suggest that during CAC development, immune system started to be suppressed in order to allow malignant transformation, in which the expression of complex branched *N*-glycans start to occur and appear to have a role. This altered glycan expression negatively regulate the immune response allowing the progression to dysplasia and carcinoma.

These evidences were supported by our data on fresh colonic biopsies from CAC patients. We observed that along the progression to LGD there was a decreased expression of $CD4^+$ T cell subset and an increase in $CD8^+$ T cells subset, which are known to be important in tumor microenvironment. Interestingly, we have observed that both subsets of T cells displayed increased expression of β1,6-GlcNAc branched *N*-linked glycans in LGD and reduced levels of the T cell activation marker, PD-1. In agreement, *MAN2A1* and *MGAT5* gene was also found to be increased in both LGD and adjacent mucosa to dysplasia comparing to normal mucosa. Taking together, our preliminary evidences, suggest that this increased expression of complex branched glycans on T lymphocytes in the dysplastic region are contributing to immunosuppressive functions of T cells allowing malignant transformation and progression. However, the number of samples has to be increased in order to sustain this hypothesis.

Sialic acid was found to be increased in colitis patient. Even though, sialylation has been mainly associated with immune suppression, in T cells, the presence of sialic acids by the increase expression of *ST6Gal1* gene is selectively related with a subtype of effector $CD4^+$ T cells that promote the chronicity of inflammation in IBD [107]. Even though, we did not observe any increased in sialic acid structures, at mRNA level we found an increased in *ST6Gal1* gene in both LGD and adjacent mucosa to dysplasia, which can be explained by the poor correlation between mRNA and protein levels that has been frequently observed in other proteins [108]. In this case, the presence of the enzyme does not correlate with the increased expression of sialic acid structures, which might indicate that the enzyme is not being functional, or the substrate are present in low abundance. Furthermore, this alteration in gene expression may not yet be reflected in the glycan profile and may be a change that will only occur in later stages of tumor progression. However, the number of samples has to be increased and further studies has to be

done to understand which are the molecules that are being affected by the altered glycosylation and what are the consequences of these alterations.

Regarding immune profile of CAC patients, we showed an increased production of IFN-γ in adjacent mucosa to dysplasia, which may indicate that the surrounding immune cells are trying to control tumor progression. However, LGD sample display a decrease in Th1 cells, suggesting a decrease in pro-inflammatory immune response. On the other hand, both LGD and adjacent mucosa displayed increased mRNA levels of *RORC*, related with Th17 cells. IL-17, released by Th17 cells, plays a dual role in tumor development, either by favoring the release of pro-tumorigenic factors by tumor and tumor-associated microenvironment, or by promoting the recruitment of anti-tumor immune cells [109]. Regarding CAC development, it has been described that IL-17A plays an important pro-tumorigenic role [110]. As so, the increased expression of *RORC* gene in the dysplastic region may indicate tumor progression.

Despite the results from protein levels and gene expression, the number of samples was insufficient to achieve a precise conclusion about the effect of glycosylation in T lymphocytes.

Our *in vivo* results have shown that *Mgat5* KO mice present less number of tumors with a less aggressive phenotype, suggesting that lack of complex structures was associated with a delayed tumor progression in CAC. Our preliminary evidences on the immune-profile of the mice revealed that KO mice presented a slightly higher percentage of PD-1 when compared with WT, suggesting an increase of T cell activation along CAC development in mice with lack complex branched *N*-glycans. Interestingly, KO mice showed slightly higher expression of *Tbet* and *Foxp3*, which are transcription factors expressed in Th1 and Tregs cells, respectively, indicating the importance of these cells in tumor immunosurveillance.

Furthermore, we also observed an increased in complex carbohydrate structures (branched *N*-glycans) along CAC development in WT mice with a decrease in the final stage, LSC, in both $CD4^+$ and $CD8^+$ T cells. This observation suggests an immunosuppressive phenotype in early stages of carcinogenesis (DESC) allowing malignant transformation. Furthermore, increased sialic acid structures showed a delay in WT mice compared to KO mice during CAC development. In fact, a study have shown that desialylation enhances proliferation and differentiation of naïve T cells [111]. As so, the early decrease in SNA observed in KO mice may indicate that T lymphocytes are being earliest activated compared to WT.

Regarding innate immune system, our evidences showed interesting differences between WT and KO mice. Remarkably, NK cells have a fundamental role in the prevention of tumor progression in the AOM/DSS-induced CAC model [112]. In fact, the modulation of glycosyltransferases GnT-V and Gnt-III correlated with the improvement of NK cell effector functions and the increase of tumor cell sensitivity to NK cell-mediated cytotoxicity [113]. As so,

the early increase in NK cells in *Mgat5*$^{-/-}$ mice correlates with the smaller number of tumors. Macrophages were also increased in the KO mice. Accordingly, knockdown of *Mgat5* gene induced stronger phagocytic capability of macrophages and enhanced the production of TNF-α and IFN-γ [95]. In fact, in LSC, KO mice showed higher expression of IFN-γ and TNF-α, corroborating the hypothesis that lack of branched glycans lead to a more anti-tumor immune environment.

Furthermore, WT mice showed higher levels of IL-17A, which was previously mentioned as a key cytokine involved in CAC development [110]. Concerning IL-10, an anti-inflammatory cytokine, we observed an increased in both animals in the last time point (LSC), suggesting a mechanism of immune evasion by tumor cells. Relationship between IL-10 and complex branched *N*-glycans was already studied in chronic infection. The authors showed that IL-10 induced the expression of *MGAT5* gene on $CD8^+$ T cells increasing the threshold for T cell activation and function [96]. If the same mechanism occurs in our model, we can speculate that even though KO mice showed higher levels of IL-10, this cytokine cannot exert its function so effectively due to the lack of complex structures.

A decrease in MR expression in macrophages and DCs was observed in cancer-induced AOM/DSS groups of both genotypes. Interestingly, WT mice shows slightly higher levels of MR in macrophages compared to KO mice, which is in accordance with the anti-inflammatory phenotype of macrophages M2 expressing positive levels of MR. In fact, MR was found to be abundantly expressed by TAMs isolated from human ovarian carcinoma being responsible for the immune-suppressive profile that characterizes M2 macrophages [114]. Taking into account these evidences we speculate that macrophages-expressing MR from WT mice may have a higher contribution for tumor progression compared to KO mice. However, expression of MR was only evaluated in the late time point (LSC) and, therefore, changes along CAC development were not evaluated.

Altogether, these results highlighted the importance of complex branched *N*-glycans in immune modulation with a significant impact in innate immune system. However, and in order to clarify these preliminary evidences, it is important to increase the number of samples analyzed. Additionally, and to further clarify these results on the impact of glycosylation alterations in immunomodulation associated with CAC development, *Mgat5*$^{-/-}$ mice could be crossed with *RAG-1*-deficient mice in order to evaluate if the observed effects are exclusively dependent on innate immunity or if adaptive immune cells have also some impact on CAC-mouse model.

Focusing on epithelial cells, results from the LSC time point showed higher expression of complex *N*-glycans in AOM/DSS WT mice compared with the DSS group, supporting the

hypothesis of this thesis. Accordingly, MHC-I showed slightly higher expression in KO mice, suggesting that epithelial cells are more visible for immune attack and, by that, KO mice develop a smaller number of tumors.

Overall, the current study contributes to our understanding of the impact of glycosylation, more specifically complex branched *N*-glycans, in the modulation of immune response along CAC development in both human and mice samples. Indeed, these structures may offer a new perspective for therapeutic and diagnostic strategies against tumor development in patients with IBD.

CONCLUSION AND FUTURE PRESPECTIVES

The work developed during this master thesis has resulted in a better understanding of the impact of glycosylation alterations during CAC development, highlighting how immune cells are affected by different glycosylation profiles. Our findings support that β1,6-GlcNAc branched *N*-glycans become overexpressed early in pre-malignancy and this early alteration could be used as a potential biomarker to stratify IBD patients accordingly with their likelihood to progress to CAC. Moreover, we have contributed to elucidate the impact of these specific glycan structures in the modulation of the surrounding immune response, proposing that this specific carbohydrate structure has a major impact in innate immune cells, contributing to an immunosuppressive phenotype associated with CAC carcinogenesis. The proposed model of this thesis is represented in **Figure 30.** However, further analysis needs to be conducted to validate these results and to better understand the mechanism behind complex branched *N*-glycans in CAC evolution.

In this regard, we need to increase the number of clinical cases analyzed in each stage of carcinogenesis to consolidate our results. Additionally, there is also a need to increase the number of fresh colonic biopsies to validate our results and to further focus not only in T lymphocytes, but also in innate immune cells and epithelial cells. Moreover, we aim to evaluate the effects in microbiome composition in the AOM/DSS-induced CAC mouse model, once intestinal homeostasis in strongly associated with microbiome composition, having a huge impact in IBD pathogenicity and cancer development. Further studies will also be conducted to better clarify the immune response profile in this model and which are the glycoproteins that are being affected in the different immune cells.

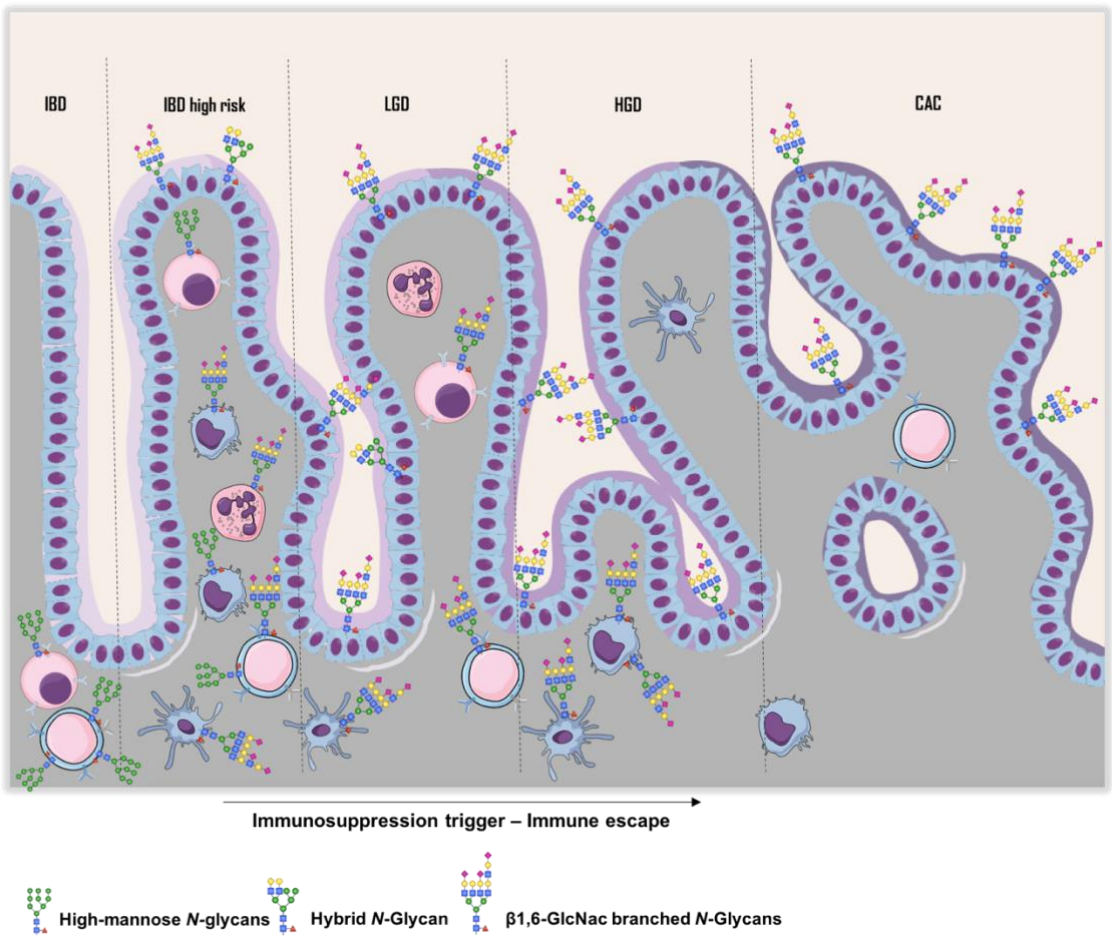

Figure 30| Proposed model. The glycans profile change over the course of CAC development. In IBD, the immune system is expressing non-branched glycan structures previously associated with an hyperactivated immune response. During the progression to dysplasia, there is a gradual increased expression of branched N-glycans that appear to be associated with the creation of an immunosuppression microenvironment that foster immune escape and malignant transformation. IBD: Inflammatory Bowel Disease; LGD: low-grade dysplasia; HGD: high-grade dysplasia; CAC: Colitis-associated Colorectal Cancer.

REFERENCES

1. UK, C.R. *Worldwide cancer incidence statistics*. 2018 [cited 2019 May]; Available from: https://www.cancerresearchuk.org/health-professional/cancer-statistics/worldwide-cancer/.
2. Organization, W.H. *Cancer*. 2018 [cited 2019 May]; Available from: https://www.who.int/news-room/fact-sheets/detail/cancer.
3. Hanahan, D. and R.A. Weinberg, *The hallmarks of cancer.* Cell, 2000. **100**(1): p. 57-70.
4. Hanahan, D. and R.A. Weinberg, *Hallmarks of cancer: the next generation.* Cell, 2011. **144**(5): p. 646-74.
5. Arnold, M., et al., *Global patterns and trends in colorectal cancer incidence and mortality.* Gut, 2017. **66**(4): p. 683-691.
6. Jasperson, K.W., et al., *Hereditary and familial colon cancer.* Gastroenterology, 2010. **138**(6): p. 2044-58.
7. Grivennikov, S.I., F.R. Greten, and M. Karin, *Immunity, inflammation, and cancer.* Cell, 2010. **140**(6): p. 883-99.
8. Rogler, G., *Chronic ulcerative colitis and colorectal cancer.* Cancer Lett, 2014. **345**(2): p. 235-41.
9. Maloy, K.J. and F. Powrie, *Intestinal homeostasis and its breakdown in inflammatory bowel disease.* Nature, 2011. **474**(7351): p. 298-306.
10. Abraham, C. and J.H. Cho, *Inflammatory bowel disease.* N Engl J Med, 2009. **361**(21): p. 2066-78.
11. Ng, S.C., et al., *Worldwide incidence and prevalence of inflammatory bowel disease in the 21st century: a systematic review of population-based studies.* Lancet, 2018. **390**(10114): p. 2769-2778.
12. de Souza, H.S. and C. Fiocchi, *Immunopathogenesis of IBD: current state of the art.* Nat Rev Gastroenterol Hepatol, 2016. **13**(1): p. 13-27.
13. Ungaro, R., et al., *Ulcerative colitis.* Lancet, 2017. **389**(10080): p. 1756-1770.
14. Feagins, L.A., R.F. Souza, and S.J. Spechler, *Carcinogenesis in IBD: potential targets for the prevention of colorectal cancer.* Nat Rev Gastroenterol Hepatol, 2009. **6**(5): p. 297-305.
15. Eaden, J.A., K.R. Abrams, and J.F. Mayberry, *The risk of colorectal cancer in ulcerative colitis: a meta-analysis.* Gut, 2001. **48**(4): p. 526-35.

16. Adami, H.O., et al., *The continuing uncertainty about cancer risk in inflammatory bowel disease.* Gut, 2016. **65**(6): p. 889-93.
17. Magro, F., et al., *Third European Evidence-based Consensus on Diagnosis and Management of Ulcerative Colitis. Part 1: Definitions, Diagnosis, Extra-intestinal Manifestations, Pregnancy, Cancer Surveillance, Surgery, and Ileo-anal Pouch Disorders.* J Crohns Colitis, 2017. **11**(6): p. 649-670.
18. Bressenot, A., et al., *Microscopic features of colorectal neoplasia in inflammatory bowel diseases.* World J Gastroenterol, 2014. **20**(12): p. 3164-72.
19. Beaugerie, L. and S.H. Itzkowitz, *Cancers complicating inflammatory bowel disease.* N Engl J Med, 2015. **372**(15): p. 1441-52.
20. Choi, C.R., et al., *Clonal evolution of colorectal cancer in IBD.* Nat Rev Gastroenterol Hepatol, 2017. **14**(4): p. 218-229.
21. Terzic, J., et al., *Inflammation and colon cancer.* Gastroenterology, 2010. **138**(6): p. 2101-2114 e5.
22. Wu, Y., et al., *Molecular mechanisms underlying chronic inflammation-associated cancers.* Cancer Lett, 2014. **345**(2): p. 164-73.
23. Elinav, E., et al., *Inflammation-induced cancer: crosstalk between tumours, immune cells and microorganisms.* Nat Rev Cancer, 2013. **13**(11): p. 759-71.
24. Lasry, A., A. Zinger, and Y. Ben-Neriah, *Inflammatory networks underlying colorectal cancer.* Nat Immunol, 2016. **17**(3): p. 230-40.
25. Kang, M. and A. Martin, *Microbiome and colorectal cancer: Unraveling host-microbiota interactions in colitis-associated colorectal cancer development.* Semin Immunol, 2017. **32**: p. 3-13.
26. Manichanh, C., et al., *The gut microbiota in IBD.* Nat Rev Gastroenterol Hepatol, 2012. **9**(10): p. 599-608.
27. Owen, J., *Kuby immunology*. 2018.
28. de Visser, K.E., A. Eichten, and L.M. Coussens, *Paradoxical roles of the immune system during cancer development.* Nat Rev Cancer, 2006. **6**(1): p. 24-37.
29. Chaplin, D.D., *Overview of the immune response.* J Allergy Clin Immunol, 2010. **125**(2 Suppl 2): p. S3-23.
30. Davies, L.C., et al., *Tissue-resident macrophages.* Nat Immunol, 2013. **14**(10): p. 986-95.
31. Morvan, M.G. and L.L. Lanier, *NK cells and cancer: you can teach innate cells new tricks.* Nat Rev Cancer, 2016. **16**(1): p. 7-19.

32. Souza-Fonseca-Guimaraes, F., J. Cursons, and N.D. Huntington, *The Emergence of Natural Killer Cells as a Major Target in Cancer Immunotherapy.* Trends Immunol, 2019. **40**(2): p. 142-158.
33. Albertsson, P.A., et al., *NK cells and the tumour microenvironment: implications for NK-cell function and anti-tumour activity.* Trends Immunol, 2003. **24**(11): p. 603-9.
34. Rescigno, M. and A. Di Sabatino, *Dendritic cells in intestinal homeostasis and disease.* J Clin Invest, 2009. **119**(9): p. 2441-50.
35. Garrett, W.S., J.I. Gordon, and L.H. Glimcher, *Homeostasis and inflammation in the intestine.* Cell, 2010. **140**(6): p. 859-70.
36. Withers, D.R., *Innate lymphoid cell regulation of adaptive immunity.* Immunology, 2016. **149**(2): p. 123-30.
37. van Wijk, F. and H. Cheroutre, *Intestinal T cells: facing the mucosal immune dilemma with synergy and diversity.* Semin Immunol, 2009. **21**(3): p. 130-8.
38. Virchow, R., *An Address on the Value of Pathological Experiments.* Br Med J, 1881. **2**(1075): p. 198-203.
39. Neurath, M.F., *Cytokines in inflammatory bowel disease.* Nat Rev Immunol, 2014. **14**(5): p. 329-42.
40. Greten, F.R., et al., *IKKbeta links inflammation and tumorigenesis in a mouse model of colitis-associated cancer.* Cell, 2004. **118**(3): p. 285-96.
41. Balkwill, F. and L.M. Coussens, *Cancer: an inflammatory link.* Nature, 2004. **431**(7007): p. 405-6.
42. Waldner, M.J. and M.F. Neurath, *Colitis-associated cancer: the role of T cells in tumor development.* Semin Immunopathol, 2009. **31**(2): p. 249-56.
43. Imam, T., et al., *Effector T Helper Cell Subsets in Inflammatory Bowel Diseases.* Front Immunol, 2018. **9**: p. 1212.
44. Anestakis, D., et al., *Mechanisms and applications of interleukins in cancer immunotherapy.* Int J Mol Sci, 2015. **16**(1): p. 1691-710.
45. Balkwill, F. and A. Mantovani, *Inflammation and cancer: back to Virchow?* Lancet, 2001. **357**(9255): p. 539-45.
46. Aras, S. and M.R. Zaidi, *TAMeless traitors: macrophages in cancer progression and metastasis.* Br J Cancer, 2017. **117**(11): p. 1583-1591.
47. Mantovani, A., et al., *Macrophage polarization: tumor-associated macrophages as a paradigm for polarized M2 mononuclear phagocytes.* Trends Immunol, 2002. **23**(11): p. 549-55.

48. Mantovani, A., et al., *Tumour-associated macrophages as treatment targets in oncology.* Nat Rev Clin Oncol, 2017. **14**(7): p. 399-416.

49. Condeelis, J. and J.W. Pollard, *Macrophages: obligate partners for tumor cell migration, invasion, and metastasis.* Cell, 2006. **124**(2): p. 263-6.

50. Bottcher, J.P., et al., *NK Cells Stimulate Recruitment of cDC1 into the Tumor Microenvironment Promoting Cancer Immune Control.* Cell, 2018. **172**(5): p. 1022-1037 e14.

51. Gardner, A. and B. Ruffell, *Dendritic Cells and Cancer Immunity.* Trends Immunol, 2016. **37**(12): p. 855-865.

52. Halle, S., O. Halle, and R. Forster, *Mechanisms and Dynamics of T Cell-Mediated Cytotoxicity In Vivo.* Trends Immunol, 2017. **38**(6): p. 432-443.

53. Speiser, D.E., P.C. Ho, and G. Verdeil, *Regulatory circuits of T cell function in cancer.* Nat Rev Immunol, 2016. **16**(10): p. 599-611.

54. Schreiber, R.D., L.J. Old, and M.J. Smyth, *Cancer immunoediting: integrating immunity's roles in cancer suppression and promotion.* Science, 2011. **331**(6024): p. 1565-70.

55. Dunn, G.P., et al., *Cancer immunoediting: from immunosurveillance to tumor escape.* Nat Immunol, 2002. **3**(11): p. 991-8.

56. Varki, A., *Biological roles of glycans.* Glycobiology, 2017. **27**(1): p. 3-49.

57. Varki, A. and S. Kornfeld, *Historical Background and Overview*, in *Essentials of Glycobiology*, rd, et al., Editors. 2015: Cold Spring Harbor (NY). p. 1-18.

58. Pinho, S.S. and C.A. Reis, *Glycosylation in cancer: mechanisms and clinical implications.* Nat Rev Cancer, 2015. **15**(9): p. 540-55.

59. Dias, A.M., et al., *Glycans as critical regulators of gut immunity in homeostasis and disease.* Cell Immunol, 2018. **333**: p. 9-18.

60. Ohtsubo, K. and J.D. Marth, *Glycosylation in cellular mechanisms of health and disease.* Cell, 2006. **126**(5): p. 855-67.

61. Marth, J.D. and P.K. Grewal, *Mammalian glycosylation in immunity.* Nat Rev Immunol, 2008. **8**(11): p. 874-87.

62. Moremen, K.W., M. Tiemeyer, and A.V. Nairn, *Vertebrate protein glycosylation: diversity, synthesis and function.* Nat Rev Mol Cell Biol, 2012. **13**(7): p. 448-62.

63. Zielinska, D.F., et al., *Mapping N-glycosylation sites across seven evolutionarily distant species reveals a divergent substrate proteome despite a common core machinery.* Mol Cell, 2012. **46**(4): p. 542-8.

64. Spiro, R.G., *Protein glycosylation: nature, distribution, enzymatic formation, and disease implications of glycopeptide bonds.* Glycobiology, 2002. **12**(4): p. 43R-56R.

65. Apweiler, R., H. Hermjakob, and N. Sharon, *On the frequency of protein glycosylation, as deduced from analysis of the SWISS-PROT database.* Biochim Biophys Acta, 1999. **1473**(1): p. 4-8.

66. Stanley, P., N. Taniguchi, and M. Aebi, *N-Glycans*, in *Essentials of Glycobiology*, rd, et al., Editors. 2015: Cold Spring Harbor (NY). p. 99-111.

67. Braakman, I. and D.N. Hebert, *Protein folding in the endoplasmic reticulum.* Cold Spring Harb Perspect Biol, 2013. **5**(5): p. a013201.

68. Caramelo, J.J. and A.J. Parodi, *A sweet code for glycoprotein folding.* FEBS Lett, 2015. **589**(22): p. 3379-87.

69. Helenius, A. and M. Aebi, *Intracellular functions of N-linked glycans.* Science, 2001. **291**(5512): p. 2364-9.

70. Chung, C.Y., et al., *SnapShot: N-Glycosylation Processing Pathways across Kingdoms.* Cell, 2017. **171**(1): p. 258-258 e1.

71. Munkley, J. and D.J. Elliott, *Hallmarks of glycosylation in cancer.* Oncotarget, 2016. **7**(23): p. 35478-89.

72. Murata, K., et al., *Expression of N-acetylglucosaminyltransferase V in colorectal cancer correlates with metastasis and poor prognosis.* Clin Cancer Res, 2000. **6**(5): p. 1772-7.

73. Nagae, M., et al., *Structure and mechanism of cancer-associated N-acetylglucosaminyltransferase-V.* Nat Commun, 2018. **9**(1): p. 3380.

74. Granovsky, M., et al., *Suppression of tumor growth and metastasis in Mgat5-deficient mice.* Nat Med, 2000. **6**(3): p. 306-12.

75. Pinho, S.S., et al., *Modulation of E-cadherin function and dysfunction by N-glycosylation.* Cell Mol Life Sci, 2011. **68**(6): p. 1011-20.

76. Carvalho, S., et al., *Preventing E-cadherin aberrant N-glycosylation at Asn-554 improves its critical function in gastric cancer.* Oncogene, 2016. **35**(13): p. 1619-31.

77. Carvalho, S., C.A. Reis, and S.S. Pinho, *Cadherins Glycans in Cancer: Sweet Players in a Bitter Process.* Trends Cancer, 2016. **2**(9): p. 519-531.

78. Pinho, S.S., et al., *The role of N-acetylglucosaminyltransferase III and V in the post-transcriptional modifications of E-cadherin.* Hum Mol Genet, 2009. **18**(14): p. 2599-608.

79. Zhao, Y., et al., *N-acetylglucosaminyltransferase III antagonizes the effect of N-acetylglucosaminyltransferase V on alpha3beta1 integrin-mediated cell migration.* J Biol Chem, 2006. **281**(43): p. 32122-30.

80. Liu, Y.C., et al., *Sialylation and fucosylation of epidermal growth factor receptor suppress its dimerization and activation in lung cancer cells.* Proc Natl Acad Sci U S A, 2011. **108**(28): p. 11332-7.

81. Lise, M., et al., *Clinical correlations of alpha2,6-sialyltransferase expression in colorectal cancer patients.* Hybridoma, 2000. **19**(4): p. 281-6.

82. Pereira, M.S., et al., *Glycans as Key Checkpoints of T Cell Activity and Function.* Front Immunol, 2018. **9**: p. 2754.

83. Johnson, J.L., et al., *The regulatory power of glycans and their binding partners in immunity.* Trends Immunol, 2013. **34**(6): p. 290-8.

84. van Kooyk, Y. and G.A. Rabinovich, *Protein-glycan interactions in the control of innate and adaptive immune responses.* Nat Immunol, 2008. **9**(6): p. 593-601.

85. Liu, F.T. and G.A. Rabinovich, *Galectins as modulators of tumour progression.* Nat Rev Cancer, 2005. **5**(1): p. 29-41.

86. Toscano, M.A., et al., *Differential glycosylation of TH1, TH2 and TH-17 effector cells selectively regulates susceptibility to cell death.* Nat Immunol, 2007. **8**(8): p. 825-34.

87. Ilarregui, J.M., et al., *Tolerogenic signals delivered by dendritic cells to T cells through a galectin-1-driven immunoregulatory circuit involving interleukin 27 and interleukin 10.* Nat Immunol, 2009. **10**(9): p. 981-91.

88. Chen, H.Y., et al., *Galectin-3 negatively regulates TCR-mediated CD4+ T-cell activation at the immunological synapse.* Proc Natl Acad Sci U S A, 2009. **106**(34): p. 14496-501.

89. Dennis, J.W., et al., *Adaptive regulation at the cell surface by N-glycosylation.* Traffic, 2009. **10**(11): p. 1569-78.

90. Brown, G.D., J.A. Willment, and L. Whitehead, *C-type lectins in immunity and homeostasis.* Nat Rev Immunol, 2018. **18**(6): p. 374-389.

91. Robinson, M.J., et al., *Myeloid C-type lectins in innate immunity.* Nat Immunol, 2006. **7**(12): p. 1258-65.

92. Saeland, E., et al., *The C-type lectin MGL expressed by dendritic cells detects glycan changes on MUC1 in colon carcinoma.* Cancer Immunol Immunother, 2007. **56**(8): p. 1225-36.

93. Rodrigues, J.G., et al., *Glycosylation in cancer: Selected roles in tumour progression, immune modulation and metastasis.* Cell Immunol, 2018. **333**: p. 46-57.

94. Beatson, R., et al., *The mucin MUC1 modulates the tumor immunological microenvironment through engagement of the lectin Siglec-9.* Nat Immunol, 2016. **17**(11): p. 1273-1281.

95. Li, D., et al., *Knockdown of Mgat5 inhibits breast cancer cell growth with activation of CD4+ T cells and macrophages.* J Immunol, 2008. **180**(5): p. 3158-65.

96. Smith, L.K., et al., *Interleukin-10 Directly Inhibits CD8(+) T Cell Function by Enhancing N-Glycan Branching to Decrease Antigen Sensitivity.* Immunity, 2018. **48**(2): p. 299-312 e5.

97. Demetriou, M., et al., *Negative regulation of T-cell activation and autoimmunity by Mgat5 N-glycosylation.* Nature, 2001. **409**(6821): p. 733-9.

98. Dias, A.M., et al., *Dysregulation of T cell receptor N-glycosylation: a molecular mechanism involved in ulcerative colitis.* Hum Mol Genet, 2014. **23**(9): p. 2416-27.

99. Dias, A.M., et al., *Metabolic control of T cell immune response through glycans in inflammatory bowel disease.* Proc Natl Acad Sci U S A, 2018. **115**(20): p. E4651-E4660.

100. Pereira, M.S., et al., *A [Glyco]biomarker that Predicts Failure to Standard Therapy in Ulcerative Colitis Patients.* J Crohns Colitis, 2019. **13**(1): p. 39-49.

101. Shinzaki, S., et al., *N-Acetylglucosaminyltransferase V exacerbates murine colitis with macrophage dysfunction and enhances colitic tumorigenesis.* J Gastroenterol, 2016. **51**(4): p. 357-69.

102. Wirtz, S., et al., *Chemically induced mouse models of acute and chronic intestinal inflammation.* Nat Protoc, 2017. **12**(7): p. 1295-1309.

103. Tang, A., et al., *Dynamic activation of the key pathways: linking colitis to colorectal cancer in a mouse model.* Carcinogenesis, 2012. **33**(7): p. 1375-83.

104. Cooper, H.S., et al., *Clinicopathologic study of dextran sulfate sodium experimental murine colitis.* Lab Invest, 1993. **69**(2): p. 238-49.

105. Bratthauer, G.L., *The avidin-biotin complex (ABC) method and other avidin-biotin binding methods.* Methods Mol Biol, 2010. **588**: p. 257-70.

106. Reily, C., et al., *Glycosylation in health and disease.* Nat Rev Nephrol, 2019. **15**(6): p. 346-366.

107. Shin, B., et al., *Effector CD4 T cells with progenitor potential mediate chronic intestinal inflammation.* J Exp Med, 2018. **215**(7): p. 1803-1812.

108. Maier, T., M. Guell, and L. Serrano, *Correlation of mRNA and protein in complex biological samples.* FEBS Lett, 2009. **583**(24): p. 3966-73.

109. Amicarella, F., et al., *Dual role of tumour-infiltrating T helper 17 cells in human colorectal cancer.* Gut, 2017. **66**(4): p. 692-704.

110. Hyun, Y.S., et al., *Role of IL-17A in the development of colitis-associated cancer.* Carcinogenesis, 2012. **33**(4): p. 931-6.

111. Pappu, B.P. and P.A. Shrikant, *Alteration of cell surface sialylation regulates antigen-induced naive CD8+ T cell responses.* J Immunol, 2004. **173**(1): p. 275-84.

112. Yoshioka, K., et al., *Role of natural killer T cells in the mouse colitis-associated colon cancer model.* Scand J Immunol, 2012. **75**(1): p. 16-26.

113. Benson, V., et al., *Glycosylation regulates NK cell-mediated effector function through PI3K pathway.* Int Immunol, 2010. **22**(3): p. 167-77.

114. Allavena, P., et al., *Engagement of the mannose receptor by tumoral mucins activates an immune suppressive phenotype in human tumor-associated macrophages.* Clin Dev Immunol, 2010. **2010**: p. 547179.

APPENDIX

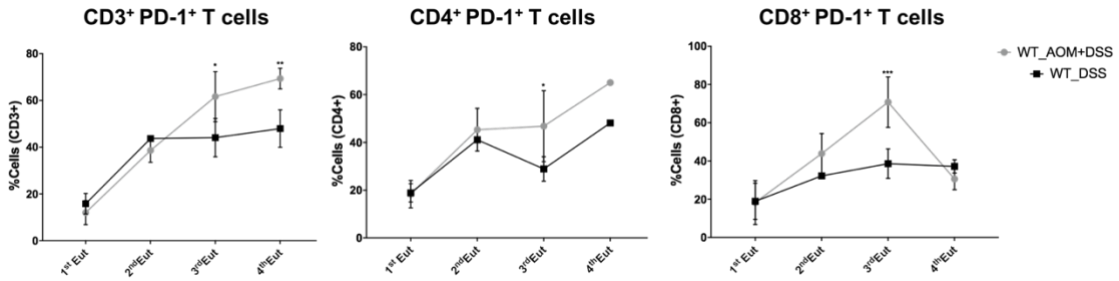

Supplementary figure 1 | PD-1 activation was not observed in the DSS group. $CD3^+$, $CD4^+$ and $CD8^+$ T cells from DSS group did not show an increase over time, when compared with the AOM/DSS group. Statistical significance was assessed by two-way ANOVA, with Turkey's multiple comparisons test: $*p \leq 0.05$, $**p \leq 0.01$, $***p \leq 0.001$.